

University of Dundee

MASTER OF SCIENCE

Lag Time and Hydrograph Form in the Upper Feshie Catchment

MacDonald, Michael

Award date:
2022

Licence:
Copyright of the Author. All Rights Reserved

[Link to publication](#)

General rights

Copyright and moral rights for the publications made accessible in the public portal are retained by the authors and/or other copyright owners and it is a condition of accessing publications that users recognise and abide by the legal requirements associated with these rights.

- Users may download and print one copy of any publication from the public portal for the purpose of private study or research.
- You may not further distribute the material or use it for any profit-making activity or commercial gain
- You may freely distribute the URL identifying the publication in the public portal

Take down policy

If you believe that this document breaches copyright please contact us providing details, and we will remove access to the work immediately and investigate your claim.

Lag Time and Hydrograph Form in the Upper Feshie Catchment



University
of Dundee

Michael MacDonald

Submitted in accordance with the requirements for the degree of Master of
Science by Research.

The University of Dundee

2022

Table of Contents

Table of Contents	ii
List of Figures	iv
List of Tables.....	vi
List of Abbreviations.....	vii
Acknowledgments.....	viii
Declaration	ix
Abstract	x
Appendices.....	129
Appendix A: Survey Derivation Report.....	129
Appendix B: R-Studio Code.....	133
Chapter 1: Introduction.....	1
1.1: Background and Rationale.....	1
1.2: Aims and Objectives.....	3
Chapter 2: Literature Review.....	4
2.1: Catchment Descriptors and Climatic Inputs.....	4
2.1.2: Antecedent Moisture.....	5
2.1.3: Elevation.....	6
2.1.4: Catchment Size.....	7
2.2: Peatland Hydrology.....	9
2.2.1: Introduction to Peatland Hydrology.....	9
2.2.2: Peatland water Fluxes.....	11
2.2.3: Surface Roughness in Peatland Catchments.....	15
2.2.4: Lag Time in Peatland Catchments.....	19
2.2.5: Impact of Restorative Management on Peatland Catchments.....	20
2.3: Summary of Peatland Hydrology.....	22
2.4: Mineral Catchment Hydrology.....	23
2.4.1: Introduction to Rocky Mineral Catchments.....	23
2.4.2: Local Contextual History and Runoff Generation.....	23
2.4.3: Summary of Mineral Catchment Hydrology	25
2.5: Importance of the Hydrometric Rating Equation.....	26
2.5.1: Introduction to the Rating Curve.....	26

2.5.2: The Empirical Rating Curve.....	27
2.5.3: Computer Modelled Rating Curves.....	28
2.5.4: The Area X Velocity Method for Rating Curve Creation.....	29
2.5.5: Summary of Hydrometric Rating Curves.....	30
Chapter 3: Study Site.....	32
3.1: The Feshie Catchment.....	32
3.2: The Study Sites.....	33
3.3: Catchment Characteristics.....	35
3.3.1 The Lower Eidart (Moine Mhor).....	36
3.3.2 The Upper Feshie Catchment.....	36
3.3.3 The Combined Catchment.....	38
Chapter 4: Methodology.....	39
4.1: Topographic Survey.....	39
4.2: Digital Terrain Model Development.....	45
4.2.1: Post Processing of the Data.....	45
4.2.2: Building the Digital Terrain Model.....	46
4.3: HEC-RAS Hydraulic Modelling for Rating Extrapolation.....	48
4.3.1: Building the HEC-RAS Model.....	48
4.3.2: Fitting the Modelled Outputs to Empirical Data.....	51
4.4: Quality Review Process.....	53
4.4.1: First Tier: Visual Analysis.....	53
4.4.2: Second Tier: Rating Application.....	53
4.4.3: The $Q = VA$ Method for Rating Extrapolation and Result validation.....	53
4.5: Hydrological Analysis.....	56
4.5.1: Application of the Newly Derived Ratings to Time Series Data.....	56
4.5.2: Event Selection and Precipitation Data.....	57
4.5.4: Event Analysis.....	60
Chapter 5: Results.....	62
5.1: Results of the Topographic Survey.....	62
5.2: Results of the Hydraulic Modelling.....	71
5.3: Quality Review Results.....	75

5.4: Results of Applying the Final Ratings to Events.....	81
5.5 Results of Lag Time Analysis.....	89
Chapter 6: Discussion.....	98
6.1: Choice of Methods.....	98
6.2: Hydrological Analysis.....	100
6.3: Study Limitations.....	105
6.4: General Implications.....	106
Chapter 7: Conclusion.....	107
References.....	110
List of Figures	
Figure 2.1.1 <i>Annual Snow Cover</i>	7
Figure 2.2.1 <i>Idealised Soil Column Example of Acrotelm and Catotelm</i>	10
Figure 2.2.2 <i>Morphology of Types of Peatland</i>	11
Figure 2.2.3 <i>Upper: Water Table Heights in Time Series; Lower: Comparison Between Rainfall on Open Mire and Beneath Canopy of Mature Birch</i>	12
Figure 2.2.4 <i>Dun Moss Hourly Rainfall and Discharge Data</i>	14
Figure 2.2.5 <i>Relative Difference Between Treatment and Control Sites for Key Hydrograph Metrics</i>	20
Figure 2.5.1 <i>Hydrological Rating Curve Example</i>	26
Figure 3.1 <i>River Feshie Catchment Delineation</i>	32
Figure 3.2.1 <i>The Study Site Catchments</i>	33
Figure 3.2.2 <i>The Physical Characteristics of the Lower Eidart and Upper Feshie Catchments</i>	34
Figure 3.3.1 <i>A Bare Peat and Hag Area on the Moine Mhor</i>	35
Figure 3.3.2 <i>A Map of the Superficial Deposits of the Study Catchments</i>	36
Figure 4.1.1 <i>Trimble R12i GNSS Rover in Use, Lower Eidart</i>	40
Figure 4.1.2 <i>Trimble R10 GNSS BASE</i>	41
Figure 4.1.3 <i>Approximate Locations of Base Stations Relative to Survey Locations</i>	42

Figure 4.2.1 <i>Representation of Surface Triangulation</i>	46
Figure 4.2.2 <i>Upper Feshie Digital Terrain Model</i>	47
Figure 4.3.1 <i>HEC-RAS Main Screen</i>	49
Figure 4.3.2 <i>HEC-RAS Geometry Tab</i>	49
Figure 4.3.3 <i>HEC-RAS Steady Flow Data Tab</i>	50
Figure 4.3.4 <i>A Theoretical Rating Curve (Left) and An Example Flood Profile (Right)</i> ...50	
Figure 4.3.5 <i>Offset Application Between Datums</i>	51
Figure 4.3.6 <i>The Solver Window in Microsoft Excel</i>	52
Figure 4.4.1 <i>Velocity x Cross Sectional Area Matrix Spreadsheet</i>	55
Figure 4.5.1 <i>Flood Event Graphed with Precipitation for August 2017</i>	59
Figure 4.5.2 <i>An Example Catchment Comparison Event</i>	60
Figure 4.5.2 <i>Mann-Whitney Wilcoxon Test Code From R-Studio</i>	62
Figure 4.5.3 <i>An Example of a Generalised Median Hydrograph</i>	62
Figure 5.1.0 <i>The Digital Terrain Models of the Three Surveyed Reaches</i>	64
Figure 5.1.1 <i>The Digital Terrain Model of Upper Feshie</i>	65
Figure 5.1.2 <i>The Digital Terrain Model of Lower Eidart</i>	66
Figure 5.1.3 <i>The Digital Terrain Model of Upper Feshie Confluence</i>	67
Figure 5.1.4 <i>The Geometry Summary of Upper Feshie</i>	68
Figure 5.1.5 <i>The Geometry Summary of Lower Eidart</i>	68
Figure 5.1.6 <i>The Geometry Summary of Upper Feshie Confluence</i>	68
Figure 5.1.7 <i>The Cross-Sectional Geometry at the Gauge- Upper Feshie</i>	69
Figure 5.1.8 <i>The Cross-Sectional Geometry at the Gauge- Lower Eidart</i>	69
Figure 5.1.9 <i>The Cross-Sectional Geometry at the Gauge- Upper Feshie Confluence</i> ...70	
Figure 5.2.1 <i>An Example Cross Section Output Table for the Gauging Station for the Reach Upper Feshie</i>	72

Figure 5.2.2 <i>The Stage Discharge Relationship at Upper Feshie from HEC-RAS</i>	72
Figure 5.2.3 <i>An Example Cross Section Output Table for the Gauging Station for the Reach Lower Eidart</i>	73
Figure 5.2.4 <i>The Stage Discharge Relationship at Lower Eidart from HEC-RAS</i>	73
Figure 5.3.1 <i>The Relationship Between Stage and Vbar for Lower Eidart and Upper Feshie</i>	76
Figure 5.3.2 <i>The Relationship Between Stage and Area for Lower Eidart and Upper Feshie</i>	78
Figure 5.3.3 <i>The $Q = VA$ Final Rating Curve for Lower Eidart</i>	79
Figure 5.3.4 <i>The HEC-RAS Final Rating Curve for Upper Feshie</i>	79
Figure 5.4.1 <i>Comparison Between Upper Feshie and Lower Eidart for 14 Events</i>	82
Figure 5.5.1 <i>Visualisation of the Catchment Lag Times</i>	91
Figure 5.6.1 <i>Median Hydrograph for Lower Eidart and Upper Feshie</i>	92
Figure 5.6.2 <i>Median Hydrograph for Lower Eidart Ranked By Peak Discharge</i>	93
Figure 5.6.3 <i>Median Hydrograph for Upper Feshie Ranked By Peak Discharge</i>	93
Figure 5.6.4 <i>Median Hydrograph for Lower Eidart and Upper Feshie for Frontal Rainfall Response</i>	94
Figure 5.6.5 <i>Lower Eidart Frontal Rainfall Response Compared to Convective Rainfall</i>	95
Figure 5.6.6 <i>Upper Feshie Frontal Rainfall Response Compared to Convective Rainfall</i>	96
Figure 6.2.1 <i>The Median Hydrographs for the Study Catchments and Their Confluence</i>	97
Figure 6.3.1 <i>The Hydrographs for 14 Events at Upper Feshie Confluence</i>	103
List of Tables	
Table 3.3.1 <i>Scottish Upland Plant Species</i>	16
Table 3.3.1 <i>Catchment Descriptors for Lower Eidart and Upper Feshie</i>	37

Table 3.3.2 <i>Soil Types of Lower Eidart and Upper Feshie</i>	38
Table 4.1.1 <i>Series of Codes Used in Trimble TSC7 For Post Processing</i>	44
Table 5.2.1 <i>Rating Equation Results from HEC-RAS</i>	71
Table 5.2.2 <i>Summarised Hydraulic Depth Outputs for Input Flows from HEC-RAS with Observed Gaugings and Stage Measurements</i>	74
Table 5.3.1 <i>Results of the 2nd Tier Quality Review Process and Precipitation Data</i>	75
Table 5.3.2 <i>Results of the Quality Review Process on Lower Eidarts Rating</i>	80
Table 5.3.3 <i>Results of the Quality Review Process on Upper Feshies Rating</i>	89
Table 5.4.1 <i>Summary Table of all 14 Analysed Events</i>	90
Table 5.5.1 <i>Summary Table of Lag Times in Each Catchment</i>	90
Table 5.5.2 <i>Results of the Mann-Whitney Wilcoxon Test</i>	91

List of Abbreviations

NFM.....	Natural Flood Management
AMCs.....	Antecedent Moisture Conditions
AOD.....	Above Ordnance Datum
CGH.....	Central Grampian Highlands
RTK GNSS.....	Real Time Kinematic Global Navigation Satellite System
$Q = VA$	Flow = Average Velocity x Area
Vbar.....	Average Velocity
DTM.....	Digital Terrain Model
RMSE.....	Root Mean Square Error
MWW.....	Mann-Whitney Wilcoxon Test of Difference
TBR.....	Tipping Bucket Rain-Gauge

Acknowledgements

This thesis submission was supervised by Dr Andrew Black of the University of Dundee. I hereby extend my sincere gratitude to him for his continued support and guidance which has transcended the writing of this thesis. Throughout the duration of this thesis, I have experienced many personal and workplace related setbacks and without Dr Black, this submission would not have been possible.

In addition, I would like to acknowledge the contribution of Dr Andrew Black in terms of the provision of data for this thesis which includes time series data of river stage and precipitation.

I would like to thank Alice Ambler for assistance with HEC-RAS in the early stages of this thesis.

I would like to thank Wildland Ltd for their support by allowing me to carry out fieldwork on their land and for transport assistance to the remote Feshie system.

I would like to thank cbec Eco-Engineering Ltd for the use of their software and some training during my employment with them.

I would also like to thank Kaya Consulting Ltd for their kind support of this thesis throughout my current employment while I have been preparing this submission.

Within this submission, the use of Autodesk® Civil 3D, R-Studio®, Edina Digimap® and all other trademarks and logos for the products of these companies remain their respective property. In addition, any other referenced marks, organisations or companies remain the property of their respective owners and more information is available on their respective websites.

The candidate confirms that the paper submitted is his own and that credit has been given where references have been made to the work of other people.

This copy is supplied on the understanding that it is copyright intellectual property and no quotations from this thesis may be published without acknowledgement.

The right of Michael MacDonald to be identified as the author of this thesis has been asserted by him in accordance with the Copyright, Designs and patents Act 1988.

© 2022 The University of Dundee and Michael MacDonald.

Abstract

This study presents findings relating to the hydrological response of the Lower Eidart and the Upper Feshie which are neighbouring sub-catchments of the Feshie catchment. These catchments have contrasting physical characteristics where the Lower Eidart has >59% mineral soil and >27% blanket peat which contrast with the Upper Feshie which has >65% blanket peat and a further 10% peaty soil.

The Vbar method has been used to calibrate the stage-discharge rating equation at the outlet of each of these gauged catchments beyond current empirical gaugings. The extended rating curve applied to a year of continuous time series gauge data to compare the hydrological response of these catchments.

Analysis of lag time to peak discharge found that the Lower Eidart catchment peaked 23 minutes sooner than the Upper Feshie, which is statistically insignificant based on a Mann-Whitney Wilcoxon Test of Difference ($P= 0.1171$). It was also found that both the Lower Eidart and Upper Feshie have a remarkably similar hydrological response to both frontal and convective rainfall based on the creation of a median hydrograph for these catchments. Lower Eidart was found to have a higher antecedent flow prior to the synthesised median hydrograph. The higher antecedent flow may contribute to the lower peak discharge observed in the time series ($11.8 \text{ m}^3/\text{s}$) when compared with Upper Feshie which had a peak discharge of $20.2 \text{ m}^3/\text{s}$. The higher baseflow observed in the time series is consistent with existing literature in the area, however, is contradictory to the Bfihost estimation found in the FEH catchment descriptors.

The Vbar method may be applicable to other upland catchments where empirical gauging data is sparse, in the context of water management and monitoring, especially where manual gaugings are not safe at higher flows.

Chapter 1: Introduction

1.0 *Background and Rationale*

It is both challenging and important to monitor upland and mountainous catchments in terms of meteorological input and catchment response (CEH, 2020). The remoteness of the mountainous uplands of Scotland presents logistical challenges for data collection, although, the monitoring of such remote and still relatively wild places may present new insights and fill the gaps in knowledge of upland catchment response to precipitation events in a time of changing climate. A multidecadal four catchment study in the Scottish west coast by Mansel (1997) observed a climate driven increase in river flows in all four catchments, with predictions for further changes in the spatial distributions of precipitation events leading to further increases in river flows across Scotland. Scotland's climate is dominated by North Atlantic maritime airflows giving rise to large volumes of precipitation annually with relatively low evapotranspiration and high runoff (Gosling, 2014). To Werrity (2000), who proposes the 'wetter-west' and a drier east, it could be assumed that the relatively eastern plateaus of the Northern Cairngorms may experience fewer extreme changes in rainfall events when compared to the west coast as these trends continue, however RLUK (2020), based on SEPA's flow records highlight that the most extreme flood events of the River Feshie (Cairngorms National Park) have occurred in the last few years. Now, in 2022, gaps in knowledge remain regarding upland precipitation and catchment response. These gaps are poignant reminders of how little is known about most upland catchments in Scotland, not least blanket peat, and mineral catchments such as those of the Upper Feshie system.

A history of deforestation, peatland draining for agriculture and anthropogenic warming of climate has led to the consideration of intense highland flooding as quasi-environmental, or human-intensified (Smith, 2013) due to decadal mismanagement and grazing pressures. Following the purchase of the Glenfeshie Estate in 2006 (Wildland, 2022), owners Wildland Limited have been pursuing a policy of rewilding (RSGS, 2014) to help "the land to achieve its full ecological potential". This policy arises in the context of decline in habitats (a severe loss in native woodland) and species (for example, Field Vole, Black Grouse, and Capercaillie). Conservation monitoring is undertaken periodically by NatureScot and by landowners, but it is not a common practice to monitor river flows in areas which are subject to land management for conservation purposes. Fortunately in Glen Feshie, there have been efforts to monitor precipitation inputs and

runoff outputs from various parts of the river catchment, and these provide the opportunity to examine hydrological behaviour in areas which have not yet been subject to focused conservation efforts, but which are expected to benefit from them in the coming years. An opportunity to better understand the hydrological behaviour of the Feshie catchment now may provide the prospect of advising future conservation action to address not only species and habitats, but also their hydrological consequences.

The restoration of peatlands is of national conservation value (NatureScot, 2022) in terms of carbon sequestration, habitat regeneration and natural flood management. Natural flood management (NFM) aims to exploit natural processes to work with nature to reduce flood risk (Black, *et al.*, 2022). Carrick, *et al.*, (2018) outlines that regeneration of surface vegetation in areas which have previously been overgrazed can enact NFM because of the protective and soil binding characteristics of the upland vegetation, such as mosses. It is on this basis that peatland restoration is expected to deliver multiple benefits, including the attenuation of storm runoff through increasing storage potential in thin alpine soils and enhancing surface roughness, “slowing the flow”, of overland runoff in hydrophobic bare peat areas. NFM interventions were classified in Lane (2017) as those aimed at reducing the rate of rapid surface runoff. A novel opportunity is presented to bridge the gaps in our knowledge of the hydrological response of headwater blanket peat and mineral soil catchments as they undergo natural regeneration which is a conservation focus at national and international scale.

The study catchments which are explained in Section 3.2 are the headwater catchments of the river Feshie. The Feshie is widely regarded as extremely flashy and exhibits an ever-changing braided zone in the mid-river (Wheaton, *et al.*, 2013). There is very little existing infrastructure in the Feshie catchment, which is within the functional floodplain, so flood risk in the area is generally considered low. The position of these catchments and the spatial intensity of the gauge network make these study catchments a suitable location to study the potential for the use of empirical methods in remote, data sparse environments. The sediment regime in the Feshie is supplied by areas of extreme erosion in the mid-river and the examination of NFM in these upland catchments is of interest for erosion management.

1.2 *Aims and Objectives*

The aim of this research is to compare the catchment response of two neighboring sub-catchments (of the River Feshie catchment) with contrasting physical characteristics.

To meet the aim of this research, some key objectives have been identified:

Objective 1: To produce reliable rating equations that extend the current ratings, which are based on low flow gaugings.

Objective 2: To validate the ratings by applying them to level data and independently evaluating the results.

Objective 3: To carry out analysis of hydrological metrics such as lag time to peak discharge and create a set of characteristic hydrographs to compare the study catchments.

Chapter 2: Literature Review

2.1 *Catchment Descriptors and Climatic Inputs*

Catchment descriptors represent the characteristics of a catchment as a single value, for example, drainage area in km². These are used in hydrological assessments, which include peak flow estimation for flood risk assessment. Methodologies for this include FEH-Rainfall-Runoff or REFH2.3, among others. These catchment descriptors have been developed for desk-based assessments of flow estimation and are particularly used in ungauged catchments.

Some key catchment descriptors included within this chapter are elevation, antecedent moisture, elevation, and catchment size. Other descriptors are included by the FEH, such as baseflow, however these have not been described in this chapter.

2.1.1 *Climatic Inputs*

Climate change is thought to have led to increased intensity and duration of precipitation events (Smith 2013) which leads to concerns relating to flood risk. Anthropogenic contributions to climate warming have been scrutinised as generating a ‘Quasi-Environmental’ risk as human drivers of climatic warming is accepted to increase flood hazard. There are many examples of how humans may intensify flood hazard such as deforestation and peatland degradation altering runoff response of a given catchment, and anthropogenic climate warming leading to changes in the intensity and duration of rainfall (Min, *et al.*, 2011; Pall, *et al.*, 2011; Scott, *et al.*, 2014). The changing global climate is discussed in Black and Burns (2002), whereby freshwater scientists have had a shift in view relating to increasing flood risk in Scotland, based on mounting evidence cited in Werritty (2002). More recent work, such as Werritty and Sugden (2013), has reinforced discussion of these potential climatic trends of increased water hazard based on key signals of anthropogenic climate warming. Burt and Holden (2002) state that further increases to the duration and intensity of precipitation events in the uplands of the United Kingdom are expected. Climate change models are uncertain due to input parameters such as emissions and global temperatures, however it is estimated that by 2050, winter in Scotland will be up to 8% wetter and 0.5 degrees warmer (McPherson, 2022).

As evidence mounts over the duration of more than two decades, there is little doubt that human-accelerated changes in climate will lead to greater pressures in the water

environment in terms of the management of water resources and increased flood risk as flooding is considered one of the central climate related hazards (Hirabayashi, *et al.*, 2013). Warming global climate trends have a direct impact on precipitation (Trenbeth, 2011) as greater warming leads to greater evaporation and surface drying thereby influencing the state of catchment wetness and increasing the air's holding capacity for water by up to 7% per 1°C of warming (Dore 2005). Dore (2015) continues that higher latitude areas will experience the greatest intensification of precipitation events in addition to an increase in rainfall duration. Overall, the current climatic trends of warming, which are believed to facilitate greater intensity and duration of rainfall events are of paramount concern for flood risk generally.

2.1.2 Antecedent Moisture

Antecedent moisture conditions (AMCs) relate to the state of wetness of the soil prior to a hydrological event (James and Roulet, 2009). There are a multitude of soil moisture-atmospheric interactions whereby soil moisture content and memory can contribute significantly to land and climate relationships (Senevirante, *et al.*, 2006a). Several studies including (Pitman, *et al.*, 2012) have demonstrated that soil moisture content has a direct impact on the severity of a flood event. AMCs significantly impact magnitude and extent of the event; this is widely agreed within literature (Lorenz, *et al.*, 2010; Quesada, *et al.*, 2012) in both drought and extreme flood situations. The wealth of literature which agree on the importance of AMCs in catchment runoff generation (for example, Zema and Blöschl, 2004; Penna, *et al.*, 2011) are insightful and well-founded, however many literature sources on the matter cite plot scale results as small as 2.8 m² (Schoener and Stone, 2019). At catchment scale, Penna, *et al.*, (2011), focussed on the threshold runoff response of an upland catchment showed a strong AMC control of the runoff generated. The research stated that catchment response time may have been dictated by soil moisture prior to the event, in dry conditions streamflow peaked prior to hillslope soil moisture whereas in wet conditions, the opposite occurred. The catchment's response was facilitated by hysteretic behaviour in the soil moisture and streamflow relationship. Additionally, AMCs were evidently important in the relationship between cumulative rainfall and total stormflow because storms of similar magnitude occurring in dry periods exhibited smaller stormflow peak discharge values than those occurring in wet conditions. An example of an event where AMCs had a significant impact on the severity of a rainfall event was the 1997 flood in Hagemann, *et al.*, (2015). Regional climate modelling indicated soil moisture contributed to the formation of extreme rainfall

climate through the control of soil moisture on soil energy availability for evapotranspiration. Due to this, spatially significant rainfall occurred giving rise to extreme levels of runoff and a significant high flow event. Vivoni, *et al.*, (2007) states that AMCs are one of three major descriptors in conjunction with catchment physical characteristics and the precipitation event structure.

2.1.3 Elevation

Elevation is a catchment descriptor which is extremely important but sometimes overlooked. Dingman (1981) documented the impact of elevation on catchment hydrology in good detail, noting that basin elevation correlates with significant variation in streamflow characteristics such as low flow, flood flow and long-term average flow. This variability can be reasonably associated with elevation-climatic interactions whereby the impact of the climate at higher altitude corresponds to the behaviour of the river. Temperature decreases with elevation due to temperature lapse rates as, generally, precipitation increases (Zhang, *et al.*, 2013) making temperature and precipitation the most important variables in an elevation based hydrological model. Due to decreased temperatures at higher elevations, it is likely that snow will cover upland catchments for much of the year, for example in the Cairngorms National Park (with altitudes of > 900 m AOD spatially significant snow cover can be expected to vary between 90 - 150 days of the year (Figure 2.1.1), a decrease from over 200 days per year in 1977 (Rivington, *et al.*, 2019). Globally, over 1.5 billion people are affected by perennial snow cover including diurnal melt and refreeze (Yao, *et al.*, 2012) by impacts to water supply. It can therefore be reasonably stated that catchment snow cover duration and extent have a significant impact on the annual hydrological runoff regime of the catchment in terms of storage, ice damming and ephemeral melt induced high flows.

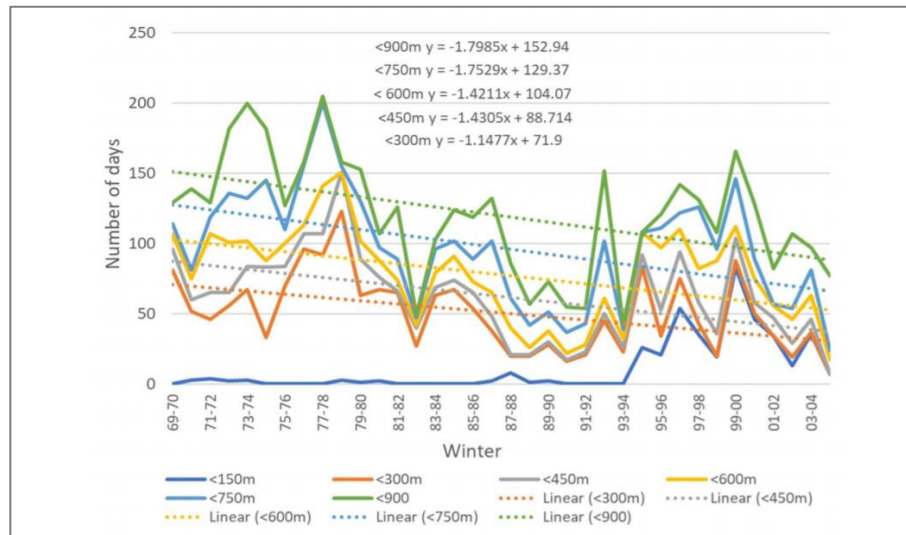


Figure 2.1.1. Annual Snow. Source: Rivington, *et al.*, (2019)

Trends estimated for the site of Whitehillocks, Cairngorm National Park, between 1969 and 2005. Anecdotally, climatic change is being estimated to reduce snow cover days by up to 52 days per year.

2.1.4 Catchment Size

The spatial extent of a catchment has a fundamental impact on how runoff is generated and conveyed through the system to the outlet. An example by Miller (1994) demonstrates that catchment size dictates the availability of absolute runoff volumes and is therefore an essential parameter in flood estimation. Pilgrim, *et al.*, (1982) asserted that most of the research on catchment response has been conducted at small spatial scales, this is accurate due to the difficulty in attaining consistent, meaningful, and reliable data in remote and or large spatial areas. (Beston and Marius 1969). The pockets of more contemporary literature that exists draws unclear and often conflicting conclusions. It may relate to the difficult hydrological question of spatial variability in physical descriptors within a catchment. Using Hortonian overland flow as an example, extreme variation in a small spatial area of surface cover leads to variability in the rate of surface runoff based on friction, so it is difficult to associate a particular runoff rate or value to this. The issue may lie in assessing homogeneity of physical descriptors as it is likely that in smaller catchments, there is a greater chance of the parent bedrock, superficial deposits and vegetation cover being the same.

Questions remain relating to large catchment hydrology and how its physical descriptors may influence runoff generation. Due to spatial variability in superficial deposits, land use, land cover, and other physical descriptors within larger catchments, it

may be reasonable to state that smaller, homogeneous, catchments are more susceptible to ephemeral storm flows from precipitation, giving them a flashier response than bigger catchments. In larger catchments, there is generally greater variability in physical descriptors with a theoretically greater storage potential, which may show a more subdued response to a precipitation event. Mimikou (1984) asserts that maximum observed flood flow and metrics such as lag time to peak discharge are increasing functions of basin size. Additionally, the variability in the catchment scale and runoff response relationship regionally is expressed and relates to the function of surface-climate interactions such as soil moisture and energy for evaporation. Overall, catchment scale is an integral parameter to flood estimation models, however due to factors such as climate over large spatial areas, variability in physical characteristics such as parent geology and land use, there is little observation-based literature since Pilgrim (1982) that describes the catchment scale and runoff relationship. However various works such as Kjeldson and Jones (2010), and Kjeldson, *et al.*, (2014) which use statistical estimation methods based on catchment descriptors to draw some conclusions on the impact of catchment area in flood extent estimation within the United Kingdom.

2.1.5 *Summary of Climatic Inputs and Catchment Descriptors*

Extensive literature, some of which is cited in Section 2.1.1, examines changing climate over the past 2 decades in relation to increased water hazard flooding. Flooding hazard is thought to be increased by anthropogenic activities on a national and global scale. In Scotland, the impacts of climate change are predicted to continue to increase the intensity and duration of precipitation events (Burt and Holden, 2010), and by 2050, winters are expected to be 8% wetter (McPherson, 2022). Catchment descriptors, as mentioned above, are a means of representing the characteristics of a catchment numerically for uses such as mathematical modelling. These descriptors are used widely in flood risk estimation, notably FEH methods, especially in ungauged catchments.

Catchment descriptors have significant impacts on runoff generating processes. In the following sections soil properties of upland catchments are discussed. The properties of the soil have a significant impact on runoff generation saturation and overland flow. Saturation flow occurs in areas where the soil becomes saturated quickly due to low storage capability (Dunne and Dietrich, 1990). Hortonian overland flow occurs in situations where the volume of water entering a soil system is greater than the volume which can be absorbed or transported (Horton, 1937).

2.2 Peatland Hydrology

2.2.1 Introduction to Peatland Hydrology

Peatlands are systems which have developed autochthonously from wetlands in low energy situations (Williams, 1990). The term peatland relates to the peat soil and vegetated land assemblage which has a wetted habitat surface leading to anaerobic conditions which are essential for peat formation (Cris, *et al.*, 2014). The perennial saturation of these wetlands leads to the creation of surface water dependant ecosystems consisting of hydrophytes (plants which require saturated conditions), which grow predominantly on blanket bog systems. Peatlands can be subdivided into different types (mesotopes) based on their hydrological input; the first type is an ombrogenous bog system receives water principally through precipitation, and secondly, fens, these systems receive telluric water from surrounding mineral fed groundwater (Ingram; 1978; Price, *et al.*, 2016). These mesotopes, although defined by hydrological input, are topographically identified in general circumstances because the telluric fens are usually at a lower elevation than the bogs because the water they receive moves downhill under gravity. In addition to having a dipped morphology when compared to ombrogenous domes. Peatlands cover roughly 20% of Scotland (NatureScot 2015), making them important considerations for hydrology, carbon sequestration and ecosystem services. There is approximately 12.5 km² of fen within this 20% and 10947.3 km² of bog Lindsay and Immirzi (1996).

The peat soil is comprised of two layers, the acrotelm which is superimposed over the catotelm (Charman, 2009). The boundary between these layers is approximately defined by the depth of the water table. However spatial and temporal changes to the boundary between these differing functional layers can occur due seasonal and spatial variations in the water table depth (Craft, 2016). The two layers have distinctly different characteristics and hydraulic properties, the catotelm is considered to have a low hydraulic conductivity due to compaction leading to low water permeability, however it is waterlogged presenting a low liquid limit (Flores, 2014). The catotelm is anaerobic with an abundance of anaerobic micro-organisms, this compact, waterlogged, and anaerobic sublayer is superimposed by the actrotelm. The acrotelm is aerobic with a high hydraulic conductivity, this layer is relatively shallow (c. 10-15 cm, (Robinson, 2006)) relative to the sometimes several-meter deep catotelm. The base of the actrotelm is at the lowest depth of the water table (Figure 2.2.1). The actrotelm contains living and dead components of sphagnum mosses and other shrub vegetation. The layering system within

the vertical soil column is important hydrologically because they impact the water fluxes within the peatland catchment, for example, storage and runoff processes. The actrotelm is thought to saturate rapidly due to a high hydraulic conductivity compared to the low hydraulic conductivity of the underlying catotelm and so questions arise as to the runoff response of peatland catchments given the widely recognised notion of peat soaking up water rather than shedding it. It is especially important to quantify the runoff response of peatland systems to create a baseline to identify key relationships between land use and runoff response (Lindsay, *et al.*, (1998) in a period of focussed conservation.

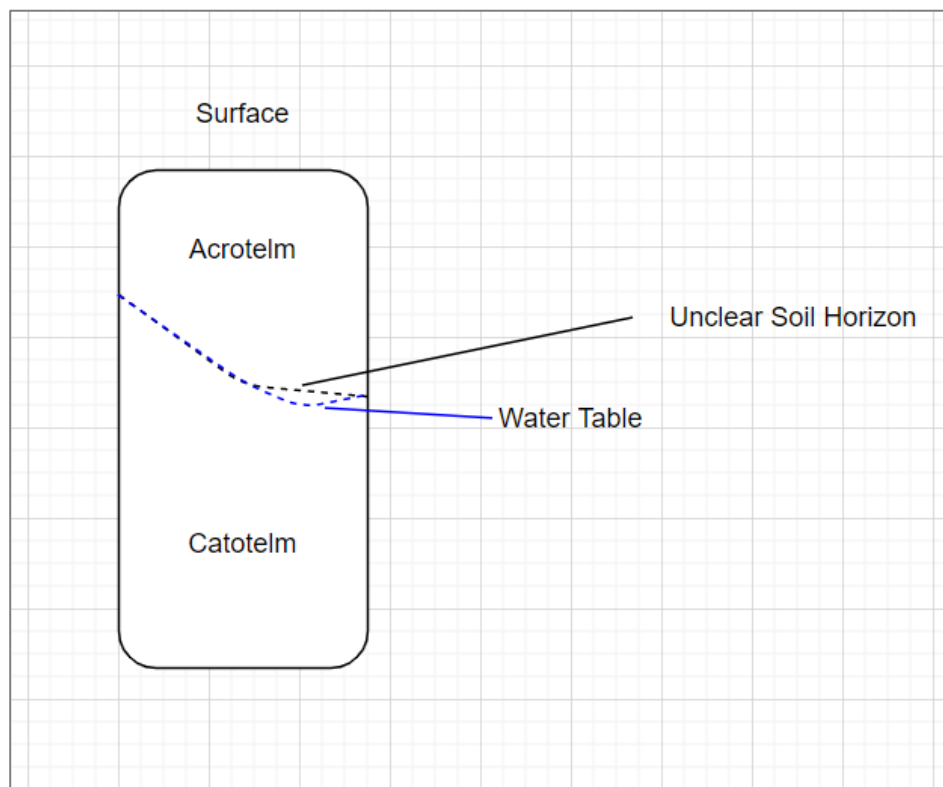


Figure 2.2.1. *Idealised Soil Column Example of Acrotelm and Catotelm.*

2.2.2 Peatland Water Fluxes

Ombrogenous systems are rain fed, meaning that precipitation is the principal input mechanism for peat bogs (Damman, 1986), whereas fens receive water from telluric groundwater sources and water shed from mire (Figure 2.2.1).

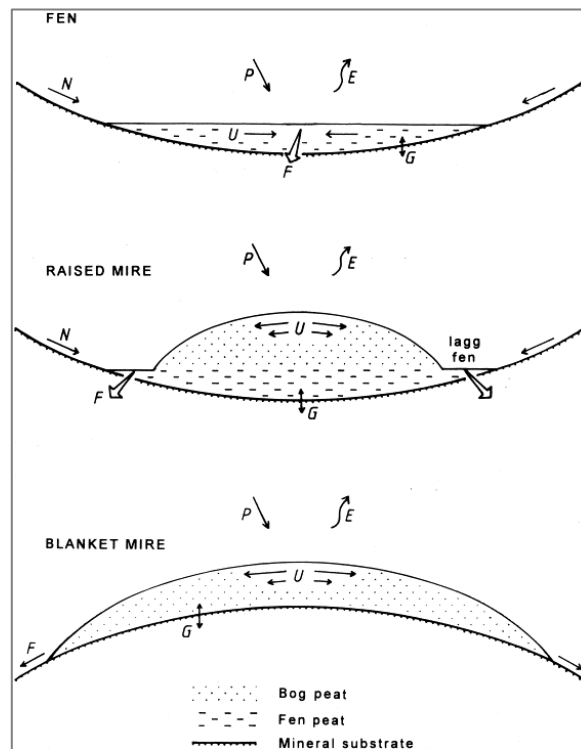


Figure 2.2.2. *Morphology of Types of Peatland.* Source: Bragg (2002).

P- Precipitation, *N*- Surface water supply, *U*- Lateral seepage in peat, *G*- exchange with deep ground water, and *E*- Evapotranspiration

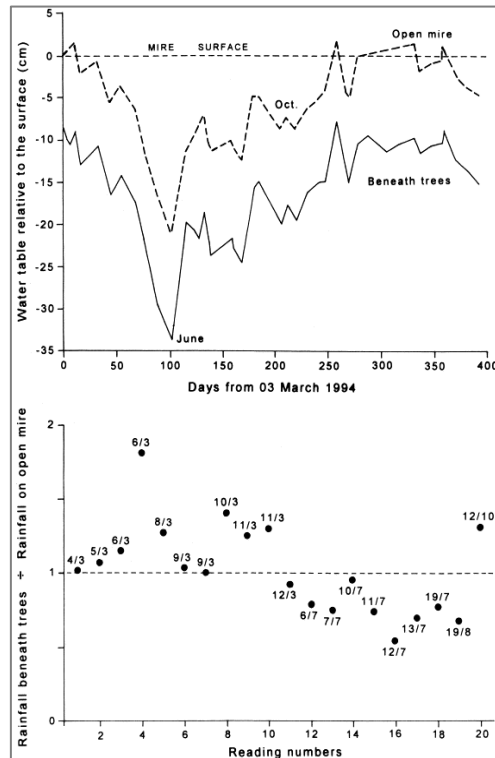


Figure 2.2.3 Upper: Water Table Heights in Time Series; Lower: Comparison Between Rainfall on Open Mire and Beneath Canopy of Mature Birch. Source: Bragg (2002)

The upper figure, utilising data collected in Kelemen and Ingram (1999) shows that in the period between 03/03/1994 and 02/04/1995, the water table was significantly deeper from the surface of the mire when under canopy when compared to the open mire.

The lower figure shows data from a study which was structured to collect precipitation through the canopy process of stem flow and throughfall. The results postulate that the crown of the tree (leafy canopy) attenuate precipitation from reaching the ground in the summer, however, serves to increase water reaching the ground in spring and autumn due to interception of ‘occult moisture’ in misty weather.

It can be seen from Figure 2.2.3 that in addition to the surface input from precipitation, surface output in the form of evapotranspiration should be considered. Ingram (1983) indicates that evapotranspiration from a peat bog is approximately equal to the potential evapotranspiration ($E/E_t = 1.1$), whereas from a fen, it is thought to be $E/E_t=1.4$. These differences are expected considering a perennially low water table.

Evapotranspiration is interconnected with vegetation, and catchment storage potential. Blanket bogs are generally accepted to be treeless (Robinson and Newson, 1986), so emphasis has previously been placed on using forest to attenuate storm runoff in up the hills. Data from pre-2000 shows that afforestation to slow runoff may be effective, these data can be seen in Figure 2.2.3.

The study from Plynimon (Robinson and Newson, 1986) showed that 68% of the precipitation reached the ground through the canopy processes of throughfall and stem

flow, although how long this took has not been documented. The other 32% evaporated from the canopy. The results show that tree cover is effective at preventing some precipitation from reaching the ground and potentially slows the remainder through canopy processes, however attention should be paid to the upper figure in Figure 2.2.3, which shows tree plantations having the effect of lowering the water table. Recent associations of deeper water tables and a decrease in a bog's ability to regulate water flows (ICUN, 2020) has led to reformation of United Kingdom forestry policy so that trees can no longer be established on peat more than 50 cm deep (RSPB, 2021). Instead, the bog's own hydrological storage and surface characteristics to regulate runoff must be utilised and maintained.

Peatland storage is variable, dependant on the mesotope. A fen is usually concave in form and is an area which other peat systems drain to as they lie at beneath ombrogenous systems. Fens can drain and receive water from the surrounding groundwater systems (Gilvear and Wilson (1995)). Ombrogenous systems, however, generally have a domed structure (Figure 2.2.2) with no telluric exchange in groundwater. A bog is perennially saturated due to net precipitation (Ingram 1978; Bragg, 2002). Perennial saturation of the catotelm layer leads to reduced storage capability within a peatland system and has implications for runoff generating processes. Additionally, storage in a superficial acrotelm (~0.1 m thick (Ingram and Bragg, 1984)), is extremely limited as the water table is confined to this layer. The low storage capability of peat soils challenges a long-standing notion that a peat bog acts like a sponge. A peat bog is a hydrologically 'flashy' system (Shuttleworth, *et al.*, 2019), shedding runoff overland instead of absorbing it. In Section 2.1.5, overland means of runoff conveyance are explained.

Peat soils have often been linked to extreme flows generated from rapid storm runoff (Wade, *et al.*, (1999)). The significance of the role of peat soils within storm generated flows is affirmed by Jarvie, *et al.*, (2001) and Soulsby, *et al.*, (2002) through empirical hydrograph analysis. A peat soil hydrograph may be categorised by a small perennial baseflow with steep rising limbs to the storm peaks. The hydrograph may also be influenced if a winter flood occurs after a dry period due to inadequate storage for attenuating winter floods. An example of this is in a study by Conway and Miller (1960) where observations of a low perennial baseflow revealed a short lag time to peak discharge. Additionally, literature which assesses the runoff regime of peatland catchments in Robertson, *et al.*, (1968) has facilitated a readjustment of the common

notion that a bog acts like a sponge attenuating runoff by absorbing and storing it. The literature which supports Robertson, *et al.*, (1968) is old yet is still accepted.

A study of the Dun Moss, Scotland, by Bragg (2002) showed that it is possible to quantify the response of mire versus other catchment soils (Figure 2.2.4), such as lithsoils, or other mineral material through gauging a series of streams which originate from various runoff origins (Smith, *et al.*, 1995). For example, a stream originating from peat and one from mineral material. Chemical separation techniques were considered for this, however, were deemed unreliable (Smith, *et al.*, 1999; Keleman and Ingram, 1999). A step further may be to calculate lag times within these streams with precipitation and stage-flow time series data to compare the response of different catchment soils. It is important to remember scale. The catchment of interest in Bragg (2002) is of very small spatial scale which is connected to temporal hydrometric values such as lag time and return time. It can therefore be utilised as a guide of how these catchments may behave, however cannot be considered fully representative of catchments at a larger spatial scale.

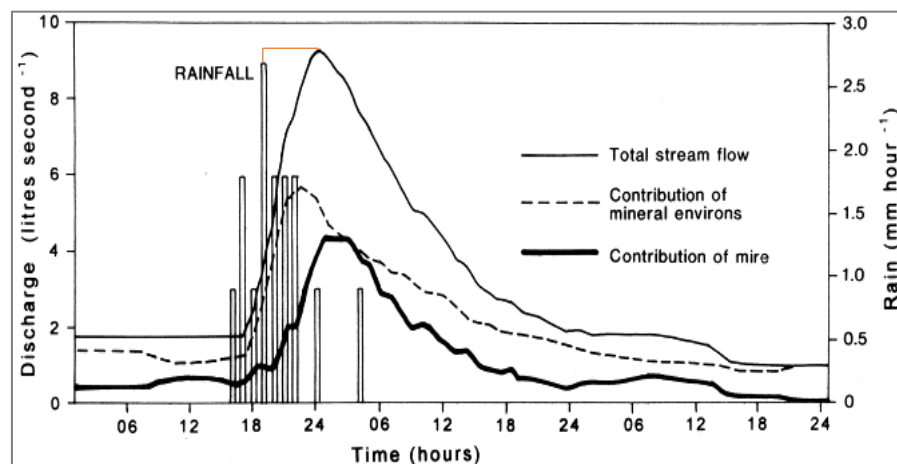


Figure 2.2.4. *Dun Moss Hourly Rainfall and Discharge Data.* Source: Bragg (2002).

Note, the discharge peak from the mire and the mineral has a difference of approximately 4 hours whereby the mire discharge is 4 hours later than the mineral, suggesting that mineral soils will peak first.

Bogs and fen peatlands differ hydrologically as bog systems are rain-fed whereas fens have the influence of groundwater exchange. It is apparent that evapotranspiration and overland runoff, due to poor storage leading to rapid saturation, are main mechanisms in which the catchment conveys water (Low, 2020). Additionally, storage within the compacted catotelm is minimal and merely contributes to the little disputed perennial baseflow in ombrotrophic systems whereas the thin acrotelm layer may contribute significantly to the shape of a storm hydrograph from a peat catchment through Hortonian





overland flow which will cause steep rising limbs on the storm hydrograph. Little is known about infiltration processes in peatland systems (Holden and Burt, 2002). It is thought that infiltration rates in blanket peat are controlled by sub-surface percolation rates resulting in the saturation of near surface layers. The low infiltration rates proposed by Holden and Burt (2002) have not been challenged in the decade since the literature was published and knowledge of infiltration within blanket peat systems remain limited.

2.2.3 Surface Roughness in Peatland Catchments

The uplands of Scotland are home to many species of vegetation which all have a significant ecological function to support the ecosystem in these remote regions. Table 3.2.1 contains some of the most found species in Scottish blanket peat environments. Many of these species are categorised as Alpine, Sub-Alpine or Arctic-Alpine (Averis, *et al.*, 2004) and are of international importance, existing in a narrow altitudinal band of >750 mAOD (Nagy, *et al.*, 2003). Surface vegetation is an important factor in the hydrological response of any catchment; however, it is especially important in upland peat and mineral catchments which have flashy hydrological regimes (Holden and Burt, 2002).

Significantly low storage and infiltration potential discussed in Section 2.2.2 emphasises the importance of surface cover in the runoff generation of these upland, headwater catchments particularly due to surface roughness. These upland species are subject to a series of pressures including land management practice and climate change (Trivedi, *et al.*, 2008) and are the focus of conservation efforts (NatureScot, 2022) to restore and conserve ecological potential. However, it is well documented in literature (for example, Shuttleworth, *et al.*, 2019) that alterations to surface vegetation will alter the overland runoff response of a catchment due to changes in surface friction.

Table 3.2.1. Common Montane Plant Species. Sources: Walker (2016), Arctic Atlas (2022), GBIF (2022), Biodiveristy Ireland (2022)

Species Name	Species Photograph
Cloudberry (<i>Hermaphroditum</i>)	
Sphagnum Moss (<i>Sphagnum Fuscum</i>)	
Grass Heath (<i>Nardus Stricta-Carex</i>)	
Woolly Fringe Moss (<i>Racomitrium lanuginosum</i>)	

As of 1983, just under 25% of mire in Scotland was protected under SSSI status (Stewart and Lance, 1983), identifying that a large proportion of Scottish moorland was open to exploitation through land management practices such as pastoral grazing by sheep. In 2015, NatureScot described the state of peat environments in Scotland as ‘unfavourable-declining’ under Article 17 of the Habitats Directive (NatureScot, 2015). To increase the agricultural yield, the carrying capacity for grazing animals must be increased through the creation of favourable conditions for heathland which subsequently are unfavourable for the peat.

It is important to understand the current grazing pressures on moorland because of the impact that grazing has on the quality and abundance of vegetation on the moorland. Areas where surface cover is reduced through grazing can lead to areas of once vegetated acrotelm being exposed and left open to erosion (Bragg, 2002) further leading to enhanced erosion through atmospheric processes and biochemical oxidation. An example of this is described in IUCN (2014) where animal footprints on bare peat become focal points for erosion due to breakage of the compacted surface exposing material to freezing and then being carried away by the wind.

Overgrazing can be applied to wild deer, such as the red deer found in the hills of Scotland. It is important to consider surface vegetation trampling from a hydrological perspective due to the potential decrease in surface friction associated with the degradation of surface vegetation and water runoff. Quinton and Hayashi (2005) emphasise the importance in surface vegetation in the attenuation of storm runoff.

Friction between surface water and vegetation is important in a peatland catchment due to the shallow acrotelm and perennially saturated catotelm giving rise to a small storage capacity; meaning that vegetation has a profound impact on a peatland catchment's hydrological response forming eco-hydrological feedback. The term eco-hydrological feedback was introduced by Price, *et al.*, (2016) where a correlated relationship between overgrazing and a flashy runoff regime are explained. Holden, *et al.*, (2008) reinforces this notion whereby surface roughness has a major role in attenuating runoff and reducing the lag time between peak rainfall and peak river flow. Furthermore, the data presented by Holden, *et al.*, (2008) presents findings of the greatest overland flow velocities occurring in areas of bare peat as well as finding that differences in the roughness of different vegetation can cause spatially complex variations in overland flow velocities. It can be reasonably stated therefore, that a high biodiversity and density of plants is desirable (Price and Whitehead, 2001); for example, Sphagnum moss is the roughest, followed by peatland mosses and grasses, heather and then bare peat although these claims were not supported with associated roughness values, and it is doubtful that they exist at this time. It is fundamentally important to understand the properties of overland flow due to it being a rapid means of runoff conveyance (Dunne and Dietrich, 1990). The main types of overland flow are explained in Section 2.1.5 where saturation excess overland flow occurs in areas where the soil becomes saturated quickly due to low storage capability. Hortonian overland flow, however, occurs in situations where the volume of water entering a soil system is greater than the volume which can be absorbed

or transported (Horton, 1937). It is noted in Holden and Burt (2002) that saturation excess overland flow is the most prevalent mechanism of overland runoff in blanket peat systems, although Hortonian overland flow does occur in areas of mineral soil which is linked to the peat landscape.

Strategic management of peatland environments requires informed decision making based on a catchment wide understanding between the connectivity of runoff delivery and precipitation (Lane, *et al.*, 2007). The literature supports this with up to 80% of runoff being thought to come from saturation overland flow in temperate blanket peat environments (Holden and Burt, 2003a; Holden and Burt, 2003b; Holden, 2006). The catchment response of a blanket peat catchment can be subdivided into two parts: the first being a more rapid and greater overland flow and secondly, a slower, yet significant, lateral seepage through the uppermost of the acrotelm and spilling through into overland flow. The data in Holden, *et al.*, (2008) may be regarded as a firm indicator of the effectiveness of Sphagnum moss in attenuating overland runoff through the high friction generated between the moss and the water. In a comparative test, a significance of $P=0.001$ exemplified the effectiveness of moss in attenuating overland runoff versus bare peat. Another important factor identified was runoff depth, however, slope was only considered a significant control overland velocity in areas of Sphagnum cover and was not in bare peat or grass areas. A noted decrease in lag time in bare peat areas is observed in Holden, *et al.*, (2007) due to poor management giving rise to a decrease in vegetated cover, it is also essential to note that vegetation, such as grass or heather still alter overland runoff velocity although they are associated with lower friction, however not as significantly as bare peat. Finally, a one cm critical depth in overland runoff was observed in Holden, *et al.*, (2007) and supported in Grayson, *et al.*, (2010) where the non-linear runoff response leads to dramatic increases in overland flow velocities after this critical threshold has been surpassed giving rise to increased potential erosion potential.

2.2.4 Lag Time in Peatland Catchments

Lag time to peak discharge is simply the time between the peak of the hyetograph and the peak of the stream hydrograph (Black, *et al.*, 2022). Lag time is useful for hydrological analysis as observed lag time is not constrained by assumptions which are required for modelling, such as input parameters. A storm hydrograph can be broken down into three major parts, the rising limb, the peak, and the falling limb. Figure 2.4.4 shows the peak of a hydrograph with a histogram of peak rainfall superimposed over it. The orange line in the figure is a visual representation of the concept of lag time. The hydrographs in Section 5.4 also show the peak rainfall and the peak streamflow in graphical form.

Although useful, the caveat is that stream response during the largest flow events have some uncertainty due to a decrease in gauging capability. Lag time within a catchment is a combination of several factors such as input, physical characteristics of the soil and land cover as well as land use (McCuen, 2005; Black, *et al.*, 2022). Observations in Synder (1938) show that lag time analysis has existed for many decades, presenting a case for its robustness as an extension to graphical hydrograph analysis (Fang, *et al.*, 2005). There are many ways to carry out lag time analysis, one way to analyse lag time is through locating the centroid of the hyetograph and then finding the peak discharge in the corresponding hydrograph as shown in Gericke and Smithers (2014) and Shuttleworth, *et al.*, (2019).

Black, *et al.*, (2022), using protocols set out in Shuttleworth, *et al.*, (2019) and Deasy, *et al.*, (2014) use a set of event characterisation rules, which must be established to ensure that each event in a series is separate (Hale and McDonnell, 2016). Another consideration for calculating lag time is the utilisation of an acceptable average. Black, *et al.*, (2022) used the median lag time as this seemed insensitive to outlier data.

Finally, a potentially significant drawback to this method is the uncertainty within the instrumentation used to collect and store the continuous time series data of streamflow and rainfall. Uncertainty can be reduced drastically by regular maintenance and uncertainties lie within the precision of the of storm depth and river stage, not the timing of the greatest recorded values. Observed data used in lag time analysis undergoes rigorous security before its use, compared against the performance of loggers and rainfall data, for example water balance checks, to ensure that the data is reliable, keeping assumptions about the data's validity to a minimum.

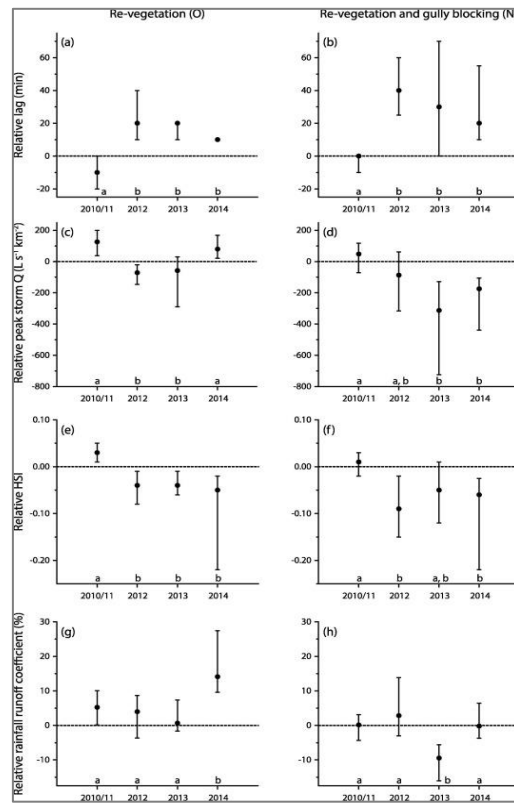


Figure 2.2.5. Relative Difference Between Treatment and Control Sites for Key Hydrograph Metrics. Source: Shuttleworth, *et al.*, (2019).

Findings for metrics; lag time (a and b), peak discharge (c and d), hydrograph shape index (e and f). Positive values indicate greater metrics at the control whereas negative values are the opposite.

2.2.5 Restorative Management on Peatland Catchments

Management of peatlands to restore damaged vegetation has given rise to studies such as that in Shuttleworth, *et al.*, (2019) whereby analysis of revegetation has yielded positive results (Figure 2.2.5). Within the study, a 106% increase in lag time was presented relative to the control along with a 27% decrease in peak flows. Typically, poorly managed peatland systems are considered flashy with a high conveyance of runoff into the river leading to high peak flows (Holden and Burt, 2003a). This is especially true in bare peat systems where overland saturation excess runoff is generated at high velocity due to a decrease in surface roughness. The Revegetation is an attempt to increase surface roughness and attenuate runoff velocities by reducing the area of hydrophobic bare peat and increasing sphagnum cover (Eggleston, *et al.*, 1993; Evans, *et al.*, 2005). No change in runoff coefficient was observed, implying that there was no change in slope storage, however hydrograph form showed wider shapes with lower peaks. Additionally, gully blocking in addition to revegetation further attenuated overland velocities, subduing the hydrograph form without any change in runoff coefficient again. No change in runoff

coefficient is useful to know as it provides evidence that runoff is attenuated by large spatial change in surface roughness and not storage, which is limited in mire environments. Pan and Shangguan (2006) reinforce this, yet it should also be considered that these data come from a single catchment study where gully blockage design may not be optimal for enhancing mire storage capacity (Milledge, *et al.*, 2015).

It is difficult to carry out a desk-based analysis of catchment response to restorative management as there is so little literature spanning an adequate temporal scale with the only current examples of comparative peatland hydrograph analysis coming from Tibet in Zhang, *et al.*, (2012) and Zhang, *et al.*, (2016). Shuttleworth, *et al.*, (2019) presents the first catchment scale evidence for hydraulic roughness as the principal descriptor-based control for peatland runoff driving the precipitation-runoff response. The findings are consistent with previous literature such as Holden, *et al.*, (2008) and Grayson, *et al.*, (2010). These additional sources facilitate assumptions that surface roughness attenuating lag time will only improve temporally as vegetation becomes more established. Revegetation as a means of NFM is due to the temporal improvement in effectiveness giving this method longevity over storage-based methods. Sphagnum is a peatland keystone species (Rochefort, 2000) due to its role in maintaining a shallow water table (Gorham and Rochefort, 2003). Strategic placement of revegetated areas may slow time to peak discharge to ~10% of the rate observed in bare peat areas. (Holden, *et al.*, 2008; Gao, *et al.*, 2016). The overall ability for revegetation to attenuate flood discharge is dependent on sub-catchment hydrograph synchronisation also, which contribute to the overall catchment hydrograph (Pattison, *et al.*, 2014) as explained in Metcalfe, *et al.*, (2018). Hydrograph synchrony is extremely important as synergy between catchments may lead to the combination of flows leading to a greater flood peak as exemplified by the Allen Water scheme in Nut and Perfect (2011). Here, sub catchment flows combined and increased the flood risk instead of reducing it.

2.3 Summary of Peatland Hydrology

Overall, there are a combination of factors which influence a peatland catchments response to precipitation. A distinction must be made between the type of peatland being observed in terms of ombrotrophic rain fed bogs and fens which can receive water through subterranean hydraulic processes and runoff from mires (Evans, *et al.*, 1999). Rain-fed mire with its perennially saturated catotelm (Gilman, 1994) and low hydraulic conductivity leads to low storage potential and thus a greater incidence of overland saturation flow as its principle means of catchment efflux (Ingram, 1989). Due to this, surface character of the mire in terms of vegetation cover is extremely important. Overgrazing, draining and general poor management may lead to surface vegetation being stripped and bare peat exposed. Bare peat and reductions in the spatial coverage of surface mosses is catastrophic hydrologically due to the decrease in surface friction between overland saturation flow and the vegetation (Roulet, *et al.*, 1992) leading to greater overland flow velocities and ultimately significantly decreased hydrological lag times and increased peak discharge.

Observed changes in lag time from multiple sources indicate that revegetating bare peat areas with Sphagnum mosses will attenuate overland runoff and in turn greatly impacting the efficiency of the catchment. The combination of restorative management techniques may greatly reduce overland flow velocities which reduce the peak discharge and create a wider, less impulsively shaped hydrograph form whilst producing no change to runoff coefficient. The caveat to this, is that there is a risk for hydrograph synchrony which may lead to tributaries peaking at the same time, leading to greater peak discharge where these tributaries combine.

2.4 Mineral Catchment Hydrology.

2.4.1 Introduction to Rocky Mineral Catchments

Existing literature regarding rocky mineral catchments has gaps, especially with regards to overall runoff response (Vasquez and Feyan, 2010) largely due to inadequate time series data. Hydrographs from a steep, headwater catchment in Italy demonstrate the potential for mineral catchments to have impulsively shaped hydrographs with steep rising limbs and short-lived peaks (Gregoretti, *et al.*, 2016). These hydrographs are initially attributed to low storage mineral soils and high incidence of bedrock exposure Jordan (1994). It is likely that these catchments can be defined as those with a high incidence of thin mineral soil and or exposed bedrock sections, although literature which defines rocky mineral catchments has not been found.

The runoff response of a catchment is a combination of many hydrological descriptors within the catchment. One of these descriptors is the antecedent soil conditions, which vary seasonally (Ledingham *et al.*, 2019). Pre-event saturation leading to extreme levels of overland runoff is cited numerous in literature (Hewlett and Hibbert, 1967; Dunn, 1978), however in the case of upland rock and mineral catchments in the Central Grampian Highlands, it is likely that these less permeable landscapes are less sensitive to antecedent moisture (Jordan, 1994) due to thin soil storage and some incidence of bedrock exposure, however, still produce rapidly formed high magnitude flood events. In terms of bedrock exposure, in some catchments this is extremely prevalent. In most upland catchments in the Cairngorms, however, bedrock more likely to be covered by a thin, superficial mineral soil layer.

2.4.2 Local Contextual History and Runoff Generation

There is a wide range of literature which explains the geological history of the Central Grampian Highlands (CGH), for example Lukas, *et al.*, (2004) where explanations of the geology of the Gaick and wider CGH can be found. The Feshie catchment (~235 km²) has an altitudinal range of 230-1262 m AOD (Soulsby, *et al.*, 2006) with the hills of the CGH rising steeply on either side.

Today, the CGH consist of many low-relief plateaus which show only minor signs of glacial modification (Phillips, *et al.*, 2006) formed from the Cairngorm paleo-surface (Ringrose and Migon, 1997; Ebert, 2009). Paleo-surfaces are relic landscapes of the pre-Quaternary which have been weathered for tens of thousands of years (Hall, 2008).

Erosion of mineral rich rocks have led to thin mineral subalpine soil which may not be easily recolonised by vegetation due to high winds and extreme seasonal weather high on the Mòine Mhór (Bragg, *et al.*, 2016).

Mountain hydrology is one of the most complex hydrological systems to monitor due to the remoteness of the landscapes. It is highly variable in space and time (Becker, 2005), and must be approached on a case-by-case basis. Hydrological response to rainfall in the mountains has undergone tremendous change within recent decades, driven by land use and climate change (De Jong, 2015). The intensification of the global hydrological cycle (Provenzale and Palazzi, 2014) created by a stepwise change in global climate warming has led to changes in precipitation patterns, for example the decreasing ratio between snow and rainfall (Serquet, *et al.*, 2011; Beniston, 2012).

The combination of these factors determines the water balance of landscape units, including moisture, evapotranspiration, and runoff generation. During an assessment of runoff generation in subalpine catchments, not only is the volume of water important but so is the relative contributions from surface and subsurface runoff. These contributions may differ considerably spatially (Buttle, 1998). Uhlenbrook and Leibundgut (1997) present an overview of runoff mechanisms in different mountainous environments. In addition, Bonnell (1998) explores the environmental factors impacting mountainous runoff. These sources both support the importance placed on the incidence of bedrock. Fissures within the bedrock sections allow for an initial abstraction of rainwater, however if rainfall continues after the hyetograph peak, overland runoff due to the low hydraulic conductivity of bedrock leads to the propagation of a large flood wave. The wave occurs through exploitation of bedrock channels leading to the rapid conveyance of rainwater in the main river channel (Boorman, *et al.*, 1995; Degetto, *et al.*, 2015). The flood wave grows rapidly as it travels downstream and contributes to an extremely steep rising limb with a short-lived peak discharge.

Hawkins, *et al.*, (2009) illustrates the minimal surface friction associated with these areas due to subalpine soils surrounding bedrock areas in mountainous catchments. Due to the lack of adequate vegetation to facilitate high friction and thus runoff attenuation, these thin soils become inundated rapidly because of low storage capacities making overland flow the principal runoff mechanism. An example is Hortonian saturation excess flow, due to the thinness of mineral and alpine soils is the runoff mechanism most associated with rocky mountain catchments (Horton, 1937; Lange, *et al.*, 2003). Hortonian overland flow is when precipitation rate exceeds the lands hydraulic

conductivity whereas Dunne overland flow occurs when the hydraulic conductivity of the soil is high, but the water table is low (Dunne, 1978; Yang, *et al.*, 2009). Additionally, Milly (1994) supports this as low vegetation cover in these upland catchments leads to low incidence of evapotranspiration, increasing confidence in the assertion that that runoff through overland flow is the main process by which a mountain catchment conveys runoff.

Given that mountains cover around 24% of Earth's surface and occupy 32% of global total runoff (Marston and Marston, 2017), it is obvious that they occur in many different environments with many different climatic influences in their hydrological regime. It is highlighted in Wohl (2010) that differing mountain environments generate profoundly different runoff regimes. Semi-arid mountains such as those found in Europe and the United Kingdom can experience ephemeral flows from rainfall or perennial flows where snowmelt augments the runoff. In other mountain ranges, such as those in Antarctica, seasonal ephemeral flows dominate and conversely mountains with warm humid climates are dominated by perennial flows with large discharge storm events. Generally, the Grampian uplands fit into the semi-arid category as the rivers which run in the valleys have a perennial baseflow with top ups from snow melt and rainfall events. The type of environment which the mountains are in determines the vegetation which would be found there. Marston (2010) outlines the important ways in which vegetation impacts mountain hydrology; 1) vegetation modifies soil moisture through interception processes, 2) organic matter in the soil can increase storage of the soil, 3) roots bind soil against piping mechanisms and soil erosion, and 4) vegetation increases surface roughness attenuating overland flow rates.

2.4.3 *Summary of Mineral Catchment Hydrology*

This section presents a general understanding of the hydrology of mountainous catchments, however literature relating to rocky mineral catchments are thwart with gaps in knowledge due to the remoteness of the study areas. There is great difficulty in achieving meaningful time series datasets relating to streamflow in these areas. Literature that does exist is highly specific to the study catchment, making a desk-based analysis extremely difficult in terms of creating an area specific overview. Hydrographs from mountainous catchments usually have a rapid rise along with a short-lived peak, which is expected from upland headwater catchments in Scotland under current land use. These hydrographs have been attributed to thin, well-draining soils and high incidence of bedrock combined with steep compact slopes.

2.5 Hydrometric Rating Equations

2.5.1 Introduction to Stage-Discharge Rating Curves.

A stage-discharge rating curve (Figure 2.5.1) is the graphical expression of the equation which describes the relationship between stage (h) and discharge (Q) for a certain point in a stream (Herschy, 1999), usually at a gauging station. At this point, manual gaugings of river Q are taken and can be plotted on a graph (x) against h (y) to represent their relationship. Stage measurements are taken using air pressure to calculate water depth at a gauging station as continuous time series data. These h - Q measurements calibrate the rating curve. An empirical rating curve is not always a fixed measure but can change over time due to changing hydraulic controls such as stream bed and bank deposition or erosion leading to a change in channel geometry. A permanent control helps assist the development of a rating curve which is resistant to temporal change. An example of a permanent control is a bedrock weir at the top of a step-pool channel. If the stream is gauged in a highly mobile area, this would be known as a shifting control. The equation used to derive the h - Q relationship varies in form, for example $Q = a(h+b)^c$ where h is stage, a is the multiplier, b is datum correction and c is the shape parameter (CEH, 2022)

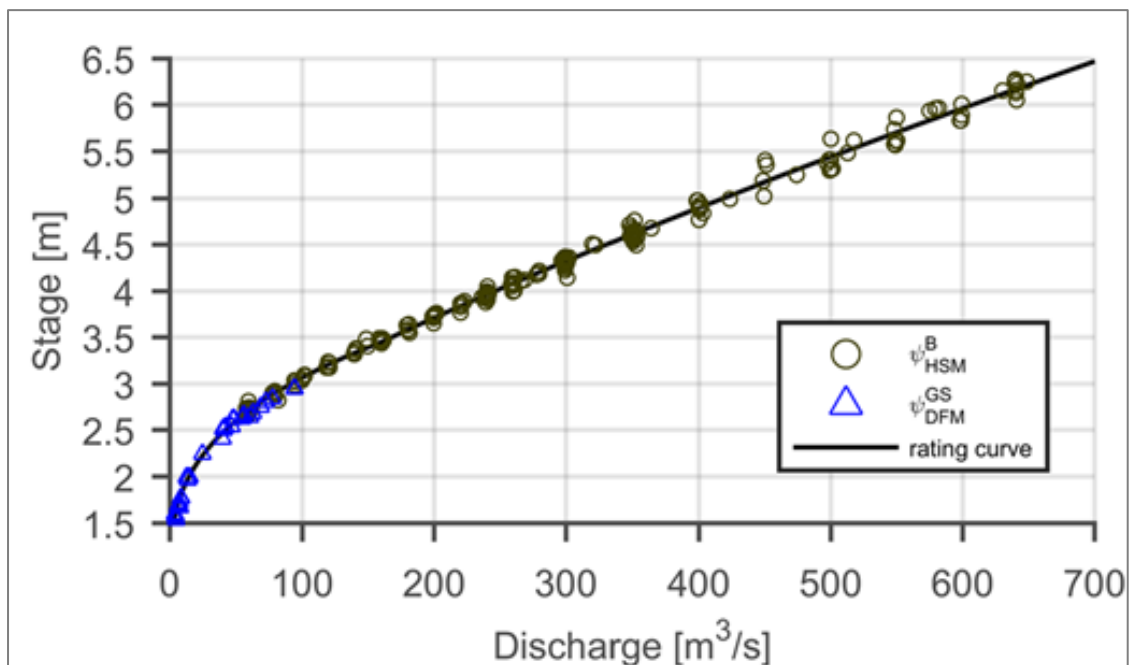


Figure 2.5.1. Hydrological Rating Curve Example. Source: Pederson, *et al.*, (2019)

2.5.2 Empirical Rating Curves

Reliable streamflow time series data is essential for hydrometric analysis, however, to achieve this can be costly and come at great physical effort to maintain (Harmel, *et al.*, 2006). Environmental managers must be able to rely on the relationship between h - Q to make strategic decisions which may impact socio-economic trajectories locally and regionally (McMillan, *et al.*, 2018; Mansanarez, *et al.*, 2019). It is extremely important to have confidence within the rating equation generated from empirical time series data due to the high risks associated with incorrect scientific conclusions (Westerberg, *et al.*, 2016; Wilby, *et al.*, 2017), this is represented in McMillan, *et al.*, (2017) by exploiting the example of hydropower industries in Norway.

Hydrometric monitoring in terms of Q is extremely difficult to manually measure for scientifically significant periods of time, thus justifying the role of the empirical h - Q rating curve (Rantz, 1982; Herschy 1993). These rating curves can be adjusted by the addition of manual gauging across a range of flows (Schmidt, 2002). However, intrinsic assumptions within the mathematical extrapolation of these curves out with gauged flows, create uncertainties within the rating curve leading to decreased confidence at the highest and lowest flows (McMillan, *et al.*, 2012; Kiang, *et al.*, 2018). As such, uncertainties within hydrological rating curves have been studied extensively, for example in Coxon, *et al.*, (2015) and Le Coz, *et al.*, (2014) giving rise to extensive research on comparisons and compensations to these uncertainties.

One of the greatest criticisms within empirical data collection through manual gauging is the physical effort required to create a rating curve which is considered acceptable. Birgand, *et al.*, (2013) proposes a minimum of 22 manual gauging per year giving rise to a series of concerns such as cost of operator payment, risk to operator due to high flows, and the reliability of the data due to flashy catchments with short lived peak flows not allowing time for the operator to travel to the gauging site as shown in Westerberg, *et al.*, 2016). Additionally, WMO (2010a, 2010b) states that the risk to the operator due to high energy flood events occurring during the night poses an unacceptable risk to life, thus acceptable means to extrapolate the curve must be achieved differently.

It is expected that climate change will increase the incidence of and peak discharge of flood events facilitating more regular mobilisation of channel bed substrate, regularly altering channel morphology, thus shifting the hydraulic controls (Milly, *et al.*, 2005; Tomkins, 2014; Hirsch and Archfield, 2015). The expected rate of change within riverbed

geometry has implications for the reliability of empirical rating curves due to the rapid demand for reliable data from expanding industries (Monanari, *et al.*, 2013; Ceola, *et al.*, 2016). These sources reinforce the concern of temporal changes to empirical rating curves however gauging station placement in resilient areas of the stream, such as bedrock zones may reduce the temporal variability of the rating curve yet may have implications for the quality of h data being recorded through a boiling effect of white water in narrow V shaped bedrock reaches. This notion gives rise to a ‘trade-off’ between reducing the need to account for a shifting control, yet boiling flows may produce a jagged h hydrograph.

2.5.3 Computer Modelled Rating Curves

The contemporary alternative to empirical rating curves is the computation of a flow model. Modelling has been said to undeniably increase the accuracy of peak flow h - Q data when compared to the uncertainties of an extrapolated manual rating curve (Kean and Smith; 2005; Lang, *et al.*, 2010). Research such as that in Reistad, *et al.*, (2007) has presented reliable h - Q estimations using HEC-RAS (Hydraulic Engineering Centre River Analysis System) with accurate input parameters. Computer modelling is highly dependent on input parameter accuracy, for example input topography and Manning’s roughness values are the two more subjective and uncertain input parameters noted widely in the literature (Acrement and Schneider, 1989; Hankin and Beven, 1998; Hardy, *et al.*, 1999).

Input parameters greatly influence the accuracy of the model and have been shown to generate accurate and reliable models (Lee, *et al.*, 2017) especially in situations of unsteady flows, curve hysteresis and ephemeral streams (Bullard, *et al.*, 2007; Clayton, and Kean, 2010). Additionally, these models can be applied to ungauged locations. Lam, *et al.*, (2016) exemplifies how accurate modelled rating curves can be, especially when supported by earlier work in Lyon, *et al.*, (2015). However, all the literature stresses the importance of the input variables as the greatest source of error (Casas, *et al.*, 2006). Due to topographic data being one of the two most important input variables, it is necessary to carry out a high-resolution topographic survey to ensure that a model has the best possible chance at creating reliable outputs.

Baldassarre and Claps (2011) highlights extrapolation uncertainties within empirically generated rating curves and propose the use of HEC-RAS, as mentioned above, due to its multi-decadal track record (Dimitriadis, *et al.*, 1957). There has been a significant increase in the use of hydraulic modelling software such as HEC-RAS in terms

of the creation of 1D, 2D and 1D-2D linked hydraulic models, especially for ungauged catchments.

HEC-RAS is not raster based (Dimitriadis, *et al.*, 2016) and thus requires low computation power to produce models which are considered acceptable. HEC-RAS has a series of solver options and is resistant to uncertainties based on surface profile oscillations (Wara, *et al.*, 2019) as tested against ADCP gaugings. The curves generated by HEC-RAS models, converse to manually gauged curves, produce outputs in discharge which are then converted to stage (Crawford, 1991; Dottori, *et al.*, 2009; Timbadiya, *et al.*, 2011). The use of HEC-RAS allows for greater understanding of $h-Q$ relationships through a range of conditions including steady and unsteady conditions (Muste and Lee, 2013). In fluid dynamics, steady state simulations are where key parameters such as velocity and viscosity among others do not change with time, whereas in unsteady situations, key parameters do change with time (Pappenberger, *et al.*, 2005; Morvan, *et al.*, 2008). Additionally, Baldasaarre, *et al.*, (2009) exemplified through 5 HEC-RAS models that modelling is optimal to support empirical gauging in certain rivers where peak flows exceed wadable conditions. A final uncertainty to consider within 1D HEC-RAS models is the computation of flow as a uni-directional mean velocity spread across the channel (Brunner, 2001), which does not allow for multi-directional flow analysis in the event of flood plains. However, given its ease of access and low computational power, the 1D model which is produced can still be considered acceptable and useful for rating curve development, especially in confined upland v-shaped valleys and constrained channels where floodplain connectivity is low. A 2D modelling approach with a high-resolution DTM mesh can represent floodplain flow pathways, yet this requires a highly detailed topographic mesh and supporting fluvial walkovers to ascertain the correct roughness parameters meaning that 2D modelling would better represent the third site in this research, however the 1D approach is considered acceptable in Ramsbottom and Whitlows (2003) best practice handbook for extrapolating rating curves.

2.5.4 *The Velocity-Area Method for Rating Curve Creation ($Q = VA$)*

In most cases, flow rating curves are approximated by least square fitting. The performance of a least square fitting is limited by measurement variability across a range of flows. Mansfreda, *et al.*, (2020) presents a four-gauging station evaluation of the area multiplied by velocity method for flow rating derivation. In principle, rating uncertainty is at least partially reduced as cross-sectional geometry is multiplied against empirical velocity observations, in a section of river where there is confidence in the empirical flow

measurements within the limited range of flows. The literature draws the conclusion that this method excels in data scarce environments, for example, remote upland gauges as the applicability of the method was evaluated using variable datasets. It is worth noting that like stage-discharge curves, the $Q = VA$ assumes steady state conditions neglecting hysteresis observed in stage and discharge during high flow events (Dottori, *et al.*, 2008) which may have an impact on the regression function extrapolation to high values. Anecdotally, if two gauging stations are in proximity, streamflow data which may be impacted by unsteadiness caused by a rapid increase in stage can be corrected using water slope and stage data (Fenton and Keller, 2001). The $Q = VA$ methodology is a version of the flow-area model (Manfreda, 2018). The traditional rating equation appears as variations of $Q = a(h+b)^c$ where a , b and c are the rating parameters (Clarke, 1999). The $Q = VA$ method can be fitted using cross sectional surveys of the riverbed topography at the gauge, making it relatively simple and sensible to implement, especially in an area of permanent control.

Comparative analysis of the $Q = VA$ in Mansfreda, *et al.*, (2020) highlighted that this method outperformed the traditional stage-discharge relationship when the sample size of empirical flow gauging were less than 10, whereas as the sample size increased, the traditional stage-discharge curve informed by $Q = a(h+b)^c$ was considered more appropriate. It is on this basis, that the $Q = VA$ method for achieving a rating equation with a high degree of confidence may be useful for remote upland gauges. This is due to the difficulty in achieving an optimal range of flow measurements to calibrate the $Q = a(h+b)^c$ method as a result of the remoteness, and danger to life during high flow events.

2.4.5 Summary of Hydrological Rating Curves.

As climate changes and the requirement for reliable rating curves grows, the environmental managers of the world increasingly depend on time series stage-discharge data. Hydrological rating curves can be developed through empirical manual gaugings at discrete locations within a stream, usually beside a gauging station. These are used to calibrate a manually constructed rating curve which is known to be very accurate in mid-range flows. However, extrapolation to extreme flows is regarded as unreliable due to some mathematical uncertainties, lowering confidence. These curves are also seen to be inaccurate at the lowest of flows. These manually developed curves require a large commitment by the operator to continually gauge the stream year-round to avoid uncertainties related to temporal variation of shifting controls and to ensure an acceptable rating curve is produced across a range of flows if the gauge location requires it. However,

these drawbacks are matched by the ease and convenience of the manually developed rating curve as one can be quickly produced and regularly updated with new gaugings. Additionally, there is no subjective input parameters to include such as topography or roughness coefficients and these curves can be produced with low cost and computation power making them a powerful tool, and the standard in hydrological analysis.

The most common alternative is computer modelled rating curves such as those which can be developed in HEC-RAS as well as several different software packages. These are shown across a great range of literature to be reliable and useful in areas of unsteady flow or ungauged locations. Models provide an insight into the $h-Q$ relationship in areas where manual gaugings may not be possible, and at the most extreme flows. However, these models require accurate input parameters, which if wrong can detrimentally impact the accuracy of the model. Subjectivity in parameters such as the appropriate roughness coefficient variable and topographic data sources can lead to highly inaccurate models. Generally, models require high computation power and a range of input variables, however HEC-RAS 1D modelling has a multi-decadal track record and a wide availability meaning that it can produce rating curves for free, meaning that for analysis of the $h-Q$ relationship, it can be a useful tool when it is correctly applied. Optimal topographic data from a high-resolution survey and LiDAR as well as correctly estimated roughness parameters can lead to models which are accurate and a reliable means to extrapolate rating data beyond gauged flows.

Finally, the $Q = VA$ methodology for rating curve creation uses surveyed topography against observed average velocity at a gauging station. Due to this, it is reasonably easily to implement. The $Q = VA$ method is more robust with a gauging sample size less than 10 measurements, so it is likely to be a reasonable methodology for the extrapolation of the empirical rating curve beyond gaugings in remote and upland areas.

Chapter 3: Study Area

3.1 *The Feshie Catchment Overview*

The River Feshie Catchment (Figure 3.1), which has an area of 230-235 km² (Soulsby, *et al.*, 2006; FEH, 2022) is a highland river basin located in the Central Grampian Highlands, Scotland. The Feshie runs from its headwaters on the Gaick plateau through a glacial trough which dissects the plateaux of the Moine Mhor and Gaick (Werritty and McEwan, 1997) down to where it drains into the Spey approximately 2 km downstream of Loch Insh. The character of the river changes enormously as it descends Glen Feshie from a classic incised headwater channel to a wider river with greater floodplain connectivity and bed substrate mobility as shown in Young (1975).

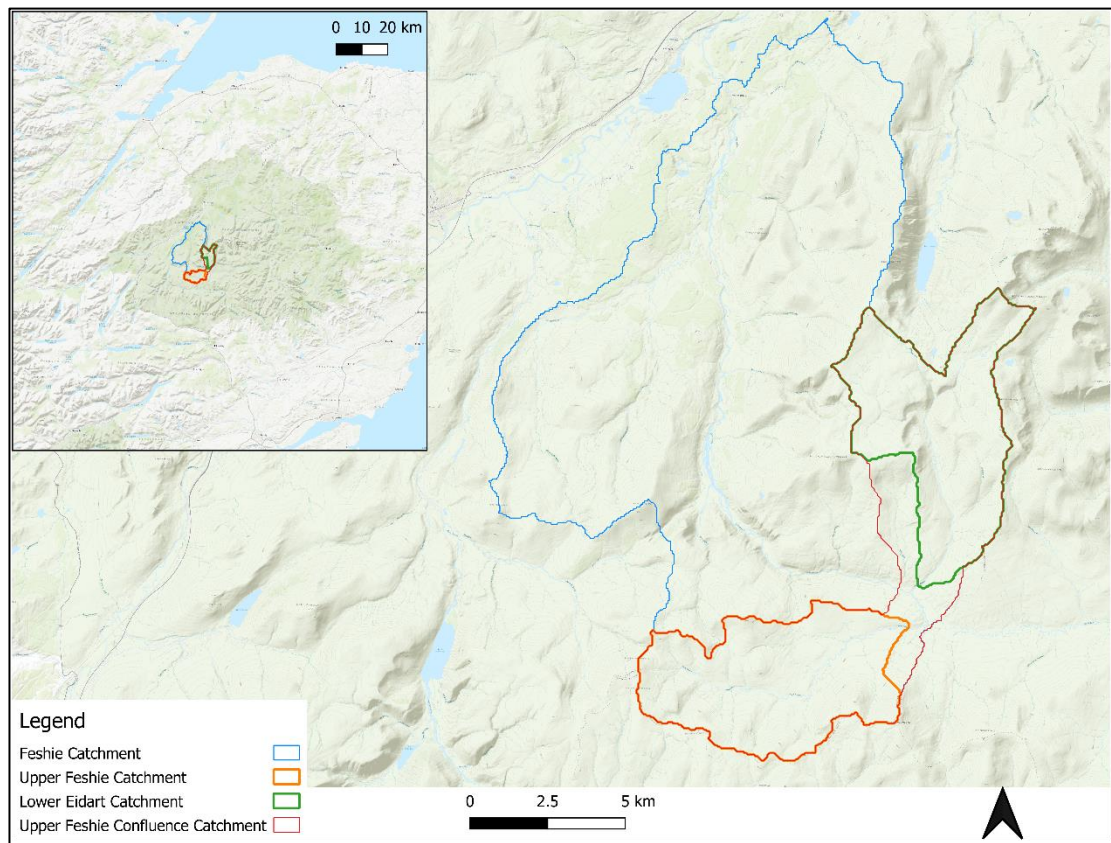


Figure 3.1. *River Feshie Catchment Delineation.* Source: FEH (2022)

Werritty and McEwen (1993) highlight that the mid-river currently reworks the Holocene valley floor through incising thick glacial outwash tills which originated from the down-wasting of the Gaick icecap (Rumsby, *et al.*, 2001) generating large volumes of meltwater which flowed under gravity through the valley we now identify as the Feshie.

3.2 The Study Sites

To meet the aim of this research, two catchments with contrasting physical characteristics were chosen for a comparison of their hydrological response. The catchments can be seen in Figure 3.2.1 and are named the Lower Eidart and Upper Feshie.

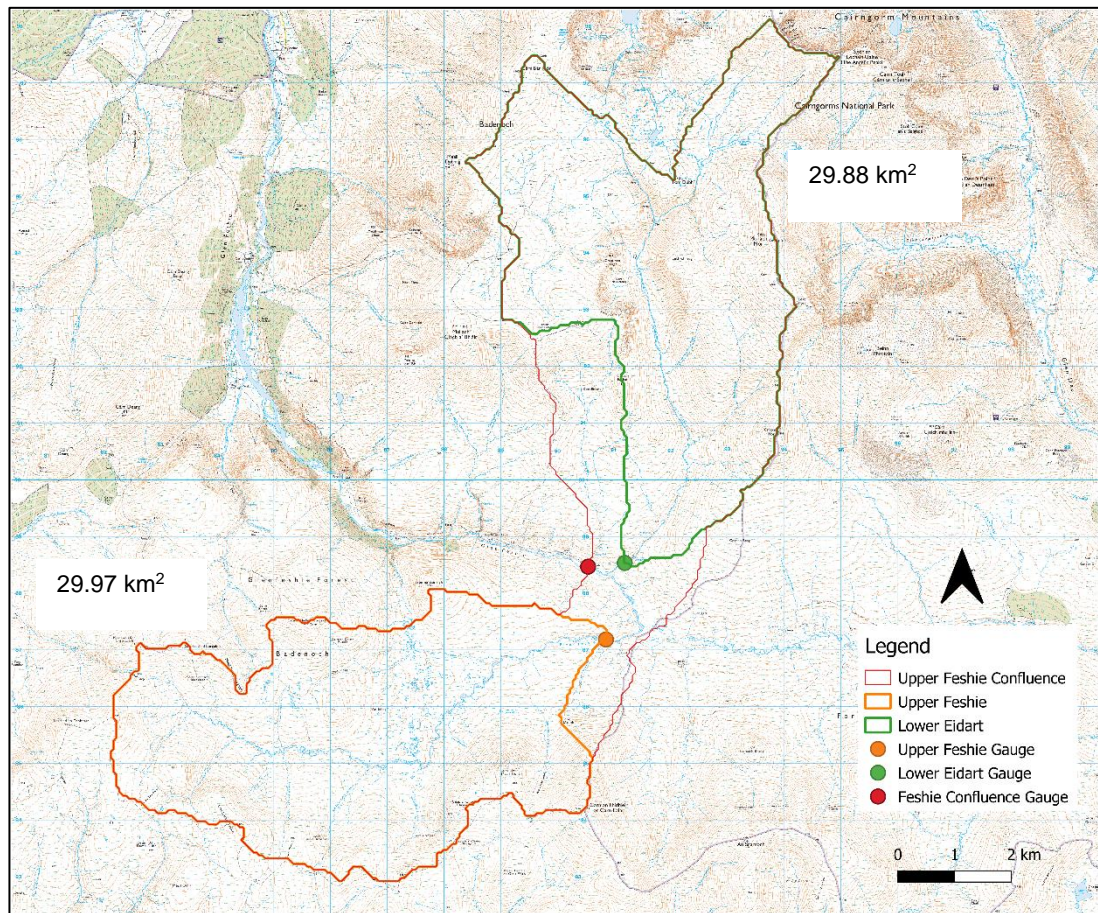


Figure 3.2.1. *The Study Site Catchments.* Source: FEH (2022)

Figure 3.2.2 presents the general catchment characteristics for the Feshie catchment. The influence of soil characteristics has long been acknowledged as one of the most important controls on the spatial variations in runoff pathways and storage potential in a catchment (Soulsby, *et al.*, 2006). Soils act as the interface between parent lithology, topography and land use making them a first-order control on the subdivision of hydrological flow pathways and storage potential (Soulsby, *et al.*, 2004). Therefore, it is important to be able to quantify runoff response of different soil types.

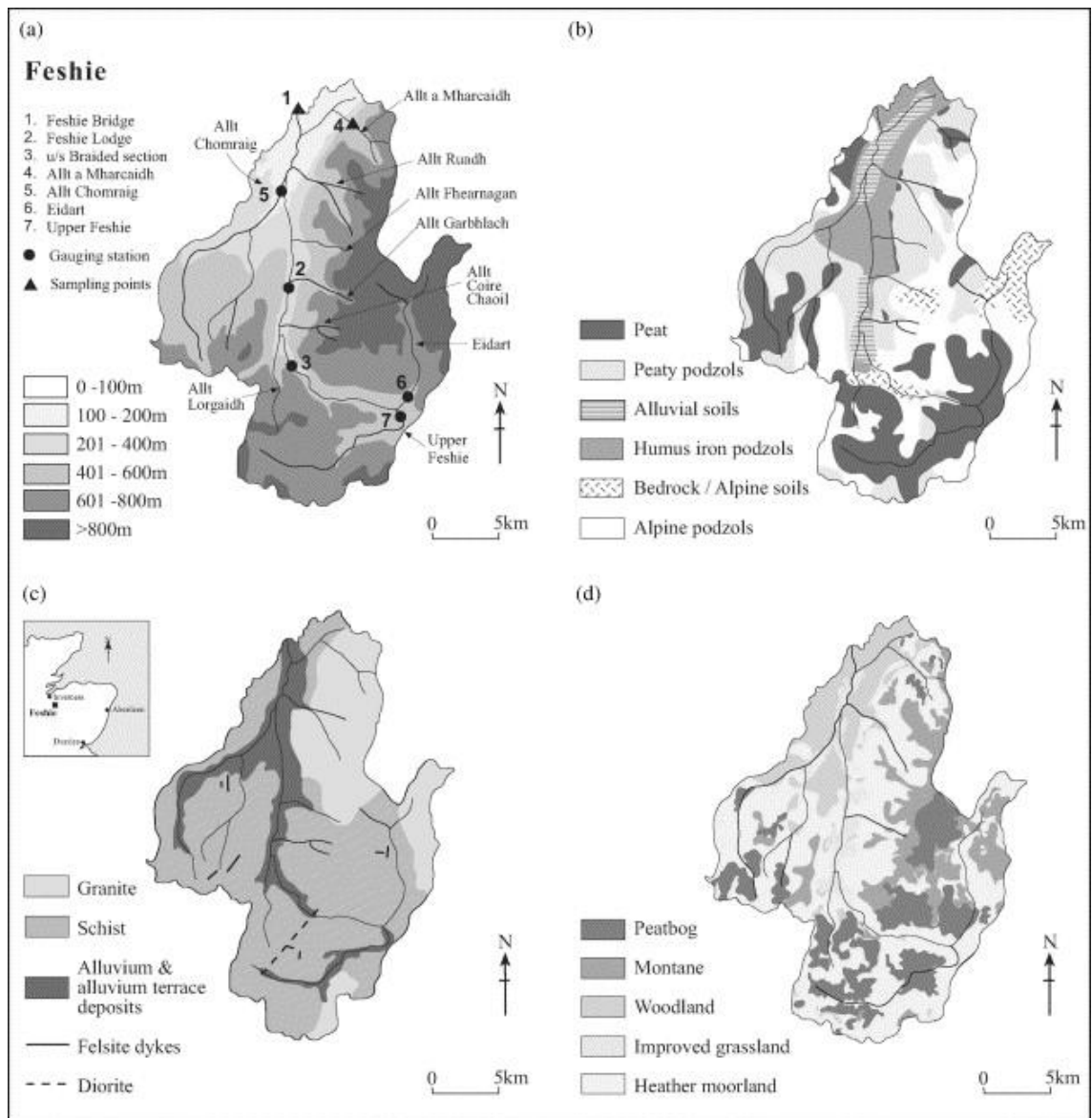


Figure 3.2.2. *The Physical Characteristics of the Lower Eidart and Upper Feshie Catchments.*
 Source: Soulsby, *et al.*, (2006).

The Lower Eidart joins the Feshie upstream of the Upper Feshie Confluence, whereby the gauge at the Upper Feshie Confluence gauges the combined catchment of Lower Eidart and Upper Feshie. Site Upper Feshie is the uppermost of the study catchments. Figure 3.2.1 highlights that the catchments of Lower Eidart and Upper Feshie are of comparable size at 29.88 km² and 29.97 km² respectively as informed by the FEH web service (FEH, 2022).

3.3 Catchment Characteristics

3.3.1 The Lower Eidart (Moine Mhor)

The Moine Mhor, or *The Great Moss* is a montane area of high conservation value in the highest reaches of the River Feshie catchment. The Moine Mhor lies as a blanket peat and mineral soil plateau with a mean elevation of 869 m AOD (Table 3.3.1). The 29.88 km² catchment drains into the river Eidart which is gauged at its outlet. Table 3.3.2 describes that the Lower Eidart is 59.5% shallow alpine mineral soil with 27.6% blanket peat.

The Moine Mhor has been categorised as a bare peat catchment for the purpose of this research due to ground proofed observations of overgrazing and trampling. Figure 3.3.1 is an example of a bare peat area with a peat hag.



Figure 3.3.1. A Bare Peat and Hag Area on the Moine Mhor. Sourced with permission from Dr Andrew Black.

Peat hags occur when water flows downwards, accelerates and erosion occurs. It occurs where peat has been exposed, often by overgrazing. As the hag gets more prominent, the erosion worsens due to increased potential energy for the water, creating an erosive feedback loop.

In addition to Figure 3.2.2, Figure 3.3.2 presents a GIS map of the superficial deposits of the Lower Eidart, Upper Feshie and combined catchments clipped from a BGS (2022) dataset.

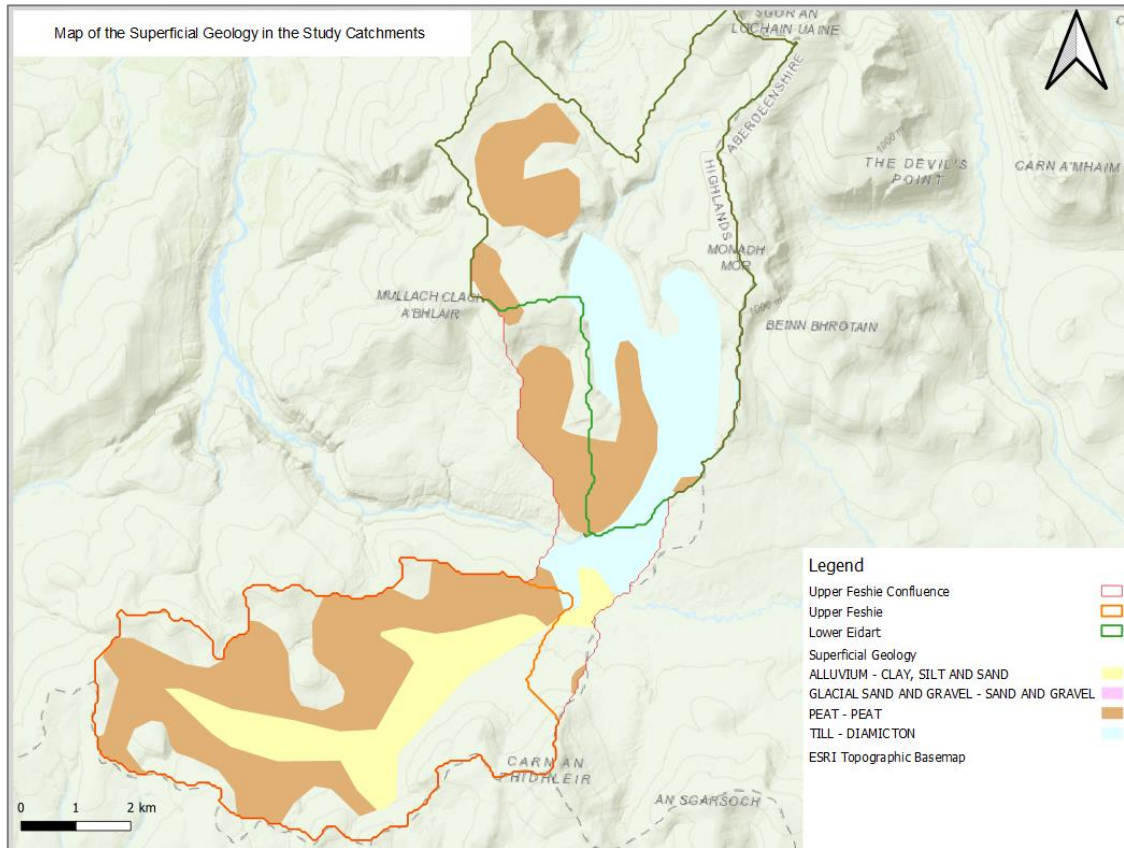


Figure 3.3.2. A Map of the Superficial Deposits of the Study Catchments. Source BGS (2022)

3.3.2 The Upper Feshie catchment

The Upper Feshie catchment can be categorised as a blanket peat catchment as it is more than 65% blanket peat (Table 3.3.2) along with 19.7% subalpine mineral soil which sits at an average elevation of 698 m AOD (Table 3.3.1). This catchment is 29.98 km².

Table 3.3.1. *Catchment Descriptors for Lower Eidart and Upper Feshie.* Source: FEH (2022). Catchment descriptors represent a feature of a catchment as a single value, for example mean altitude (Altbar).

Descriptor	Catchment	
	Lower Eidart	Upper Feshie
Outlet	291200788550	290850787200
NGR	NN 91200, 88550	NN 90850, 87200
Area	29.88km ²	29.98km ²
Altbar	869m	698m
Aspbar	204 degrees	63 degrees
Aspvar	0.25	0.21
Bfihost	0.363	0.532
Bfirhost19	0.291	0.382
Centroid E	291,947m	286,570m
Centeroid N	793,594m	785,532m
Dplbar	7.11km	6.99km
Dpsbar	171.1m/km	132.5m/km
Farl	0.999	0.977
Fpext	0.0184cm	0.0416cm
Fpdbar	0.273cm	0.553cm
Fploc	0.875	0.727
Ldp	12.27km	13.47km
Propwet	0.72	0.72
RmedH1	10mm	9.8mm
Rmed1D	42.8mm	37.3mm
Rmed2D	64.2mm	54.8mm
Saar6190	1,666mm	1,438mm
Saar4170	1,773mm	1,668mm
Sprhost	58.85%	53.74%
Urbconc1990		
Urbext1990		
Urbloc2000		
CatchmentRain C	-0.019	-0.019
catchmentRainD1	0.452	0.415
CatchmentRainD2	0.534	0.507
CatchmentRainD3	0.381	0.393
CatchmentRainE	0.248	0.246
CatchmentRainF	2.411	2.397
GridRainD1	0.444	0.437
GridRainD2	0.518	0.534
GridRainD3	0.374	0.375
GridRainC	-0.018	-0.018
GridRainE	0.245	0.244
GridRainF	2.332	2.335

3.3.3 The Combined Catchment.

The catchments of Lower Eidart and Upper Feshie join at site Upper Feshie Confluence. The Upper Feshie Confluence catchment contains both blanket peat and postglacial moraine deposits (Figure 3.3.2) as both sub catchments are included within the overall catchment. The superficial deposits of this catchment can be observed in Figure 3.3.2. The immediate vicinity of site Upper Feshie Confluence is dominated by stratified fluvial till deposits of mostly sand and gravel which have been sorted. There are also deposits of blanket peat at a slightly higher elevation on the valley sides along with some alluvium.

Table 3.3.2. *Soil Types of Lower Eidart and Upper Feshie.* Source: Soulsby, *et al.*, (2006)

Superficial Deposits		
Soil (%)	Upper Feshie	Lower Eidart
Peat	65.1	27.6
Peaty Podzol	10.1	9.6
Subalpine	4.5	3.5
Shallow Alpine	19.7	59.5
Alluvial	0.5	0

Chapter 4: Methodology

To undertake this research, time series flow and precipitation data were provided by Dr Andrew Black along with rating equations for the gauging stations which gauge the study catchments. These rural catchments present issues for calibration gaugings and so the first element of this research was to extend the rating equation beyond the manual gaugings. Two methods were employed for this, HEC-RAS 1D hydraulic modelling and the $Q = VA$ method. Validation of these results by visual analysis, application to the level data and $Q = VA$ verification in a three-tier process was the second element. Finally, analysis of hydrological metrics such as lag time to peak discharge and hydrograph form were undertaken once the ratings were judged to be adequate. To undertake the modelling, a high-resolution topographic survey was required as there is no high-resolution topographic data available for the rural catchments in this study.

4.1 *Topographic Survey*

During review of existing topographic data for the study area, it was found that a high-resolution topographic survey of each site must be undertaken using precise instrumentation to be able to meet the aims of this research. For this reason, a Trimble R12i Real Time Kinematic Global Navigation Satellite System (RTK-GNSS) was selected for use with a Trimble TSC7 controller. The GNSS was selected due to its ability to measure and store georeferenced elevation data of high precision as well as having a tilt compensator so the surveyor can take measurements in un-wadable and out of reach areas of the channel geometry. The survey equipment is pictured being used in Figure 4.1.1. GNSS for river survey use is justified in Lee and Choi (2007) who state that GNSS survey is 15.3% more time efficient relative to conventional survey methods such as a Manual Total Station or Dumpy Level. The 2007 source exemplifies the usefulness of GNSS in river surveys yet is over a decade old and the 15.3% time saving is likely considerably higher today, however no recent revision of this statistic has been located.



Figure 4.1.1. *Trimble R12i GNSS Rover in Use, Lower Eidart.*

The GNSS works using a roaming sim card which utilises any mobile network signal which is available in the area, however, due to the remoteness of the survey sites in this research, no mobile phone coverage existed. Due to this, a Trimble R10 GNSS base was used to work in tandem with the R12i rover in a base and rover system. The base is set up with no fixed position, so it is set to autonomous mode meaning that it receives satellite signals at a pre-defined time step throughout the day (IC, 2021). The Trimble R10 base, pictured in Figure 4.1.2, therefore becomes a position of known high accuracy because several hours of satellite signal generates an accurate base position after post processing. The R12i rover connects to the base through a radio link and all observations measured by the RTK are relative to the base position at this stage before post processing. During post processing, georeferenced observations relative to the base can be used to confirm the observations true position relative to OS Datum Newlyn. As stated, the base and rover system are linked through radio signal, so the base placement was essential for speed and reliability of the communications throughout the survey.



Figure 4.1.2. *Trimble R10 GNSS BASE.*

To set the base up as shown in Figure 4.1.2, a high vantage point was in the middle of all 3 survey reaches (Figure 4.1.3) to ensure a strong radio connection could be maintained between the base and rover all day. Once an appropriate area had been located, the tripod was erected and the GNSS base was attached before its height was measured to a control pin by a Disto. The Disto was double checked against a conventional measuring tape for accuracy on the first set up and used alone on the second set up. Once the base height had been entered into the controller, the base was then connected to the rover.

The R12i had been pre-tuned to the R10 base before the field visit to ensure that set up did not waste valuable survey time. Due to the rolling nature of the hills in the Upper Feshie catchment, the base had to be erected twice, due to the rolling topography reducing signal strength. The base and rover system do not theoretically require line of sight due to radio wave propagation and the role of the ionosphere in radio communication (Poole, 1999). Short distance radio communication, however, is reduced by the mountainous topography and therefore two base set ups were required. However,

this was not an issue due to the efficient nature of the equipment meaning that set up took approximately 10 minutes each time.

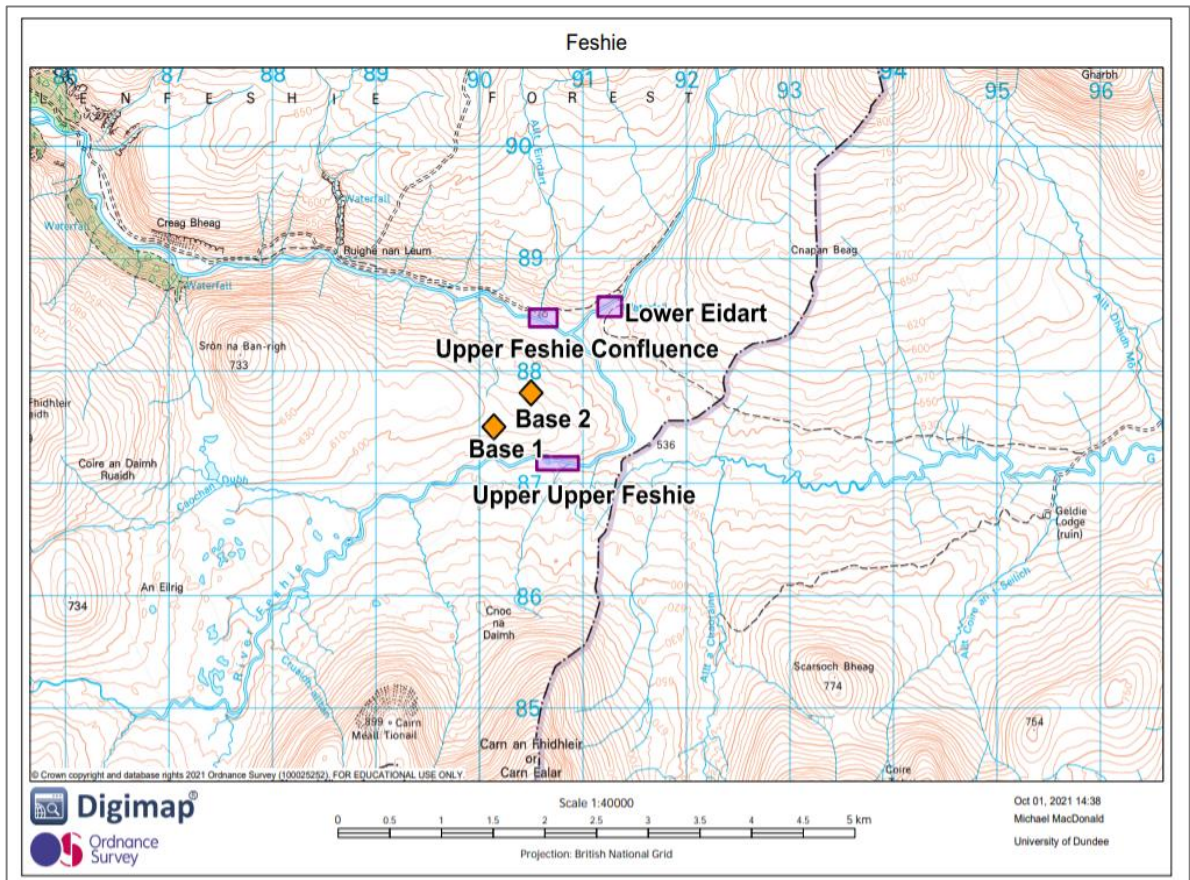


Figure 4.1.3. *Approximate Locations of Base Stations Relative to Survey Locations.* Source: Edina Digimap (2022)

Once the base and rover were set up and connected, the survey team travelled to the survey reach and began the topographic survey. Hydraulic models are subject to two main sources of error, topographic data input and incorrect roughness coefficients (Filion and Karney, 2003; Bessar, 2020). In terms of topographic data input, two main types of survey can be undertaken: scatter based and cross sectional, depending on the type of simulation which is being undertaken within the modelling software.

A scatter-based survey includes taking a scatter of points at pre-determined resolution (for example one-two m). To undertake this survey, points would be measured at one-two m intervals in zigzags so that surface triangulation can be achieved in Autodesk Civil 3D software, which aids the creation of a highly detailed Digital Terrain Model (DTM) which is the required resolution for 1D/2D and 2D modelling. However, for a low to high flow simulation of a flood event, primarily with high flows remaining in-channel, a 1D model informed by a highly detailed cross-sectional survey was chosen, with several scatter-based data observations being taken at confluence sites as representing these in cross section form is very difficult. To carry out the cross-sectional survey, the river was traversed, taking measurements with the GNSS. These cross sections were taken in a feature-based way, meaning that cross section locations were chosen based on hydraulic features such as riffles and pools.

Before the survey was undertaken, a walkover of the reach took place so that main hydraulic controls were identified. Obtrusive objects such as boulders, changes in bed gradient (which attenuates flow facilitating pool and riffle formations (Leopold and Maddock, 1953)) and stage-independent bedrock control pool and cascade sections were all carefully considered as it is recognized that these features of the channel geometry play a role in river stage in both low and high flows. Additionally, the downstream boundary condition of the hydraulic model is paramount in terms of model accuracy (Pappenberger, *et al.*, 2005; USACE, 2021) so particular attention was paid to the downstream end, ensuring that the reach to be modelled finished in an area of smooth flow and not on a control feature such as a weir or boulder riffle. To carry out the survey, the RTK operator would begin at the highest point of the local flood plain, taking measurements with the RTK at every change of slope, water's edge and change in bed geometry. A series of codes are assigned to each of these different parts of the survey so that post processing can be more efficient. A non-exhaustive list is included in Table 4.1.1 below.

Table 4.1.1. *Series of Codes Used in Trimble TSC7 For Post Processing.*

Code	Code Meaning
Fp	Flood Plain
WSE	Water Surface Elevation
Bar	Bar
Bed	Bed
Toe	Toe of Bank
ToB	Top of Bank
PoS	Point on Slope

4.2 Digital Terrain Model Development

4.2.1 Post processing of Survey Data

Once the survey was completed, the autonomous data from the Trimble R10 GNSS base was downloaded in conjunction with the measured topographic data from the Trimble R12i GNSS rover. These data were inserted into Trimble Business Centre software to process the measured topographic data, which was relative to the base, bringing these data in to line with OS Datum Newlyn. The processing adjusts the relative positions to correct them spatially within the designated coordinate system (OSGB 1936). The software was run several times, until the errors were within the defined threshold (within 30 mm vertically and 60 mm horizontally). A derivation report can be found in Appendix A. The derivation report simply outlines the derived georeferenced elevation data from the mathematic derivation of each measurements position in the Trimble Business Centre software.

4.2.2 Building the Digital Terrain Model

The corrected elevation data was uploaded into Autodesk Civil 3D CAD software for creation of a DEM for each of the three survey sites. Surface creation is an involved multi-step process which has been summarized in this chapter. The points were uploaded in PENZD format meaning, point number, easting, northing, elevation, and description. Point descriptions are important because they inform the creation of polylines, which are considered definitions of the surface. Triangulation of the surface cannot cross polylines, so these are used to define the banks of the river which enriches the accuracy of the surface to represent the actual topography of the surveyed area. Break lines are created by joining the dots whereby a polyline is drawn between certain points (Figure 4.2.1). Triangulation between polylines creates the 3D DTM as highlighted in Figure 4.2.1.

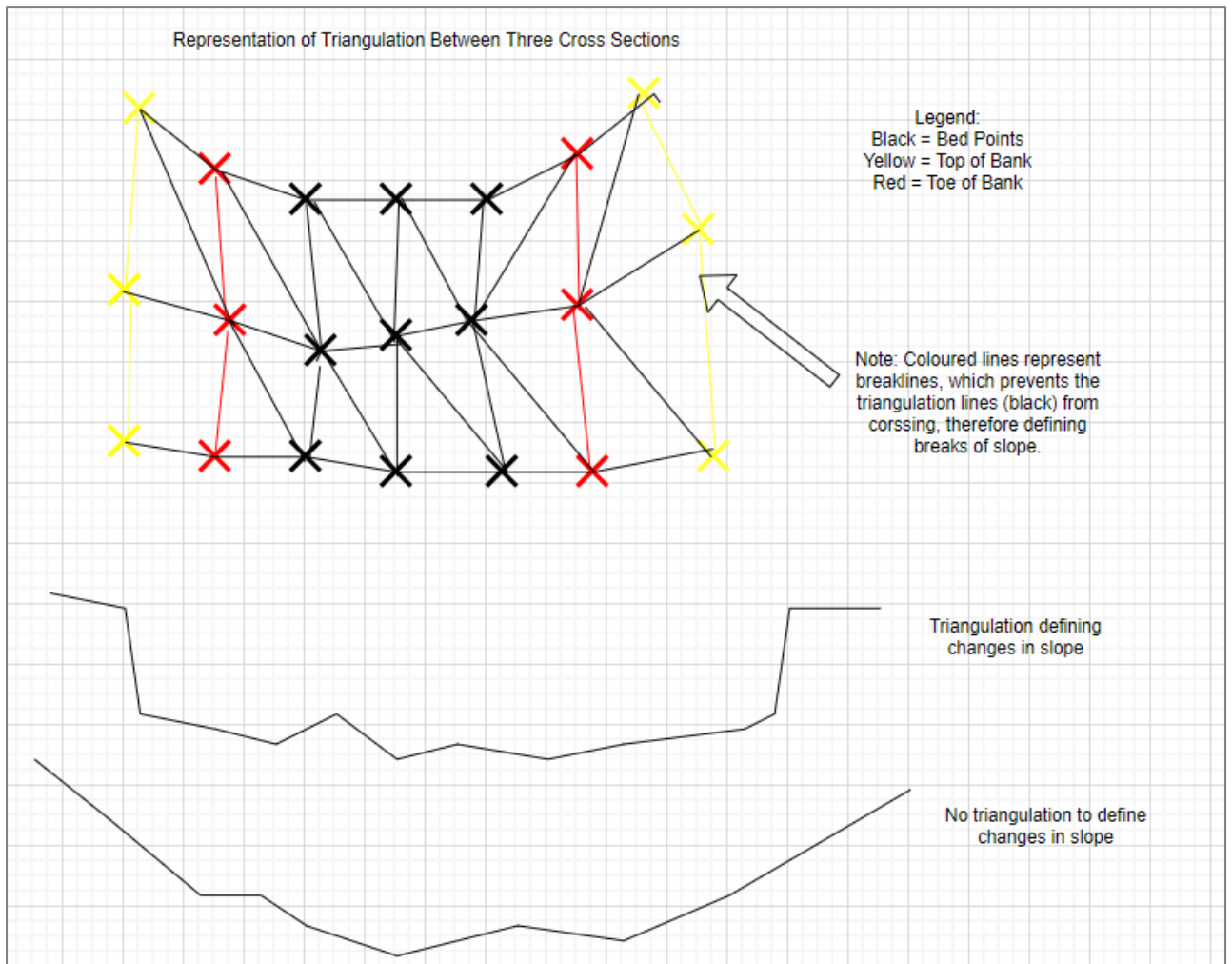


Figure 4.2.1 *Representation of Surface Triangulation.*

Once a surface has its polyline definitions and has been triangulated, it can be checked through implementation of 0.1 and 0.5 m contour lines (Figure 4.2.2). The contour lines make visual checking of the surface easier as the banks and bed are clearly shown, meaning that if anything does not look like it makes sense, then it is easily noticeable and can therefore be investigated.



Figure 4.2.2. Upper Feshie Digital Terrain Model.

After the surface has been created and checked, a series of sample lines must be created to represent a series of cross sections. To do this, a channel alignment, or long profile, is drawn along the reach and loaded into the sample line function in Civil 3D along with a pre-defined spacing. In this research, 10 m intervals were chosen as these are regular and seemed to fit the reach for computation of flows later in the modelling process. Cross section spacing is a central parameter to the reliability of a 1D flood computation. A study which compared four flood models to test the impact of cross section spacing found that there was little difference in mean absolute error between the four models, however there was a lot of variability in the computed spatial extent of flood water. The variability is caused by the wider spatial distribution of cross sections leading to an absence of required topographic data and therefore geometric influences on the hydraulic processes within the river (Ali, *et al.*, 2017). However, an unduly detailed topographic DTM of the water course can lead to model instabilities and may even reduce

the model accuracy due to rounding errors, this is shown in Samuels (1990) whereby once an optimal cross section spacing has been achieved to fit the physical flood wave and represents the bed geometry, additional cross sections increase error potential. Therefore, cross section resolution must strike a fine balance in detail, appropriate to the task, for example in flood forecasting, a coarse topographic DTM is considered appropriate, however for high resolution flood inundation mapping, a finer resolution is required (Castellarin, *et al.*, 2009). The sample lines were exported from Autodesk Civil 3D as a GeoTIFF. In Figure 4.2.2, the gradient of the channel alignment details is noted for modelling later.

4.3 HEC-RAS Hydraulic Modelling for Rating Extrapolation

4.3.1 Building the Hydraulic Model

To perform the flow computation, HEC-RAS 5.0.7 was utilised as it is freely available and is cited widely as a reliable software (Patel, *et al.*, 2017) in flood risk literature. To perform the flow computation, HEC-RAS was opened, and a new project was created (Figure 4.3.1). In the project, the reach to be modelled was named appropriately. Once the project had been named, the river geometry was uploaded into the software section for river geometry.

The section for geometry opens as a blank panel, then the user must then import the surveyed geometry as shown in the workflow in Figure 4.3.2. Once the cross-section drawing is uploaded, it will show the thalweg alignment (long profile), and cross section sample lines (Figure 4.3.2). After this, the Manning's n friction values can be inserted into the software. The values selected for this research were 0.05 for the banks and 0.033 and were informed by consultation with work by Chow (1959) where a series of values and associated channel descriptions are provided. The frictions were chosen based on rocky, upland channels with little in-channel vegetation.

The second step of developing the flow computation is to input the initial conditions (Figure 4.3.3), as well as several flows (represented as PF for Profile Flow in the software) in addition to reach boundary conditions. The boundary condition can be input in several ways in HEC-RAS, for example, a hydrograph, normal water depth and

gradient. In this instance, the gradient was chosen. The several flows which are input populate the theoretical rating curve which this software has been selected to produce.

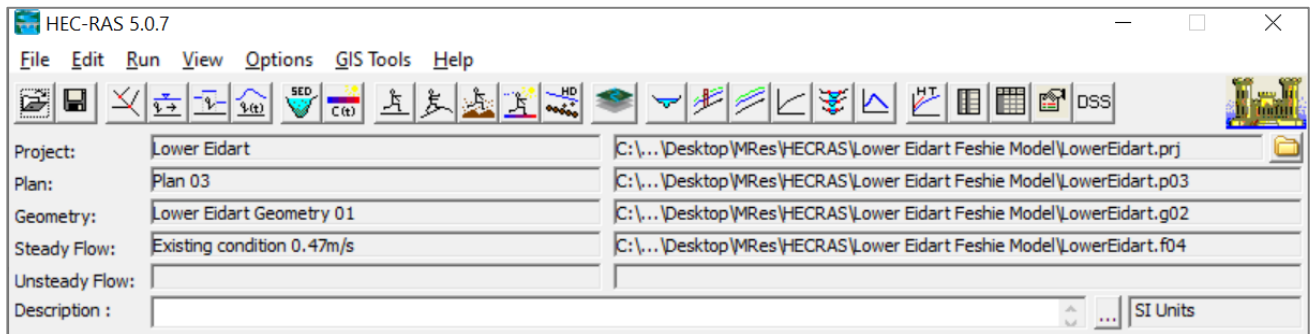


Figure 4.3.1. HEC-RAS Main Screen.

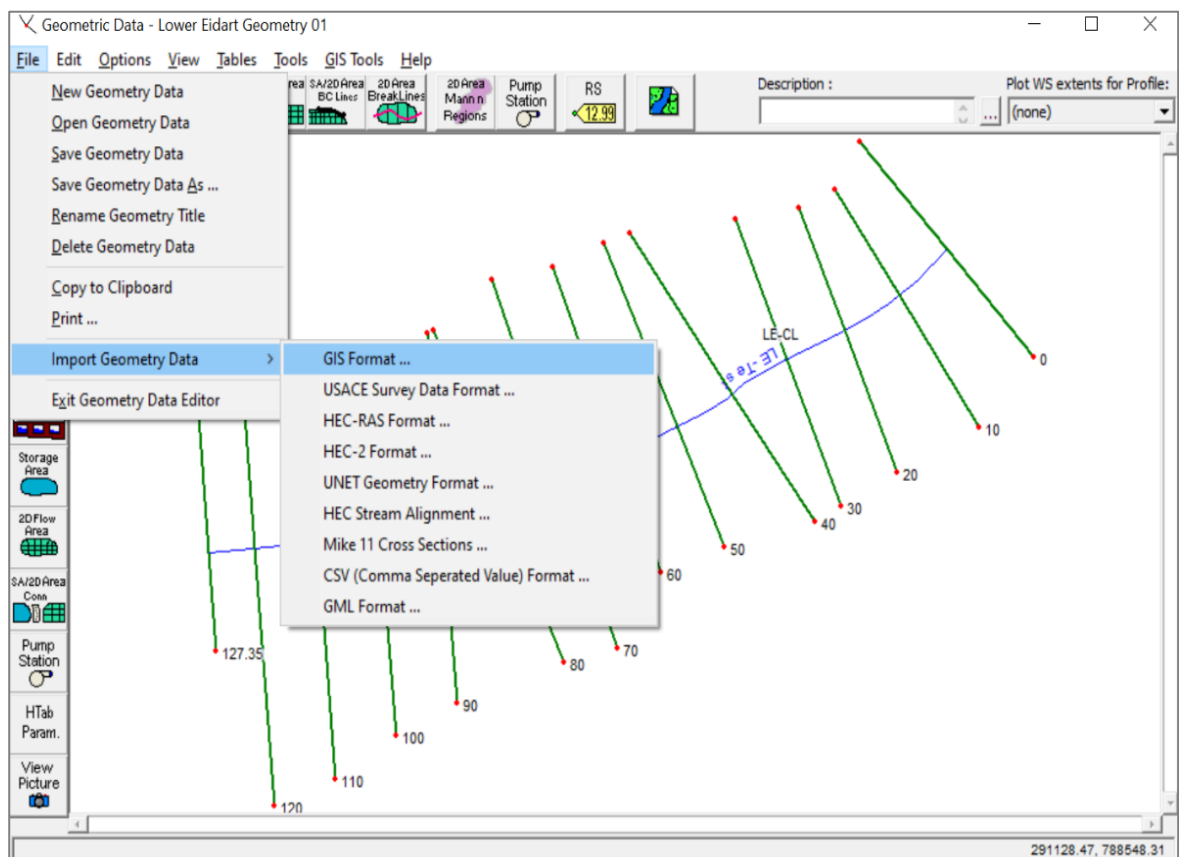


Figure 4.3.2. HEC-RAS Geometry Tab.

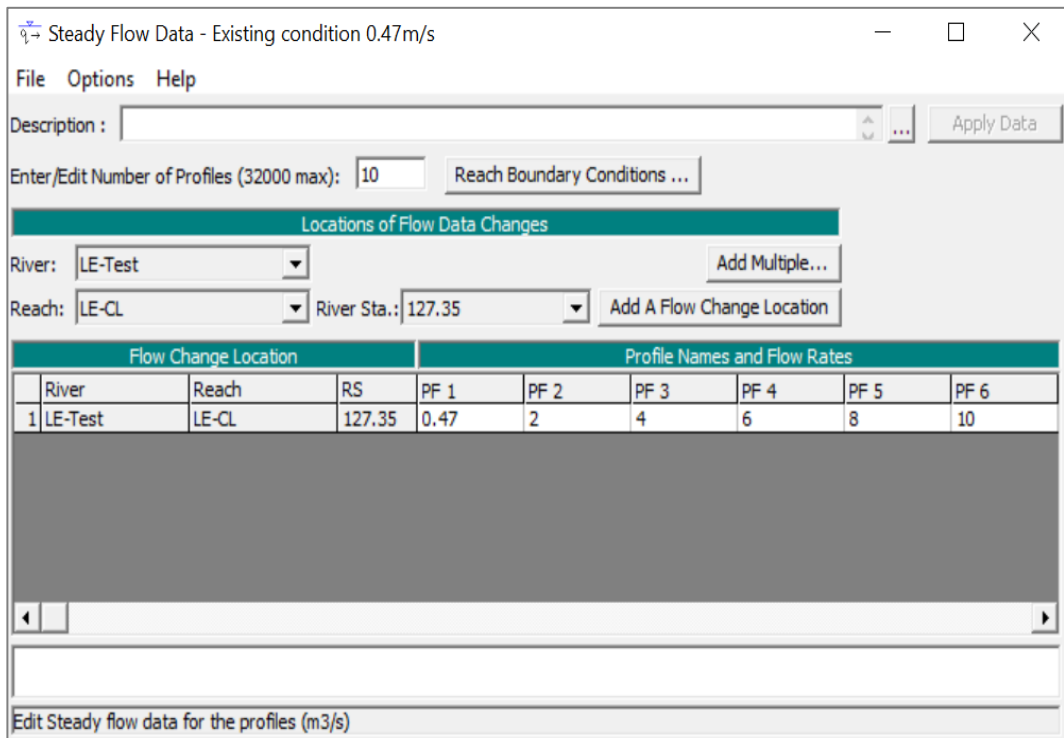


Figure 4.3.3. HEC-RAS Steady Flow Data Tab.

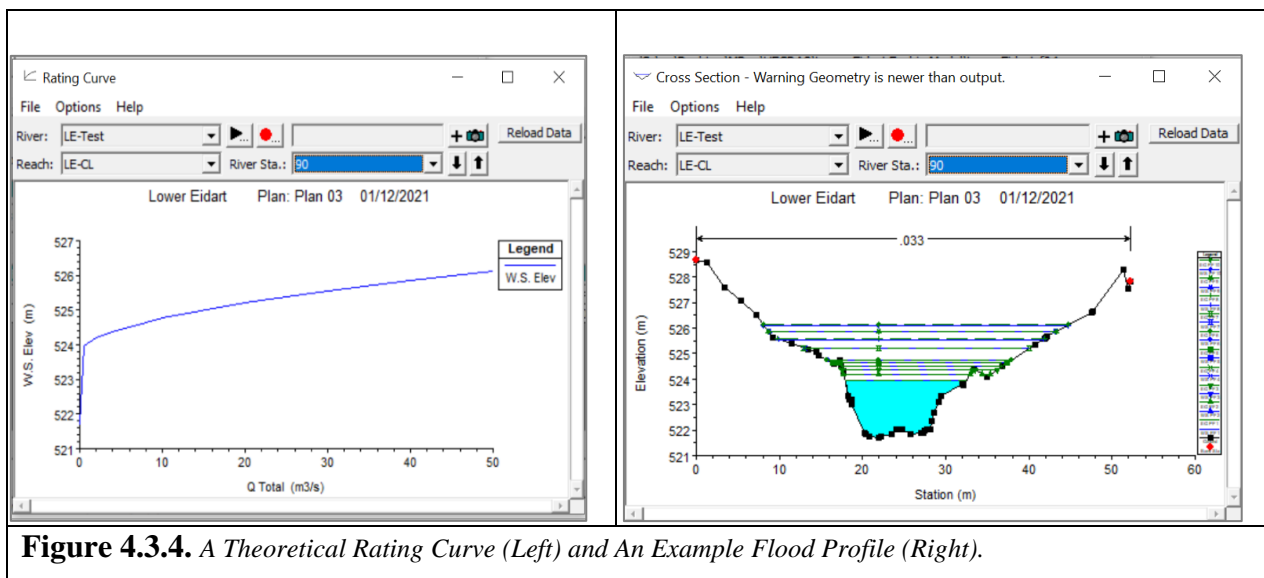


Figure 4.3.4. A Theoretical Rating Curve (Left) and An Example Flood Profile (Right).

4.3.2 Fitting Modelled Outputs to Empirical Data

The theoretical stages computed by HEC-RAS are relative to the software datum and are expressed in metres. However, stage measurements taken at the time of ADV gaugings are taken from a permanent bolt placed above the water level and are expressed initially as a negative value.

To bring the theoretical rating curve into line with observed gaugings, an offset was applied. It is assumed that there is a 1:1 ratio between a change in stage in observed field measurements and a change in stage in the HEC-RAS model. To achieve the offset value, the observed stage can be subtracted from the HEC-RAS stage on the day of the gauging. The offset constant can be applied to the manual gaugings by adding the offset to the observed local stages. Figure 4.3.5 illustrates the difference between the two datums.

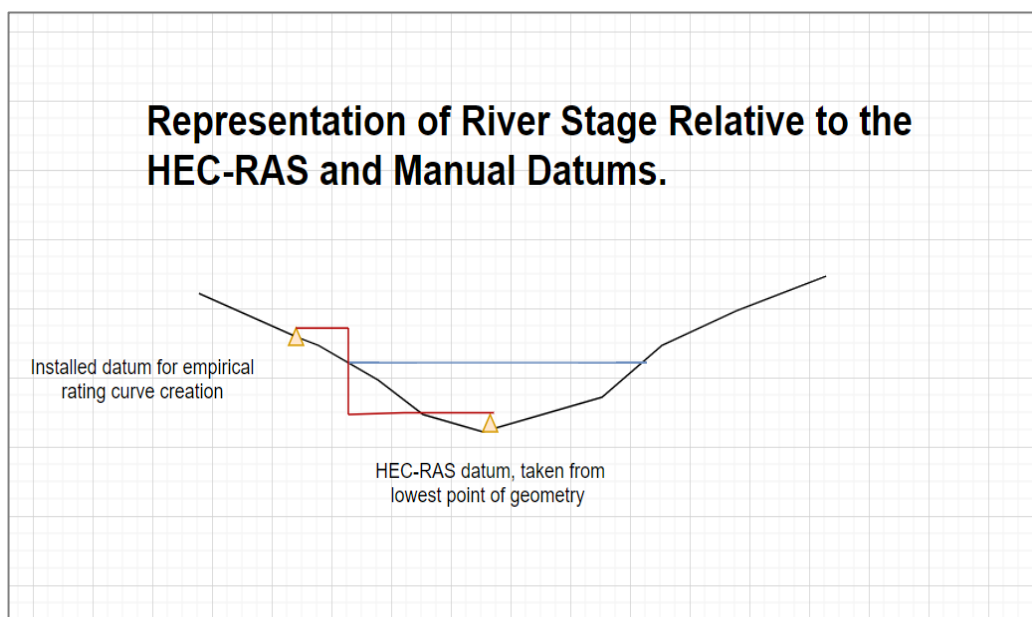


Figure 4.3.5. *Offset Application Between Datums*

Once a dataset regarding the Q - h relationship has been achieved it is then possible to derive a rating equation, using the equation $Q = a(h+b)^c$ where Q = discharge, a = the multiplier, h = stage, b = the datum correction (stage at zero flow), and c = the shape parameter (CEH, 2022). A set of values for a , b and c are input into the equation and are initially informed by Hydata manual produced by the Centre of Ecology and Hydrology (Ramsbottom and Whitlow, 2003) and the equation is solved using the series of combined

stage values from manual readings and HEC-RAS. Once a series of $Q-h$ flows are achieved, the error between the flows computed by HEC-RAS and those calculated using the baseline equation is calculated and then the error squared is calculated. Once these have been calculated, the next step of the rating derivation process is to calculate the initial Root Mean Square Error (RMSE) of the $Q-h$ data. The solver function under ‘Data’ in Microsoft Excel was used for this (Figure 4.3.6)

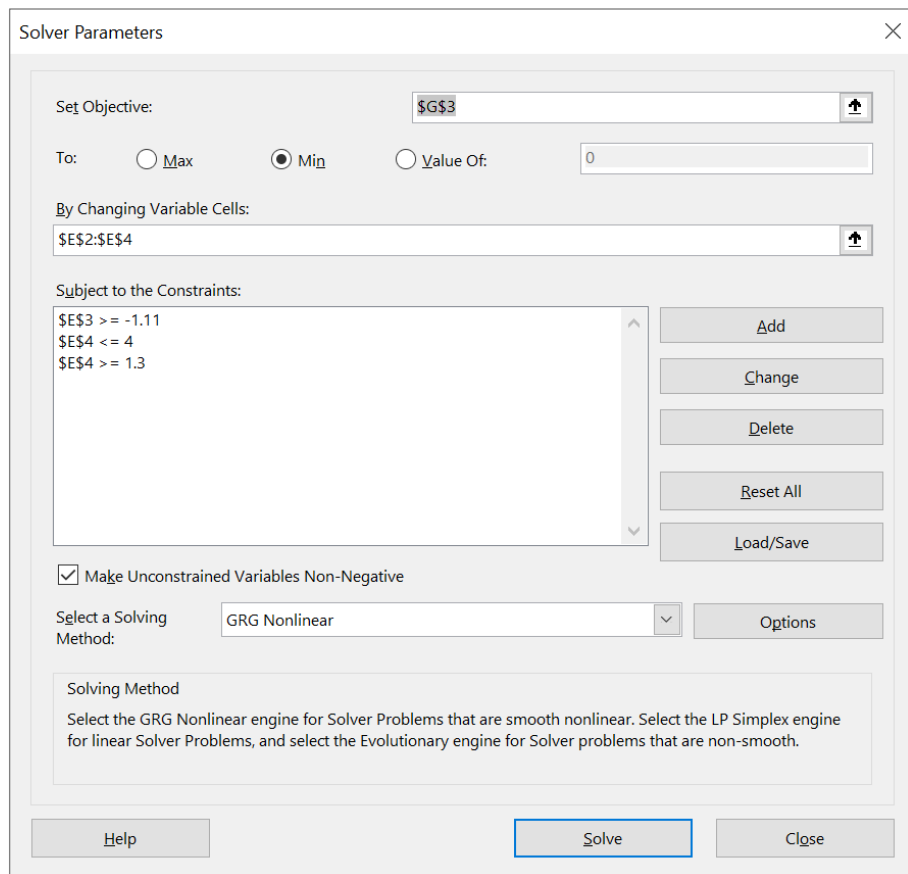


Figure 4.3.6. *The Solver Window in Microsoft Excel*

Within the solver, the objective cell is selected, this cell should contain the current RMSE value, and the objective is set to minimum before the variable cells containing the a, b and c values are selected. It is important to set constraints to the solver so that Excel does not calculate values which are not accurate. The constraints are informed by the Hydata user manual (IoH, 1987) Once the Solver has run, the RMSE value should become smaller, and closer to 0. An RMSE of 0 would imply a perfect rating, and is not likely to be achieved, however the reduced RMSE value and the variable values of a, b and c have been set to best fit the data. The rating parameters are therefore solved. A quality check

of the rating can be achieved by graphing a broad range of flows and stages using the derived rating equation and identifying any discontinuity in the curve.

4.4 *Quality Review Process*

4.4.1 *First tier: Visual Analysis*

The first step of checking the derived rating equation is to visually check the data used for the rating derivation. The $Q-h$ data should form a smooth, convex curve which does not have any significant discontinuity in slope.

Divergence of the $Q-h$ relationship from the Solver and HEC-RAS can highlight the requirement for a multi-part equation over a single rating. A multipart equation, which is fitted to individual portions of the data, is supposed to represent different limbs of the hydrometric rating curve, where each limb is separated by curve breakage or discontinuity. A multi-part equation can better represent the $Q-h$ relationship across the entire range of flows in both simple and complex channels (Holmes, 2018).

4.4.2 *Second Tier: Rating Application and Water Balance*

Another quality check is to sense check the rating equation in terms of assessing catchment water balance. To do this, the rating equation must be applied to continuous time series stage data so that a series of derived flows at the gauging station can be calculated (Peck, 1983). The derived flow can then be used to calculate mean annual runoff which can be checked against precipitation input into the catchment to judge if the rating equation is sensible. It is assumed that the extensive rain gauge network in the area is representative of the area and are accurately capturing the precipitation. An 18 Tipping Bucket Rain gauge (TBR) study by Stransky, *et al.*, (2007) showed that there can be underestimation of rainfall by up to 30% if the TBR is not calibrated, so there is room for uncertainty if the rain gauge network is not maintained.

4.3.3 *Third Tier: The $Q = VA$ Method for Rating Extrapolation and Result validation*

Review of the modelling results using mean annual runoff described in Chapter 6 showed that the mean annual runoff for the reach Lower Eidart was substantially overestimated by the results of the HEC-RAS modelling. Therefore, another verification method was deemed necessary.

The verification method which was selected for this was the $Q = VA$, or velocity multiplied by cross sectional area method. To carry out this method, the cross section at

the gauging station was used along with the lowest possible water surface to calculate the wetted area at the water surface. Microsoft Excel was then used to calculate the wetted area in millimetric increases in stage at the cross section of the gauging station. In addition to this, a series of empirical gaugings were used to calibrate the spreadsheet by using the manually recorded stage and discharge information to achieve a velocity at a given stage. Figure 4.4.1 displays a screenshot of the $Q = VA$ spreadsheet. A series of $Q-h$ values are generated in the spreadsheet and can therefore be used in the same way as the HEC-RAS $Q-h$ data, in the Excel solver. The details of this method are outlined in section 4.3.2 of this chapter. A rating derivation can be achieved, and if required, a multipart equation can be used also, to fit the $Q-h$ equation to the data.

Once a series of rating equations have been achieved using the $Q = VA$ method, they were applied to the continuous time series stage data in the same way that the HEC-RAS ratings were, as described in this chapter. Then, a series of flows can be used to calculate mean annual runoff and verify the results of the HEC-RAS or identify divergence in the results.

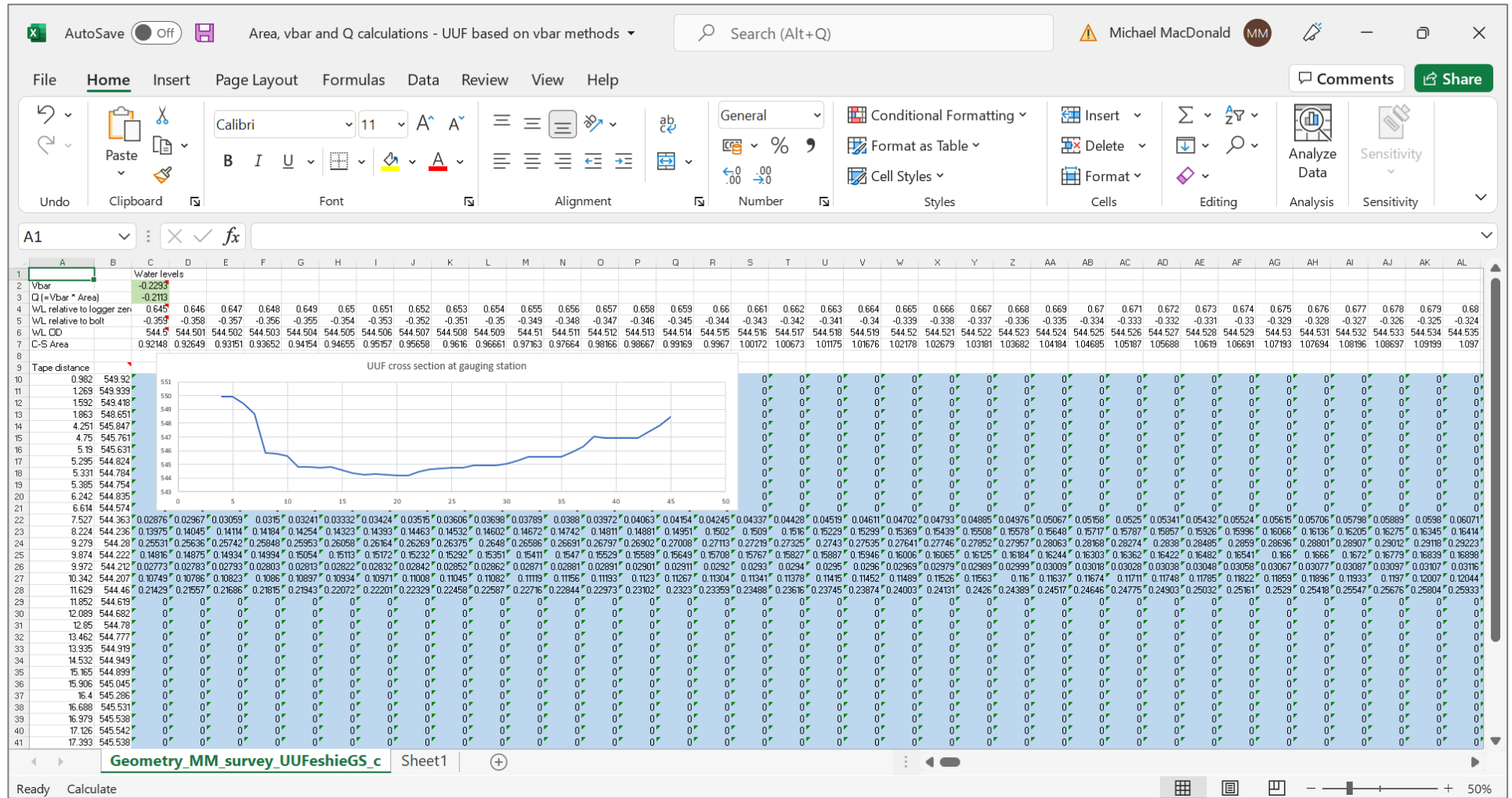


Figure 4.4.1. Velocity x Cross Sectional Area Matrix Spreadsheet.

4.5 Hydrological Analysis

The ratings were applied to the data so that the third objective of this study could be achieved, to carry out analysis of lag time to peak discharge and hydrograph form in these catchments.

4.5.1 Application of Newly Derived Ratings to Time Series Data

The new rating equations which have been derived from a combination of the HEC-RAS hydraulic modelling and the $Q = VA$ method were applied to continuous time series river stage data which were provided by Dr Andrew Black to aid this research.

Flow break points which separate the different limbs of the rating were converted to stage break points by rearranging the stage-discharge rating equation. The rearranged equation took the form of:

$$Q = a*((h+b)^c)$$

$$Q/a = (h+b)^c$$

$$(Q/a)^{1/c} = h+b$$

$$((Q/a)^{1/c}) - b = h$$

The stage break points were then used in a nested IF Statement to act as divisions between the data which each rating applied to. An example of the IF Statement used is:

=**IFERROR**(**IF**(E158646<=N\$158651,N\$158648*((E158646+N\$158649)^N\$158650),
,Q\$158648*((E158646+Q\$158649)^Q\$158650)),**"0"**).

Within the above IF Statement, the break points are highlighted in bold text, the Excel command states that if the value in the respective cell (italics) is less than/greater than the break point (bold) then apply the following rating equation, for example:

$$\text{IF}(E158646 \leq \mathbf{N\$158651}, \mathbf{N\$158648} * ((E158646 + \mathbf{N\$158649})^{\mathbf{N\$158650}})$$

The IF Statement is then stating that the rest of the stage data should conform to the final part of the rating. To visually clarify the two parts of the rating being used, two different colours have been used. Finally, the commands which have a yellow highlight are IFERROR commands, meaning that if there is any issue with the data which this nested IF Statement is being applied to, then Excel should insert a 0 value, so that the remainder of the data is unaffected in terms of calculation of an average flow and to aid fluency of applying formulae to the whole dataset where an '#ERROR' message would disrupt the workflow. The IF Statement was then applied to the continuous series for the reaches Lower Eidart and Upper Feshie. Application of a series of new ratings to Upper Feshie Confluence would be useful in the validation of these ratings, however lack of available data for Upper Feshie Confluence prevented its inclusion in this study.

4.5.2 Event Selection and Precipitation Data

To meet the aims of this research, it is crucial that flood events chosen to compare the response of the catchments are representative of the response of each respective catchment. Due to this, precipitation data was used to inform flood events which occurred due to uniform precipitation occurring across the entire study area, encompassing both sub-catchments. To do this, monthly flows for both catchments were plotted on a graph with precipitation data. Events which signaled a response in one catchment but not the other such as snowmelt or localised convective rainfall events were omitted. Convective rainfall generally occurs for a shorter duration with more intense rainfall than frontal rainfall (Thurai, *et al.*, 2016). Frontal rainfall occurs over a longer duration with steady rain which is generally not localised (Met Office, 2022) frontal rainfall was regarded as an ideal form of precipitation input for comparing the catchments in this study.

Figure 4.5.1 represents an example graph with monthly river flows and precipitation. Flood events were selected by identifying the events which occurred in both catchments simultaneously as it appeared likely that these events would have occurred from precipitation which occurred in both catchments.

Instruments at gauging stations are generally reliable, however if the instrument becomes exposed to air during low flows or is poorly placed and damaged during high flows, they can be a source of uncertainty as it is not easy to get to their remote location to check them often. Additionally, the climate has an impact on these instruments due to the extreme cold in the remote uplands of Scotland. The cold leads to the depletion of batteries and therefore potential gaps in the time-series data as well as freezing the instruments themselves. However, the data is rigorously checked, and periods of uncertain data are omitted from further analysis.

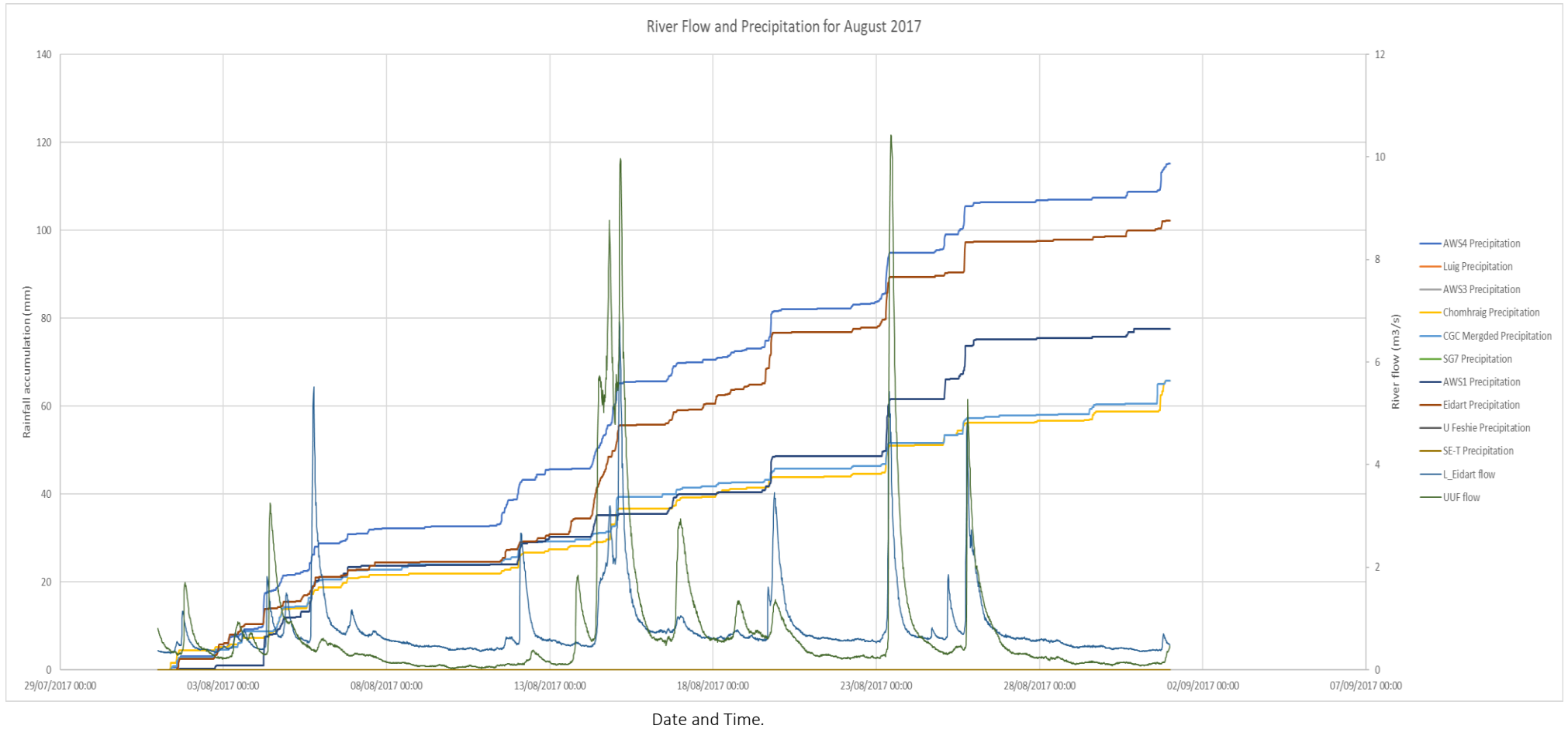


Figure 4.5.1. Flood Event Graphed with Precipitation for August 2017.

4.5.3 Event Analysis

The chosen events were graphed for visual analysis with precipitation data as seen in Figure 4.5.2, as in Lombard and Holschlag (2018). The peak discharge and timing were extracted and form a summary table as seen in Chapter 5, in Table 5.4.1 and Table 5.5.1. In addition to these values, the date and time of the peak of the precipitation was also noted from the singular rain gauge which covers both catchments. The peak of the rainfall was used for the lag time analysis as Black, *et al.*, (2021) mentions that it is one of many variations used when estimating time balance between rainfall and discharge.

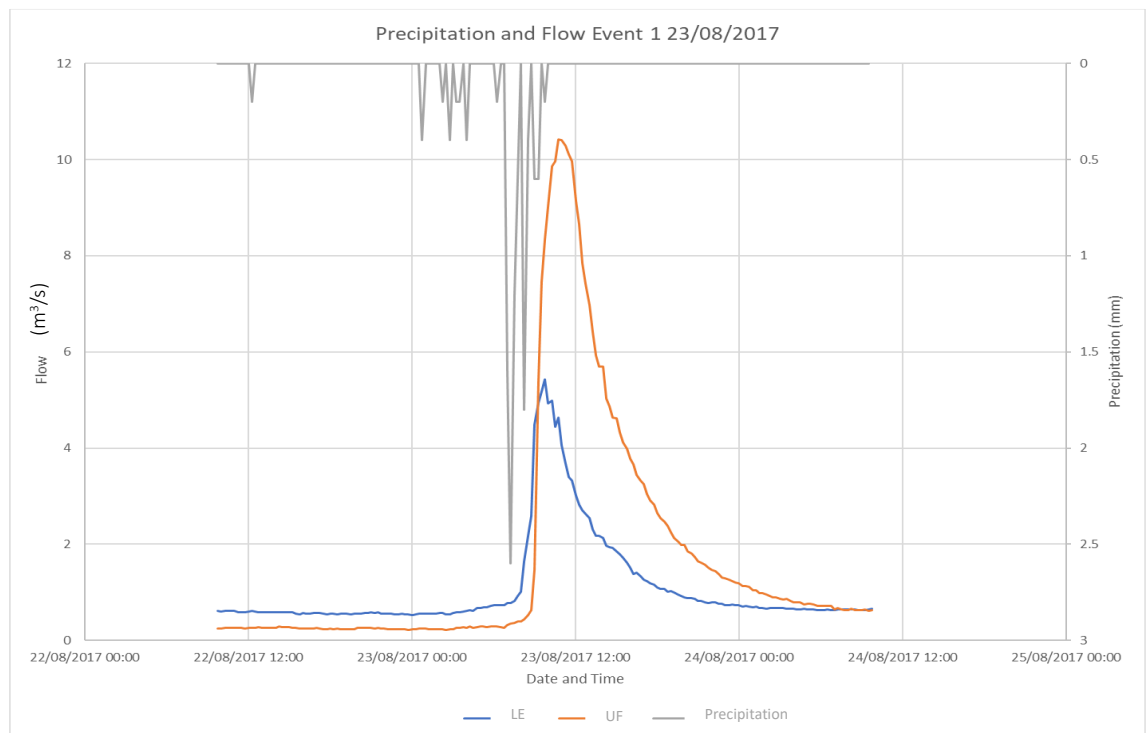


Figure 4.5.2 An Example Catchment Comparison Event.

Once a table of values had been achieved in terms of lag time to peak discharge, a statistical test was undertaken to calculate the significance of the difference in lag time to peak discharge in each catchment. The choice of statistical test is an important consideration and to decide which test would be required, a Shapiro-Wilk Normality Test (Shapiro and Wilk 1965). was first utilised to test if the lag time data for each catchment was normally distributed.

The data were not normally distributed as shown in Table 5.5.2 (Chapter 5, section 5.5) so the Mann-Whitney Wilcoxon Test of Difference was chosen similarly to Black, *et al.*, (2022). R-Studio software was chosen to carry out the statistical test as it is freely available and easy to use. The exact code used to carry out this test can be found in the appendices (Appendix B).

In addition to lag time analysis, hydrograph form from each event has been used to calculate a characteristic hydrograph. The requirement for a characteristic hydrograph shape of a given catchment is the basis of Archer, *et al.*, (2000). A characteristic hydrograph may be used in the exploration of the hydrological response of the two contrasting catchments in this study.

This method includes the generalisation of the shape of flood hydrographs which have been observed in time series data at gauging stations. The method may be split into three steps which can all be conducted using Microsoft Excel.

The first step is to derive the duration of exceedance of specific percentages of the event peak discharge. An example of percentages include: 10%, 20%, 30%, 40%, 50%, 60%, 70%, 80%, 85%, 90%, 95%, where the peak discharge is 100% of the flow of the event. The duration of exceedance can be synthesised before and after the peak by normalising the time of each event peak discharge to 0, this should create a more realistic, asymmetric hydrograph profile. The second step is to calculate the median value at each percentile of the peak flow after each event has been lined up and the peaks normalised to 0 hours. The median has been selected due to its insensitivity to outlier events, for example, an event with a particularly long duration may unduly influence the mean value for each percentile. The third step is to test the sensitivity of the analysis, this methodology can be applied to various subsets, for example, by ranking the events by peak discharge, input precipitation or seasonality. An example of what the graph should look like may be found in Figure 4.5.4 below.

In the median hydrograph synthesis in this research, events had already been selected to use clean hydrographs with one peak, or with minor secondary peaks which are not likely to largely skew the median values. The 14 events from which the hydrographs were synthesised were also chosen to omit snowmelt events so that reliable comparisons between the 2 catchments being assessed within this research could be made. The events chosen for this analysis are restricted considerably by the continuity of the time series data collected, as these are upland catchments, instrumentation is less likely

to perform to the ideal standard, and with all statistics, a greater sample would increase confidence within the analysis.

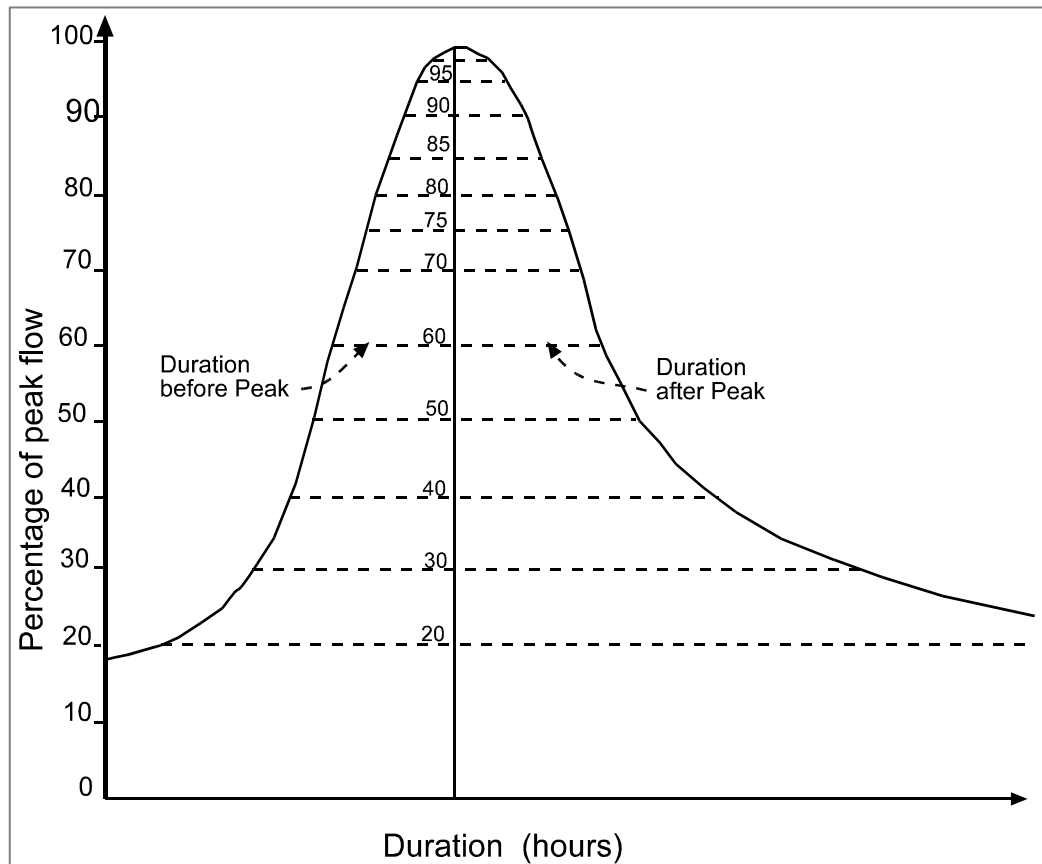


Figure 4.5.4. An Example of a Generalised Median Hydrograph. Source: Archer, *et al.*, (2000).

Chapter 5: Results

The results of this research are presented in the following chapter. Upper Feshie Confluence was descoped from the rating extension and validation process due to both time constraints and the constraint that the gauging station data for the study period was not continuous due to instrumentation failure. Therefore, no results for Upper Feshie Confluence will be presented except for the topographic survey and the creation of a median hydrograph on the basis of combining the flows from Upper Feshie and Lower Eidart.

5.1 Results of the Topographic Survey

The processed outputs from the topographic survey can be observed in Figures 5.1.0, 5.1.1, 5.1.2. and 5.1.3. The results are presented in the form of 2D elevation banding for the purpose of visualisation. The overall range of elevations surveyed were 508-517

m AOD and are represented in graduations of 0.5 m. Figures 5.1.1 and 5.1.2 display a significant thalweg feature whereas in Figure 5.1.3, the thalweg is less defined until the run-out pool.

Figures 5.1.4, 5.1.5 and 5.1.6 represents the gradient and horizontal distance of the three reaches which have been surveyed and modelled. Figure 5.1.4 represents Upper Feshie with a riverbed gradient of -0.016 and a horizontal distance of 262.124 m. Figure 5.1.5 highlights that Lower Eidart has a gradient of -0.016 and a horizontal distance of 124.755 m. Finally, Upper Feshie Confluence is 247.554 m long with a gradient of -0.017 (Figure 5.1.6). These features are extremely important input parameters for hydraulic modelling as reach length can have a significant impact on the stability of a model, and gradient can be used in 1D HEC-RAS modelling as the normal depth boundary condition.

Figures 5.1.7, 5.1.8, and 5.1.9 are representations of the surveyed topography at each reach gauging station. The cross-sectional geometry is a particular important output from the topographic survey as it can be used for various analysis, including independent verification of the modelling process. Figure 5.1.7 shows that Upper Feshies thalweg occurs at 10 m across the section at an elevation of 544.2 m AOD. Figure 5.1.8 shows that Lower Eidarts thalweg occurs at 522.3 m AOD, and at 23 m across the cross section. Finally Figure 5.1.9 shows that Upper Feshie Confluence has a thalweg at 507.3 m AOD, which occurs at 29 m across the cross section.

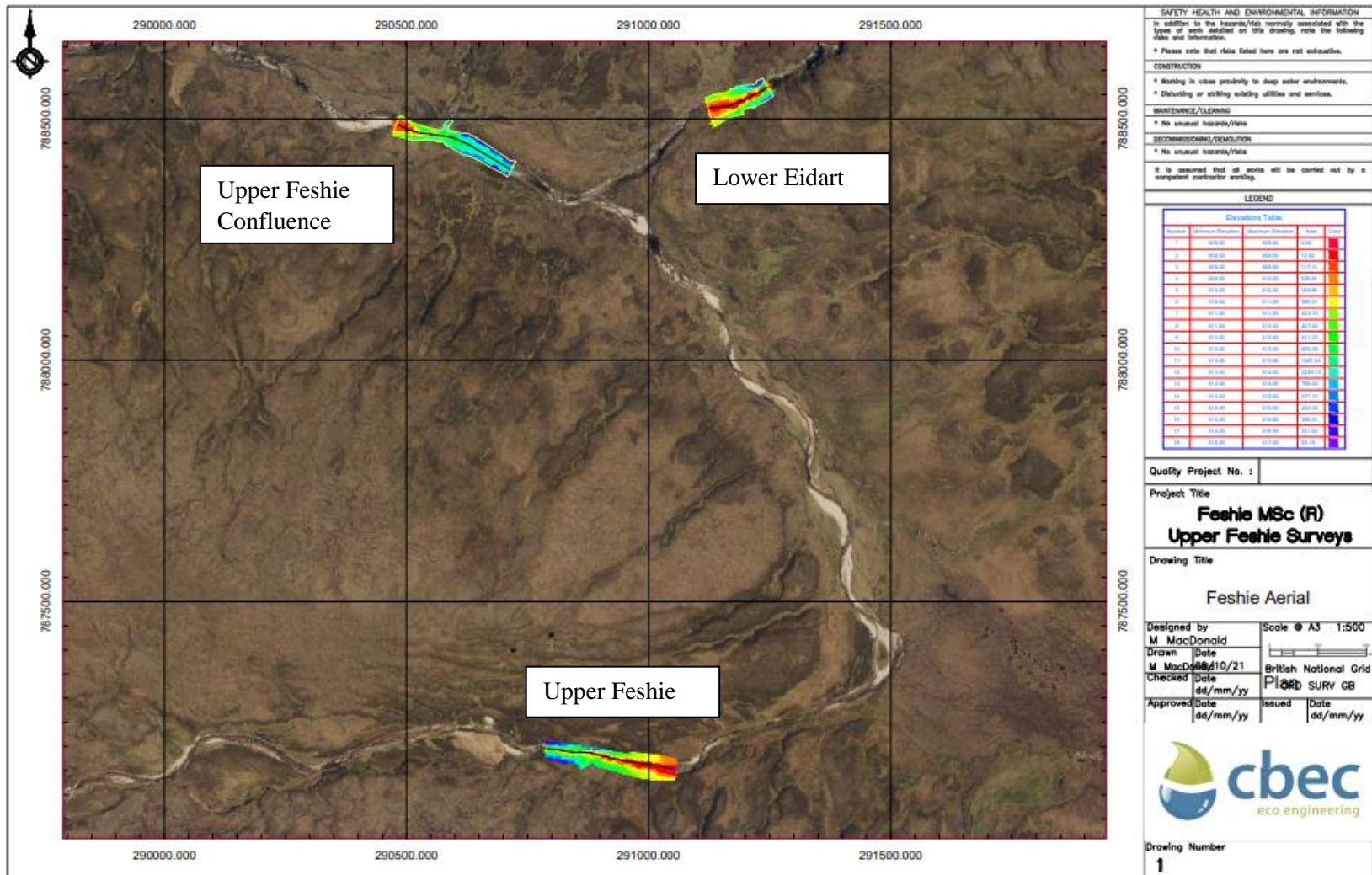


Figure 5.1.0 The Digital Terrain Models of the Three Surveyed Reaches. Scale Enhanced in Figure 5.1.1

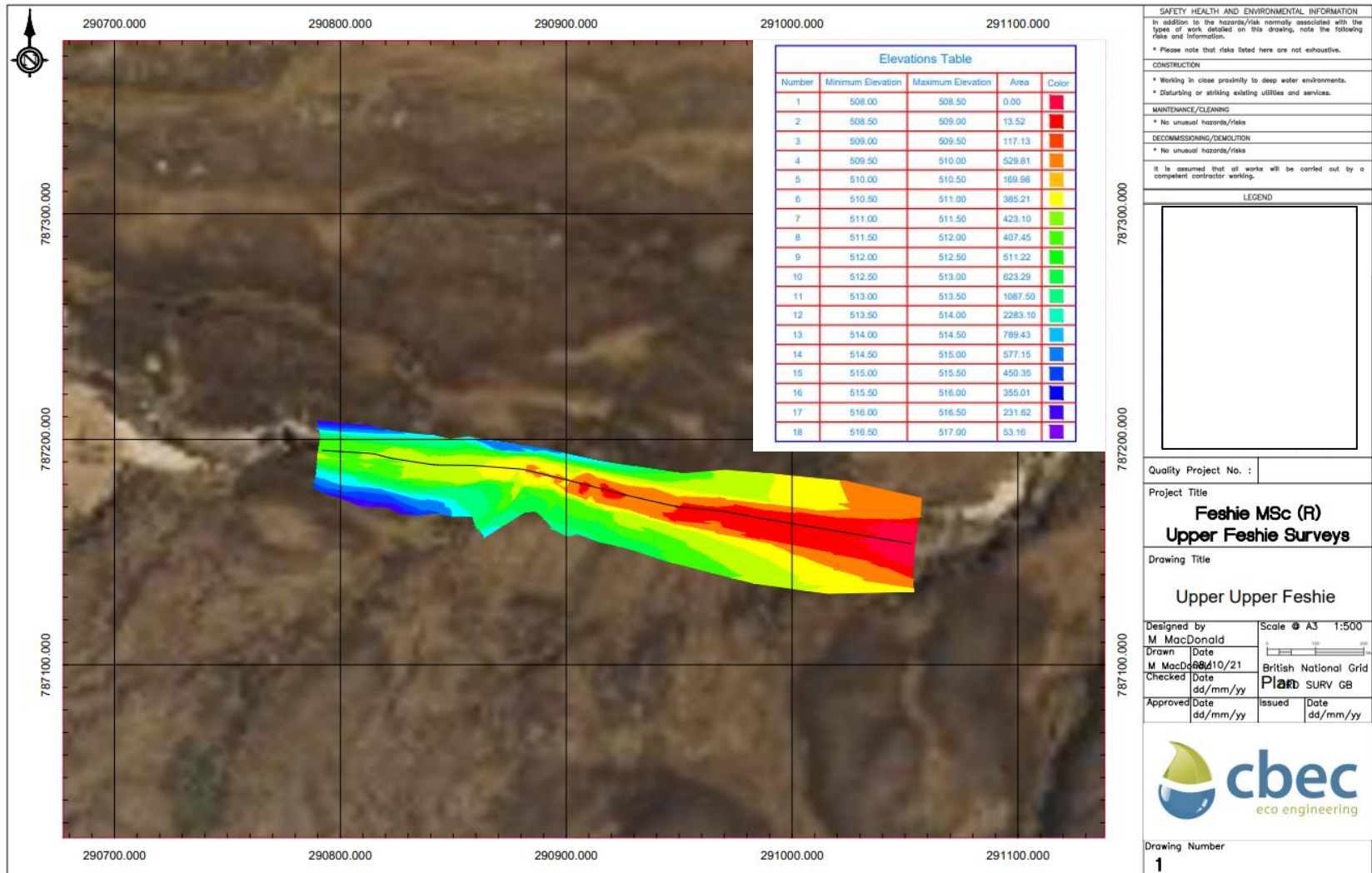


Figure 5.1.1 The Digital Terrain Model of Upper Feshie.

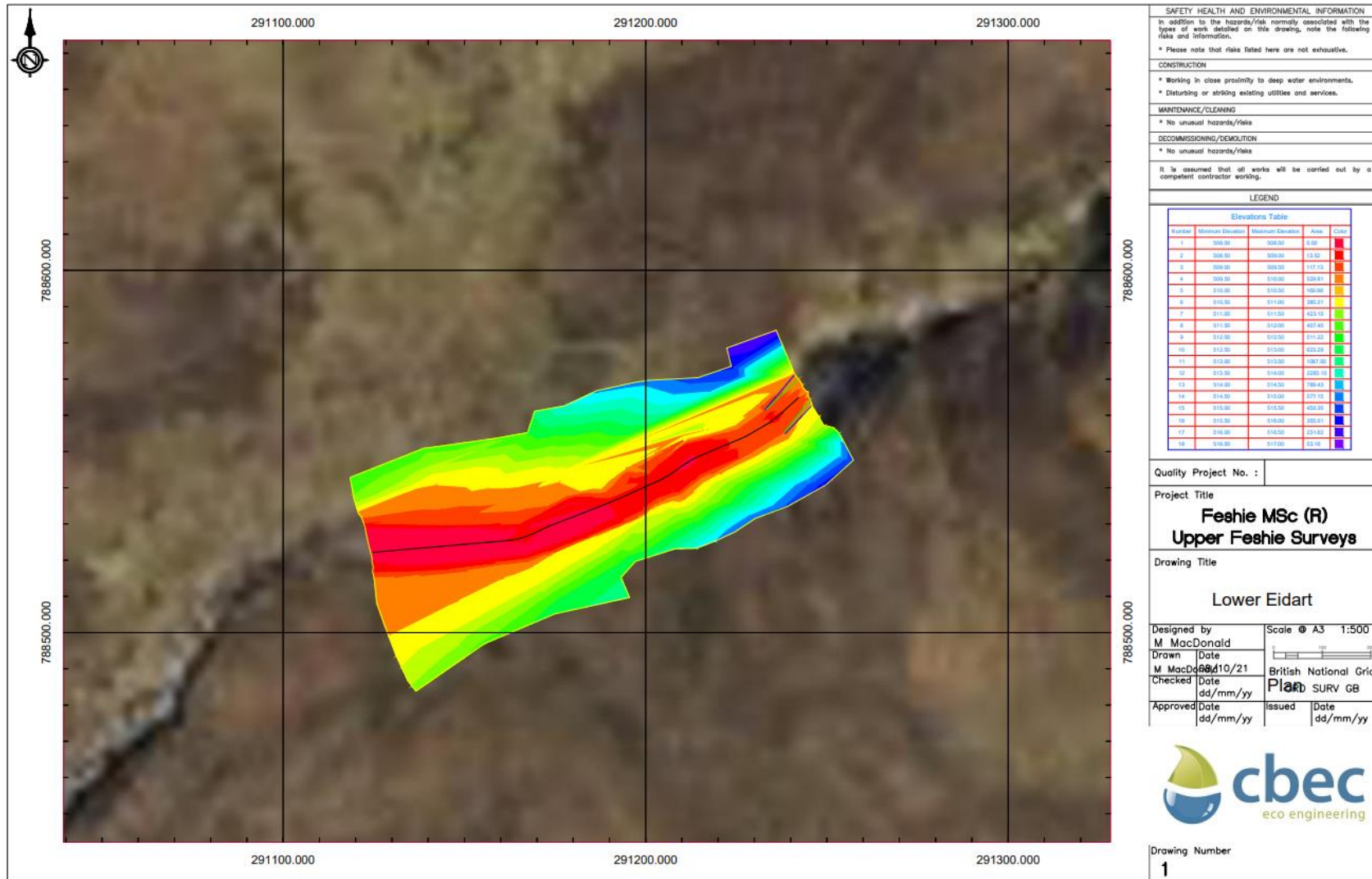


Figure 5.1.2 The Digital Terrain Model of Lower Eidart. Scale Enhanced in Figure 5.1.1

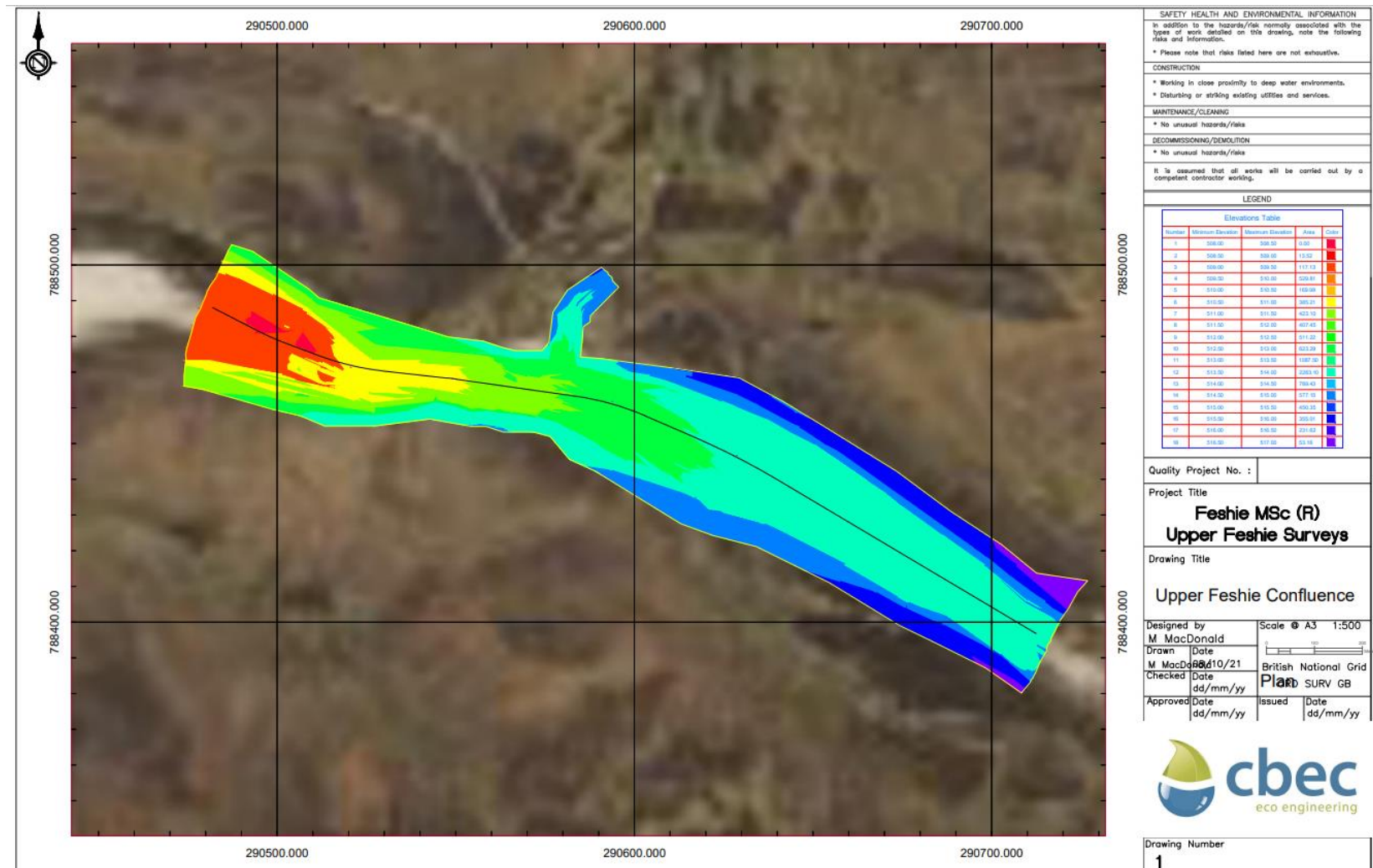


Figure 5.1.3 The Digital Terrain Model of Upper Feshie Confluence. Scale Enhanced in Figure 5.1.1



Figure 5.1.4 *The Geometry Summary of Upper Feshie.*

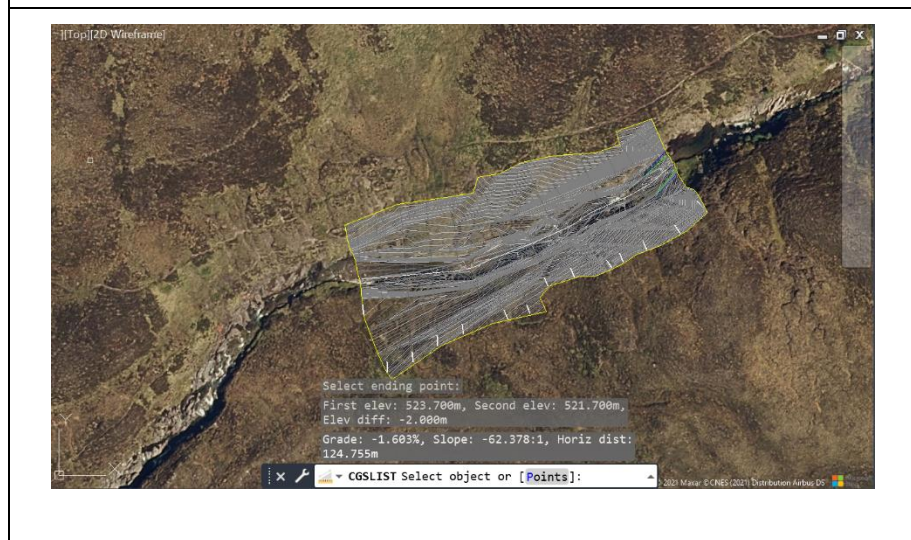


Figure 5.1.5 *The Geometry Summary of Lower Eidart.*



Figure 5.1.6 *The Geometry Summary of Upper Feshie Confluence.*

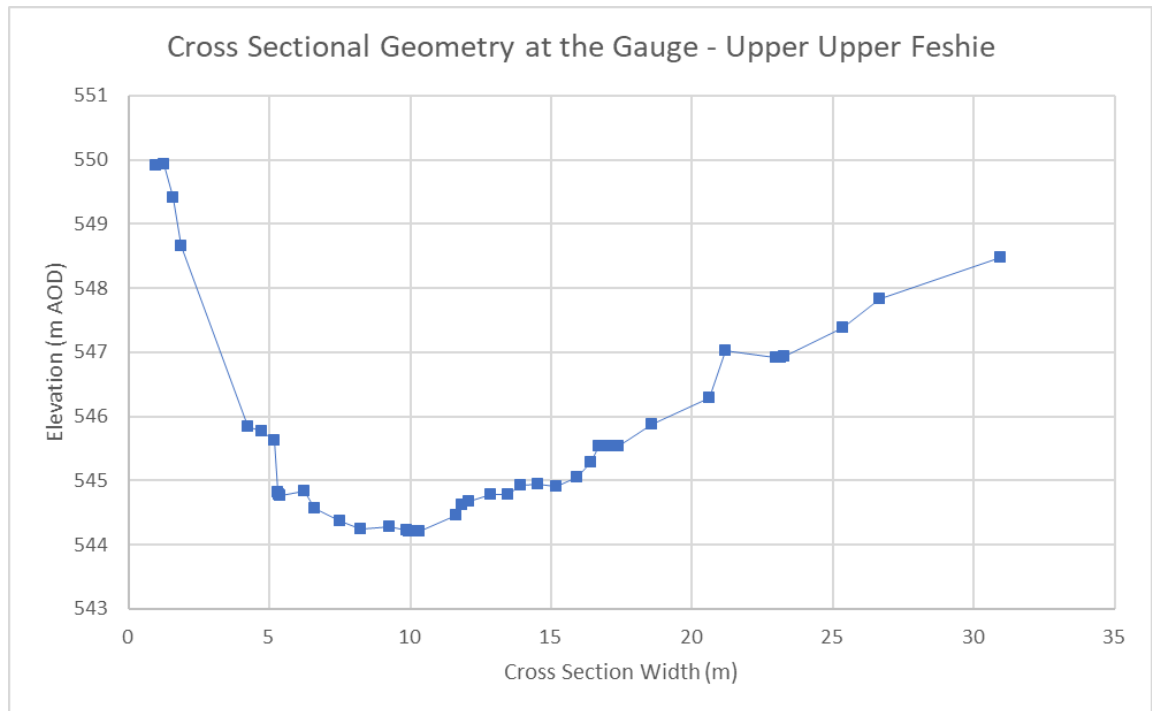


Figure 5.1.7 *The Cross-Sectional Geometry at the Gauge - Upper Feshie.*

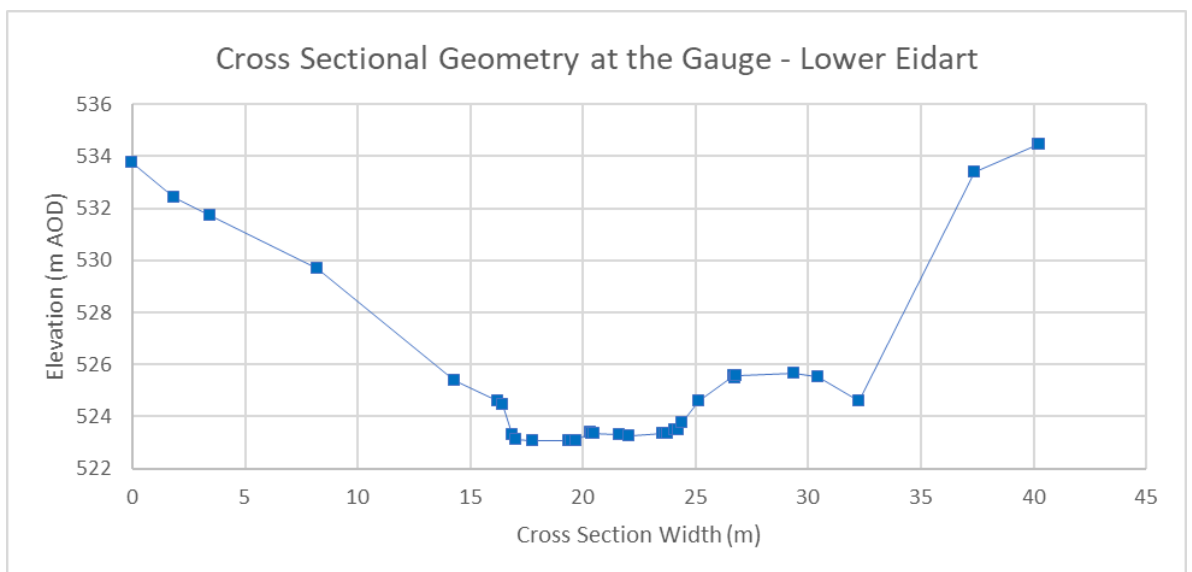


Figure 5.1.8 *The Cross-Sectional Geometry at the Gauge - Lower Eidart.*

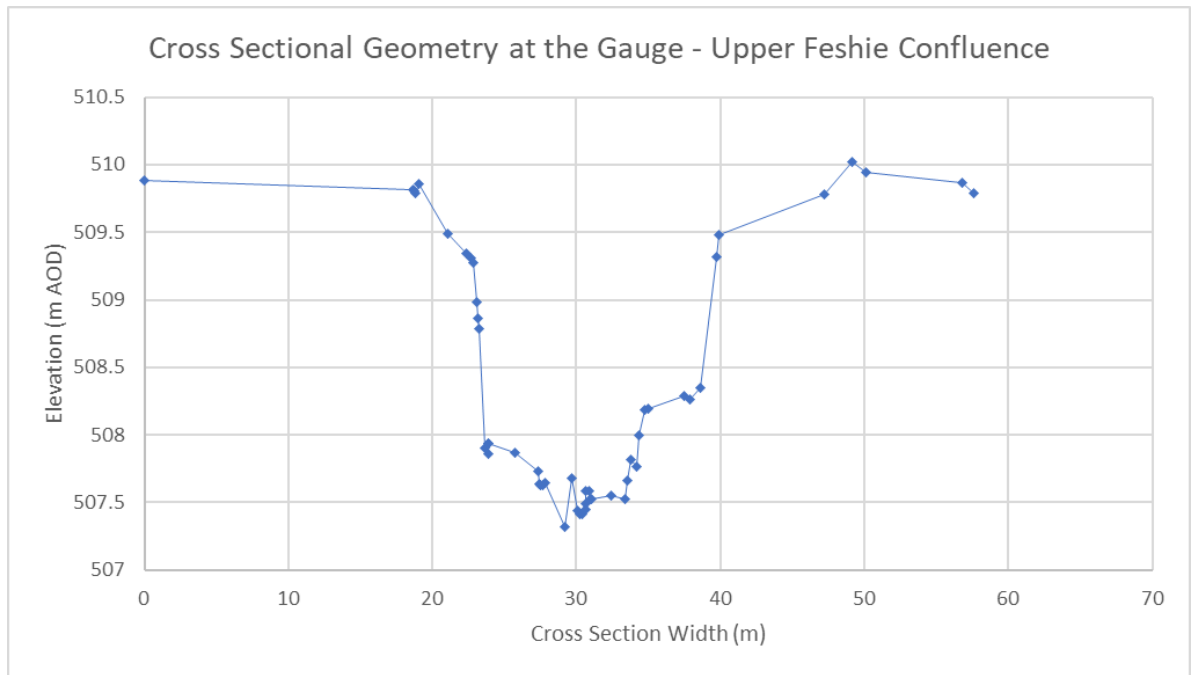


Figure 5.1.9 *The Cross-Sectional Geometry at the Gauge- Upper Feshie Confluence.*

5.2 Results of the Hydraulic Modelling.

Summary output tables from the HEC-RAS modelling can be observed in Figures 5.2.1 and 5.2.3. These include a summary of computed outputs from the input ‘PF’ or profile flows. For the purpose of this research, the hydraulic depth for the input flow was required. A summary table is generated for each input flow and at each cross section. At PF1 (0.38 Q m³/s) at Upper Feshie (Figure 5.2.1), a hydraulic depth was calculated at 0.45 m. At Lower Eidart (Figure 5.2.3), for an input flow of 0.47 m³/s a hydraulic depth of 0.70 m was calculated. These three input flows were chosen as they were the flows recorded on the day of the survey so that a comparison of observed stage and HEC-RAS stage could be made.

Figures 5.2.2 and 5.2.4 show the graphical expression of the stage-discharge rating equations generated by the hydraulic depth values that are exemplified in Figures 5.2.1, 5.2.3 and which were chosen to cover a range of flows from dryweather flows to extreme floods corresponding to at least 3 m³/s per km² (expected to be close to probable maximum flood based on Acreman (1989)). These rating curves were the expression of the rating equations which were derived from the HEC-RAS, which can be seen in Table 5.2.1. Due to the creation of several hundred of these output tables, the output summary tables from the gauging stations have been presented in this chapter. The output values from all the output tables were collated and are summarised in Table 5.2.2. It is from Table 5.2.2 that the rating curves in Figures 5.2.2 and 5.2.4 are calibrated.

Table 5.2.2 contains the stage-discharge data which inform the equations noted in this chapter. In addition to the HEC-RAS stages, there are several empirical flow gaugings which pre-date this research. These data have been provided and were included in the equations.

Table 5.2.1. Rating Equation Results from HEC-RAS

Reach	Equation	Corresponding Figure
Upper Feshie	$Q = 33.4(h-1.1)^{1.5}$	5.2.2
Lower Eidart	$Q = 18(h-0.83)^4$	5.2.4

Plan: Plan 01 Feshie_UUF UUF-CL RS: 40 Profile: PF 1					
Element	Left OB	Channel	Right OB		
E.G. Elev (m)	546.21				
Vel Head (m)	0.00				
W.S. Elev (m)	546.21				
Crit W.S. (m)					
E.G. Slope (m/m)	0.000014				
Q Total (m3/s)	0.38				
Top Width (m)	13.00				
Vel Total (m/s)	0.06				
Max Chl Dpth (m)	0.75				
Conv. Total (m3/s)	101.2				
Length Wtd. (m)	10.00				
Min Ch El (m)	545.46				
Alpha	1.00				
Frctn Loss (m)	0.00				
C & E Loss (m)	0.00				
Element					
Wt. n-Val.		0.033			
Reach Len. (m)	10.00	10.00	10.00		
Flow Area (m2)		5.85			
Area (m2)		5.85			
Flow (m3/s)		0.38			
Top Width (m)		13.00			
Avg. Vel. (m/s)		0.06			
Hydr. Depth (m)		0.45			
Conv. (m3/s)		101.2			
Wetted Per. (m)		13.55			
Shear (N/m2)		0.06			
Stream Power (N/m s)		0.00			
Cum Volume (1000 m3)		0.00			
Cum SA (1000 m2)		0.40			

Errors, Warnings and Notes

Warning: The conveyance ratio (upstream conveyance divided by downstream conveyance) is less than 0.7 or greater than 1.4. This may indicate the need for additional cross sections.

Select River Station

Figure 5.2.1 An Example Cross Section Output Table for the Gauging Station for the Reach Upper Feshie.

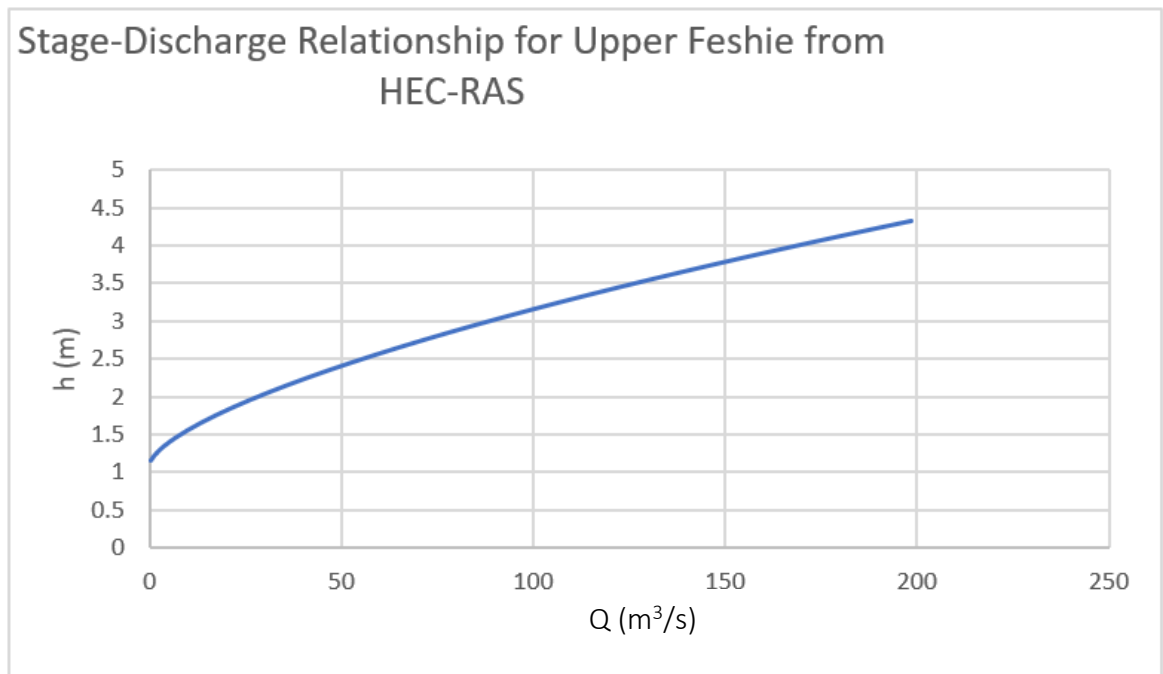


Figure 5.2.2 The Stage Discharge Relationship at Upper Feshie from HEC-RAS.

Cross Section Output

File Type Options Help

River: LE-Test Profile: PF 1

Reach: LE-CL RS: 20 Plan: Plan 03

Plan: Plan 03 LE-Test LE-CL RS: 20 Profile: PF 1

Element	Left OB	Channel	Right OB
E.G. Elev (m)	523.95		
Vel Head (m)	0.00		
W.S. Elev (m)	523.95		
Crit W.S. (m)			
E.G. Slope (m/m)	0.000014		
Q Total (m ³ /s)	0.47		
Top Width (m)	7.99		
Vel Total (m/s)	0.08		
Max Chl Dpth (m)	0.91		
Conv. Total (m ³ /s)	123.7		
Length Wtd. (m)	10.00		
Min Ch El (m)	523.05		
Alpha	1.00		
Frctn Loss (m)	0.00		
C & E Loss (m)	0.00		
Wt. n-Val.		0.033	
Reach Len. (m)	10.00	10.00	10.00
Flow Area (m ²)		5.57	
Area (m ²)		5.57	
Flow (m ³ /s)		0.47	
Top Width (m)		7.99	
Avg. Vel. (m/s)		0.08	
Hydr. Depth (m)		0.70	
Conv. (m ³ /s)		123.7	
Wetted Per. (m)		8.88	
Shear (N/m ²)		0.09	
Stream Power (N/m s)		0.01	
Cum Volume (1000 m ³)		0.10	
Cum SA (1000 m ²)		0.16	

Errors, Warnings and Notes

Enter to move to next downstream river station location

Figure 5.2.3 An Example Cross Section Output Table for the Gauging Station for the Reach Lower Eidart.

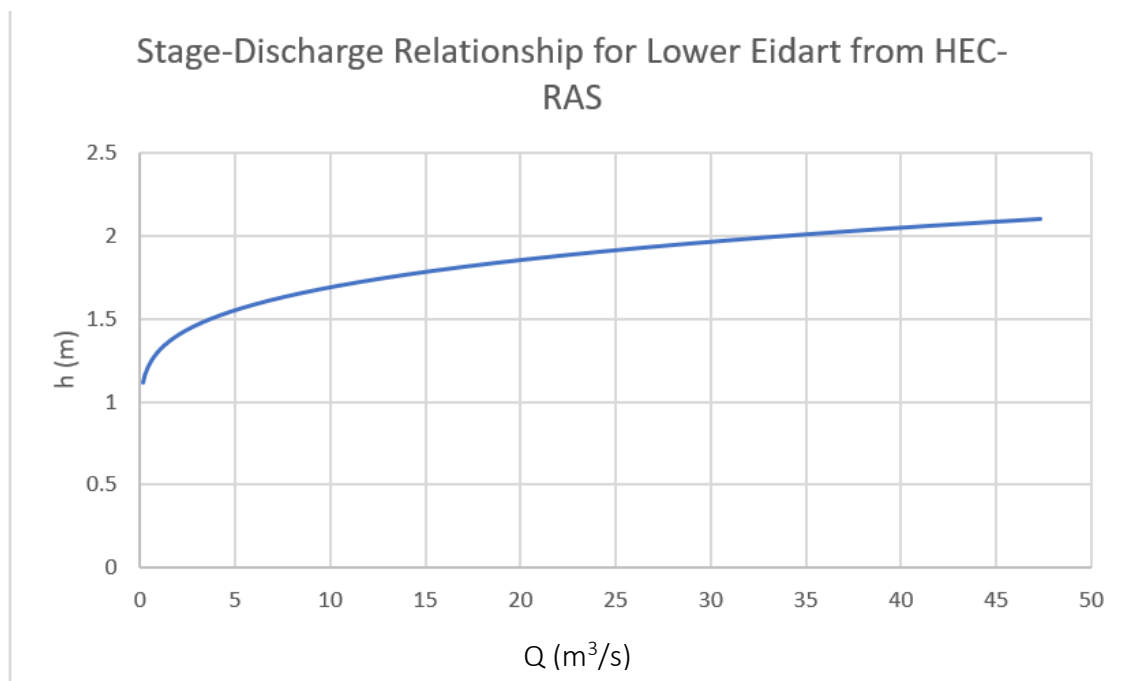


Figure 5.2.4 The Stage Discharge Relationship at Lower Eidart from HEC-RAS.

Table 5.2.2 Summarised Hydraulic Depth Outputs for Input Flows from HEC-RAS with Observed Gaugings and Stage Measurements.

Upper Feshie		Lower Eidart	
Q (m ³ /s)	Stage (m)	Q (m ³ /s)	Stage (m)
Gaugings			
1.20	1.31	0.532	1.249
0.52	1.20	0.174355	1.176
0.93	1.30	0.256134	1.201
0.59	1.23	0.410749	1.246
0.61	1.23	0.274739	1.194
1.07	1.30	0.131731	1.149
0.97	1.30	HEC-RAS	
0.49	1.21	0.37	1.22
0.16	1.12	2.00	1.41
HEC-RAS		4.00	1.56
0.47	1.21	6.00	1.57
2.00	1.41	8.00	1.62
4.00	1.51	10.00	1.65
8.00	1.65	12.00	1.66
10.00	1.71	12.50	1.69
12.00	1.73	13.00	1.72
14.00	1.75	13.50	1.74
16.00	1.77	14.00	1.75
18.00	1.79	14.50	1.76
20.00	1.80	15.00	1.77
25.00	1.84	15.50	1.78
30.00	1.86	16.00	1.79
35.00	1.87	18.00	1.83
40.00	1.90	20.00	1.88
45.00	2.00	25.00	2.00
50.00	2.10	30.00	2.10
55.00	2.16	35.00	2.15
60.00	2.22	36.00	2.16
65.00	2.29	37.00	2.16
70.00	2.36	38.00	2.16
75.00	2.42	39.00	2.16
80.00	2.48	40.00	2.16
85.00	2.54	41.00	2.17
90.00	2.59	42.00	2.17
95.00	2.64	43.00	2.18
100.00	2.69	44.00	2.19
150.00	3.19	45.00	2.20
200.00	3.50	50.00	2.30
		55.00	2.40
		60.00	2.50
		65.00	2.59
		70.00	2.69
		75.00	2.78
		80.00	2.88
		85.00	2.96
		90.00	3.05
		95.00	3.13
		100.00	3.21
		150.00	3.84
		200.00	4.33

5.3 Quality Review Results

A three-part quality review process was used to verify the results of the HEC-RAS modelling. The first and second tier of quality review process were visual analysis and then application of the derived ratings to assess water balance. A description of what was deemed visually acceptable is noted in Chapter 4. If the visual analysis presented issues with the rating equations, a multi-part rating was used as detailed in Chapter 4.

The second part consisted of applying the derived rating equation to the time series data to initially sense check the results. Once the rating had been applied, observation of the data was carried out to look for issues, for example flows which seem disproportionately high or low and unrealistic water balance. Table 5.3.1 outlines the results of applying these equations to gauge if the peak flow and mean annual runoff appear to be reasonable results in the context of these catchments. The results outlined in Table 5.3.1 show that the results of the initially derived rating equation are an unrealistic 715 m³/s and a mean annual runoff of 1600 mm for the Lower Eidart catchment. Additionally, the Upper Feshie catchment produced a peak flow of 20.2 m³/s and 1268 mm of mean annual runoff. These results are representative of the time series data they were applied to (01/08/2017-22/06/2018) which had approximately 1400 mm of rainfall observed in the rainfall. Additionally, Soulsby, *et al.*, (2006) presents that Lower Eidart receives 1653 mm of annual precipitation depth with Upper Feshie receiving 1423 mm. It is possible that the rain gauges from which these precipitation data were observed could over or underestimate precipitation observations based on calibration, refer to Section 4.4.2.

Table 5.3.1 Results of the 2nd Tier Quality Review Process and Precipitation Data.

HEC-RAS		
River	Peak Discharge (m ³ /s)	Mean Annual Runoff (mm)
Lower Eidart	715	1600
Upper Feshie	20.2	1268
Q= VA		
Lower Eidart	11.8	1183
Upper Feshie	20.2	1268
Average Precipitation Depth (mm (Soulsby, <i>et al.</i> , 2006))		
Time Series	Lower Eidart	Upper Feshie
~1400	1654	1423

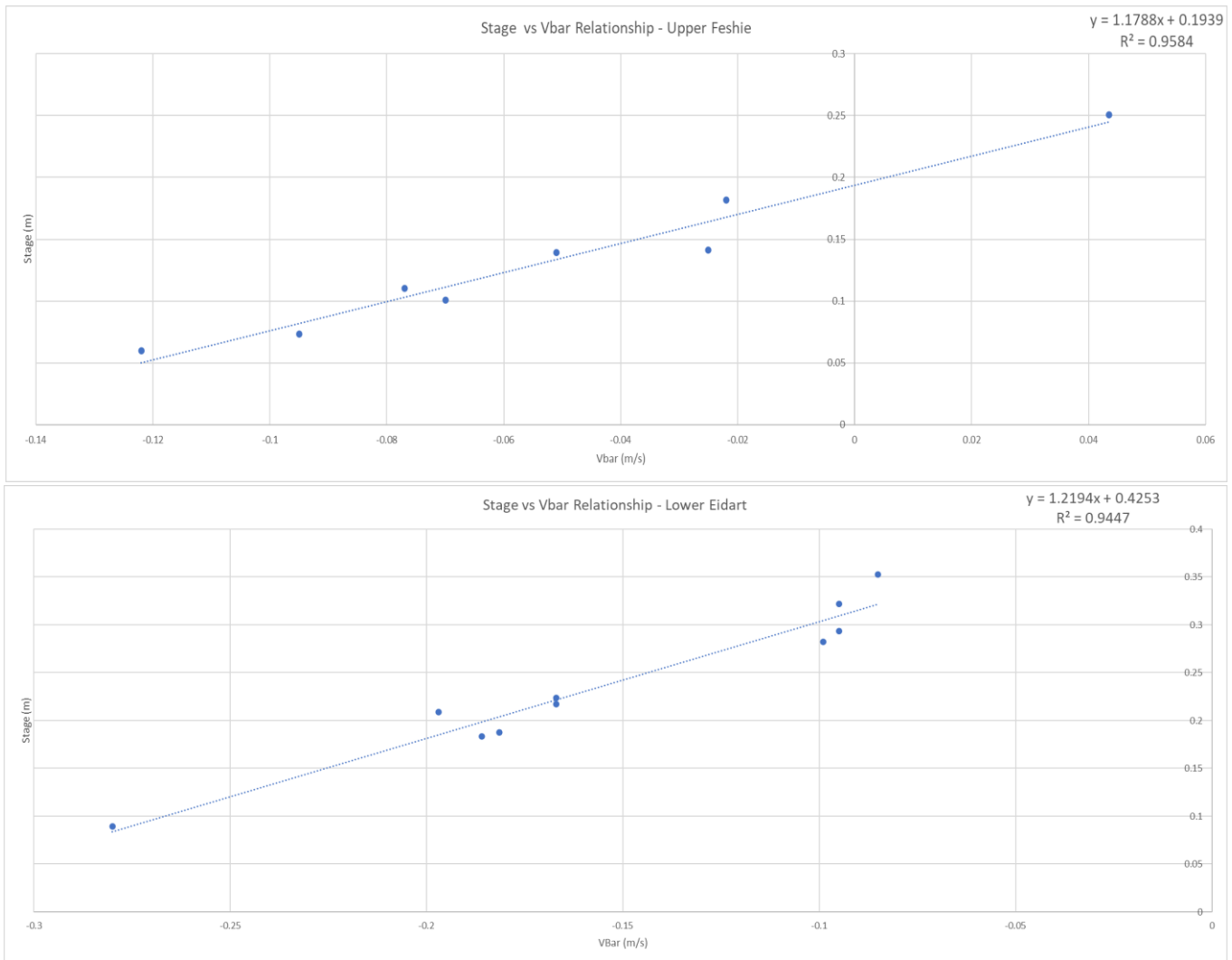


Figure 5.3.1 *The Relationship Between Stage and Vbar for Lower Eidart and Upper Feshie.*

The third tier of the quality review process was the use of the velocity multiplied by the cross-sectional area ($Q = VA$) method. The $Q = VA$ method is explained in Chapter 4 and can be extremely useful for the verification of the modelling as the $Q = VA$ is considered a standalone methodology for rating curve creation (Ramsbottom and Whitlow, 2003). Figures 5.3.1, 5.3.2 and 5.3.3 are the results for the sequence of steps in the $Q=VA$ method. Figure 5.3.4 is a rating equation generated by HEC-RAS but was included in this section for ease of visualisation between the ratings.

Figure 5.3.1 highlights the relationship between average velocity and stage which is the first step which is the first step in the $Q=VA$ method. Figure 5.3.1 highlights which average velocity occurs at which stage. The second step is presented in Figure 5.3.2 where the relationship between stage and cross-sectional area. The concave curve shown in Figure 5.3.2 is a result of a non-linear relationship between an increase of wetted cross-

sectional area as river stage increases. The significance of this relationship increases as river stage increases due to wetted area width. An example of this is detailed in Figure 5.3.2 where the river stage is a critical influence on the significance of the increase in wetted area as stage increases. In Figure 5.3.2, a stage increases of one meter from a river level of one-meter leads to an increase in wetted area of 12 m² whereas a stage increase of one meter from a prior river level of two metres leads to a change in wetted area of 15 m². Finally, if the researcher can establish the mean velocity (\bar{V}) at a given stage from Figure 5.3.1 and the wetted cross-sectional area at the same given stage (Figure 5.3.2) then they can apply the formula $Q=VA$ to get a flow in m³/s which is the stage-flow relationship, as presented in Figure 5.3.3.

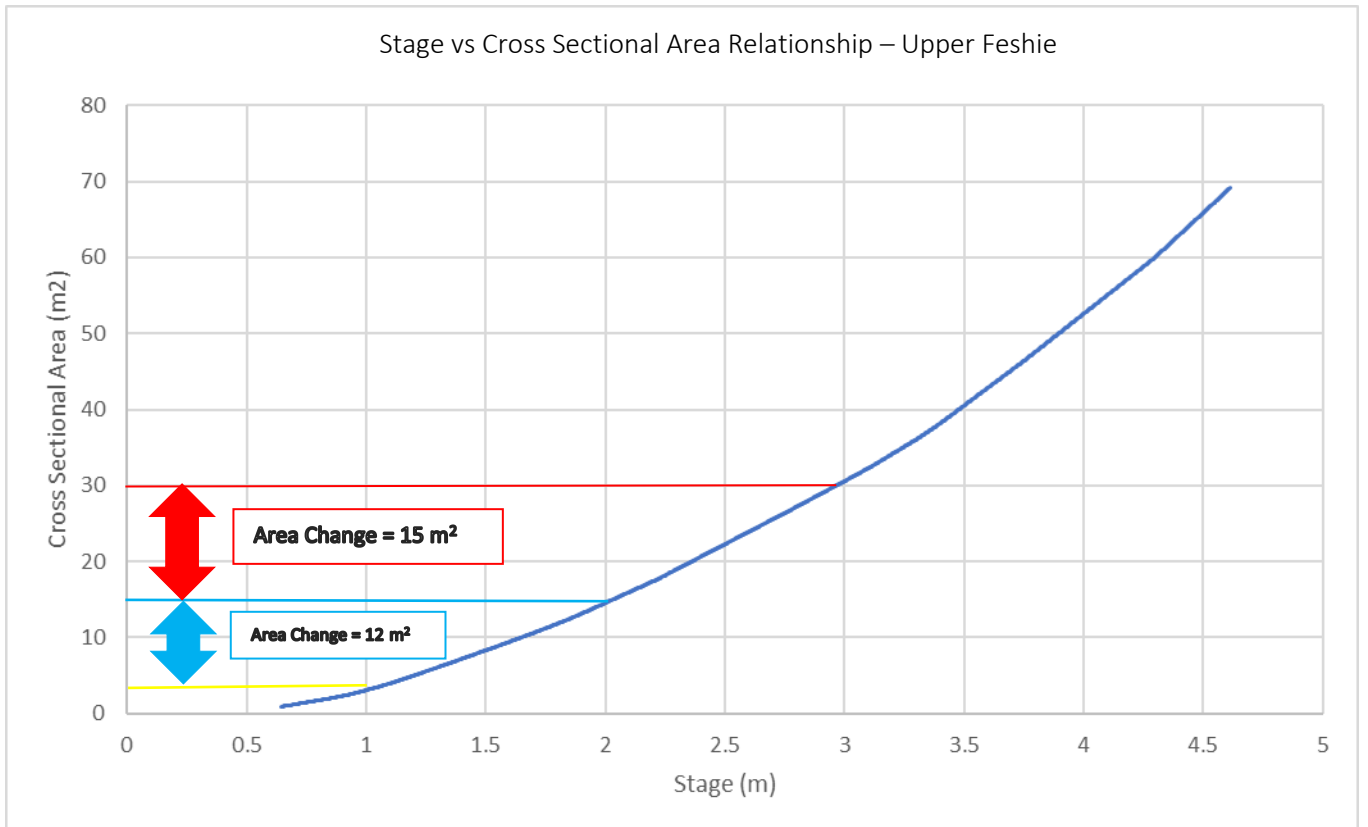


Figure 5.3.2 *The Relationship Between Stage and Area for Lower Eidart and Upper Feshie.*

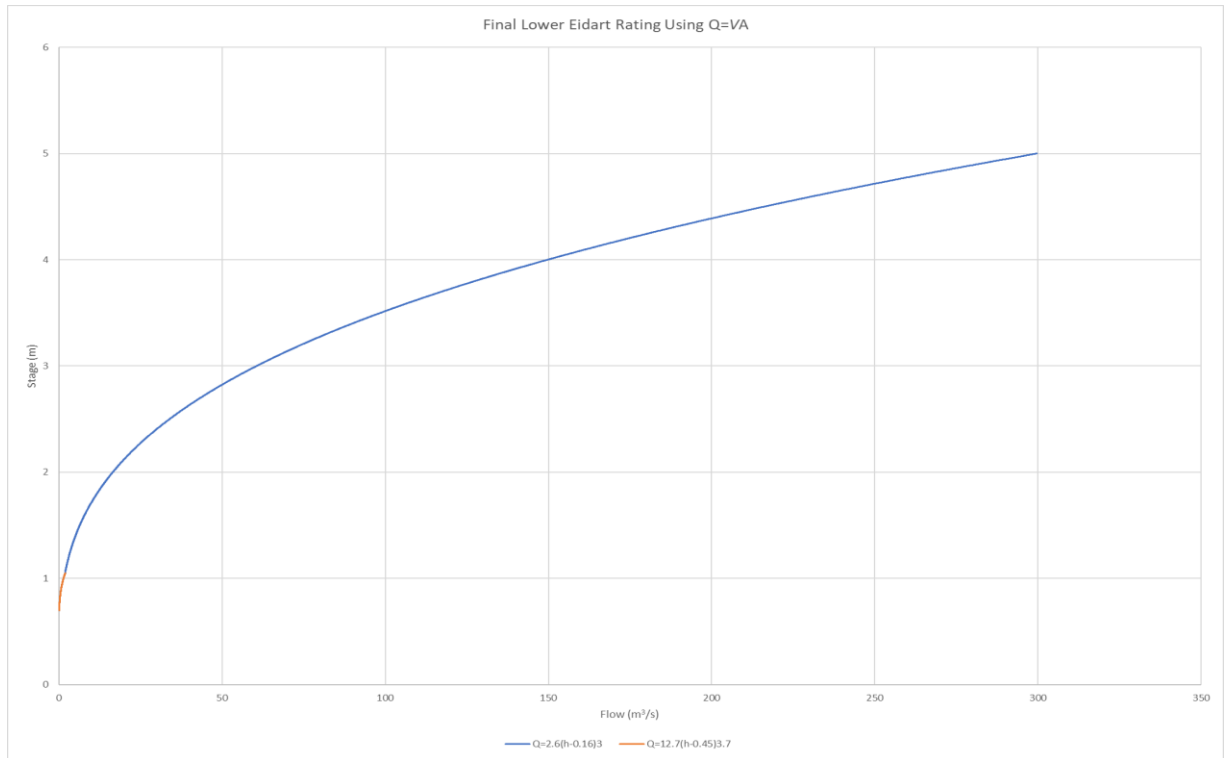


Figure 5.3.3 The $Q = VA$ Final Rating Curve for Lower Eidart

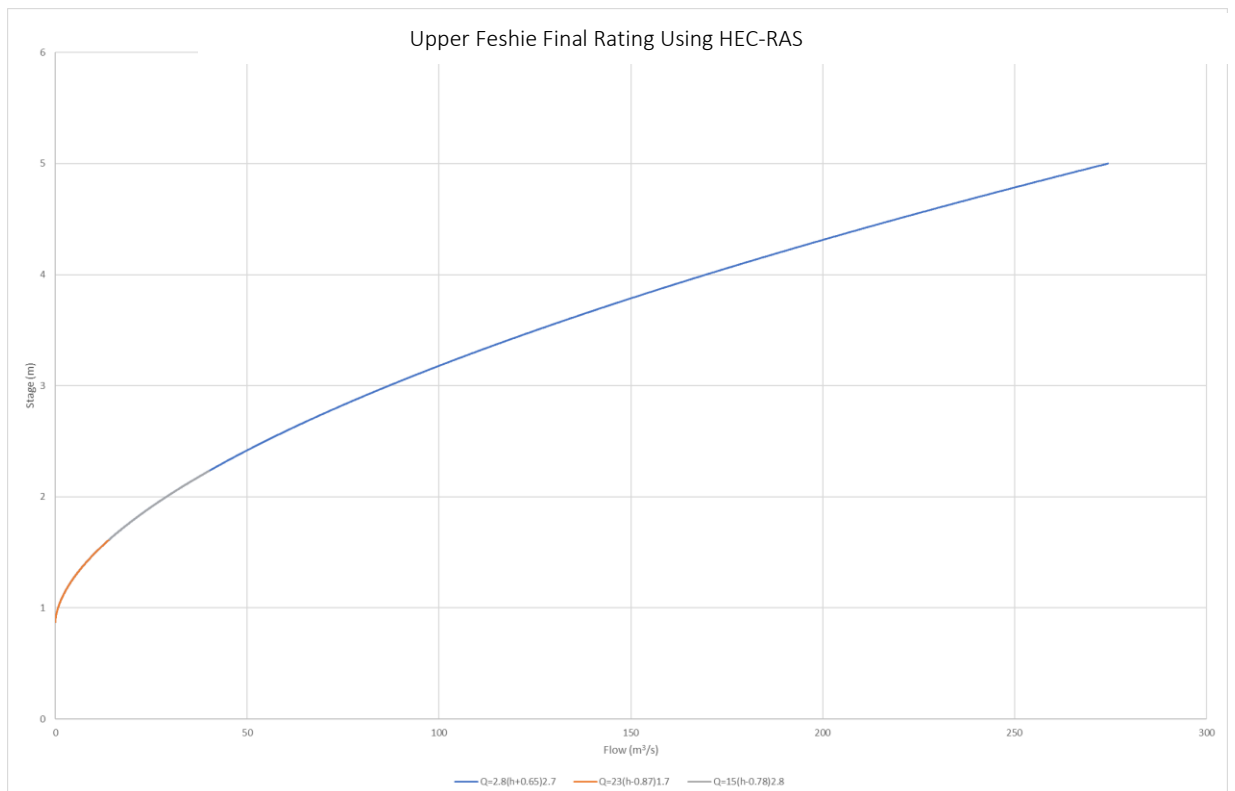


Figure 5.3.4 The HEC-RAS Final Rating Curve for Upper Feshie

Table 5.3.1 describes the results obtained using the $Q = VA$ method, highlighting that the results for Lower Eidart were $11.8 \text{ m}^3/\text{s}$ and 1183 mm of annual runoff depth.

The results generated by the $Q = VA$ method were extremely different from HEC-RAS for Lower Eidart with a peak flow of $703.2 \text{ m}^3/\text{s}$ less than the HEC-RAS estimation $715 \text{ m}^3/\text{s}$ being observed in the time series and 417 mm less mean annual runoff being calculated for a period of record with approximately 1400 mm of rainfall. In addition, Soulsby, *et al.*, (2006) presents that mean precipitation in the Eidart catchment is 1654 mm and is 1423 mm for the Upper Feshie catchment so a mean annual runoff of 1600 is not permissible as other factors such as evaporation and storage come into play.

Figure 5.3.3 demonstrates the final rating curve for Lower Eidart which is made up of a two-part rating equation where the limb parameters and breakpoints are described in Table 5.3.2. Additionally, Table 5.3.3 describes the final rating for Upper Feshie. The final rating for Upper Feshie can be observed in Figure 5.3.4 and was generated by HEC-RAS modelling and the solver, fitting the curve to the data. The letters in Tables 5.3.2 and 5.3.3 correspond to the parameters of the rating equation, which takes the form of $Q = a(h+b)^c$. The numbers that appear alongside each parameter correspond to a particular limb of the rating equation, in the case of Lower Eidart, limbs one and two. Break point, or BP, relates to the point where one part of the rating equation changes to another, for example from $Q = a_1(h+b_1)^{c_1}$ to $Q = a_2(h+b_2)^{c_2}$. These break points are recorded in terms of flow.

Table 5.3.2 Results of the Quality Review Process on Lower Eidarts Rating.

Rating Parameters	a1	12.66	a2	2.64	Bp1 (m ³ /s)
Lower Eidart	b1	-0.45	b2	-0.16	1.05
	c1	3.7	c2	3	

Table 5.3.3 Results of the Quality Review Process on Upper Feshies Rating.

Rating Parameters	a1	23.39	a2	15.2	a3	2.79	Bp1 (m ³ /s)	Bp2 (m ³ /s)
Upper Feshie	b1	-0.45	b2	-0.78	b3	0.65	14	40
	c1	3.7	c2	2.8	c3	2.66		

5.4 Results of Applying the Final Rating to Events

Application of the final rating curves to the time series data is a key part of identifying events for direct comparison between catchments. The resultant events can be observed in the text, in Figures 5.4.1 which contains all 14 flood event comparisons.

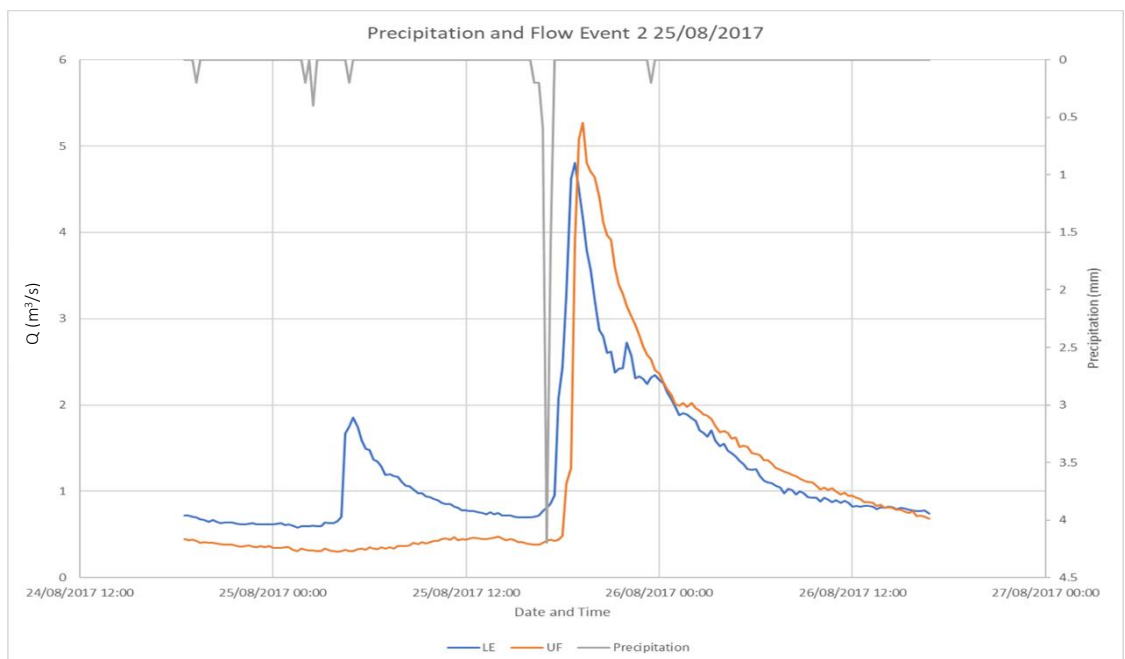
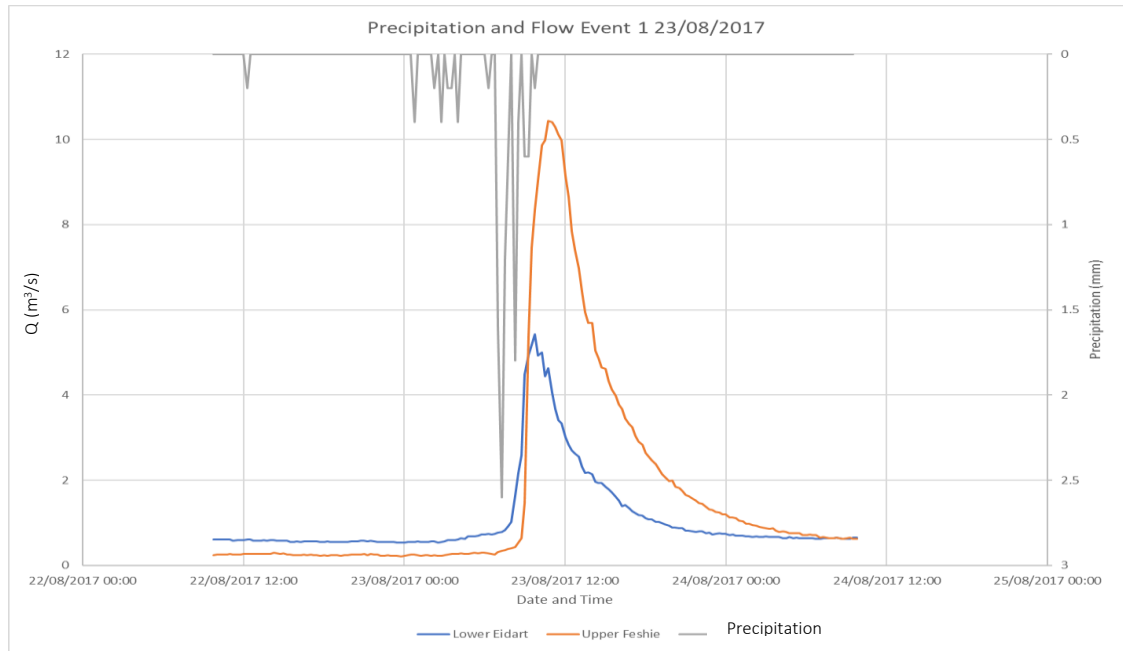


Figure 5.4.1. Comparison Between Upper Feshie and Lower Eidart for 14 Events.

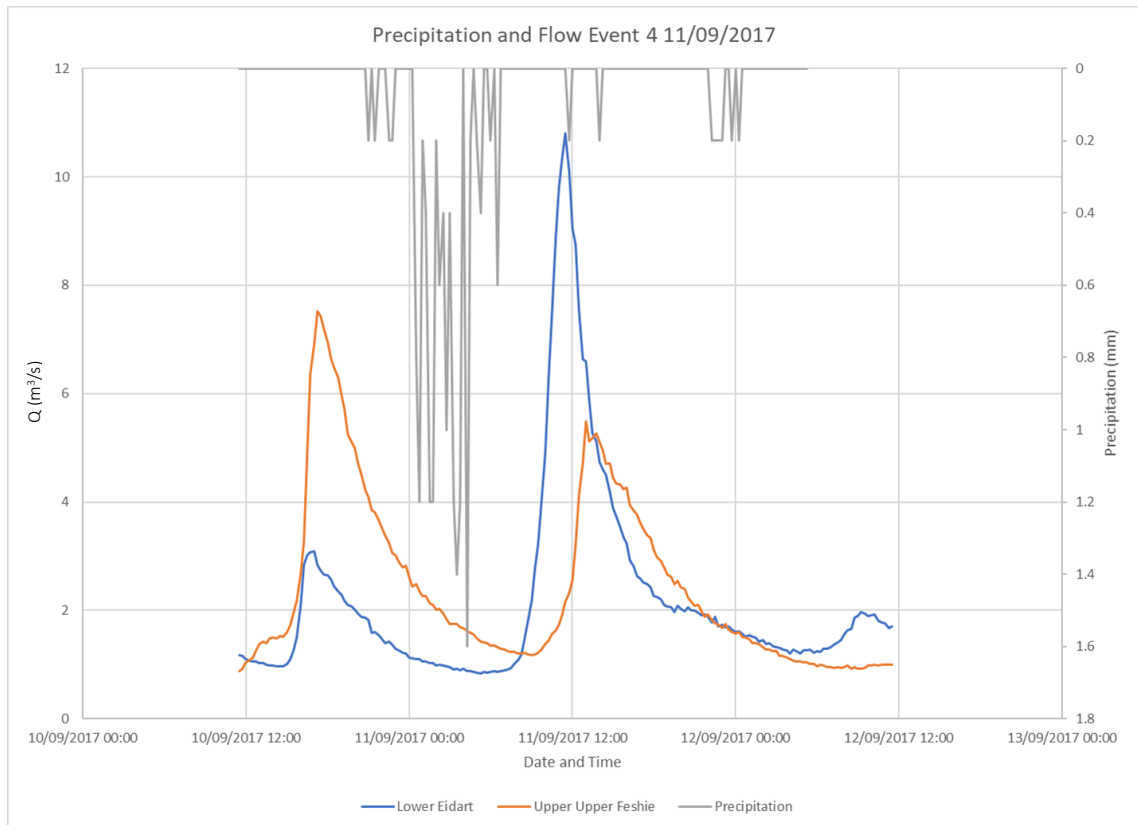
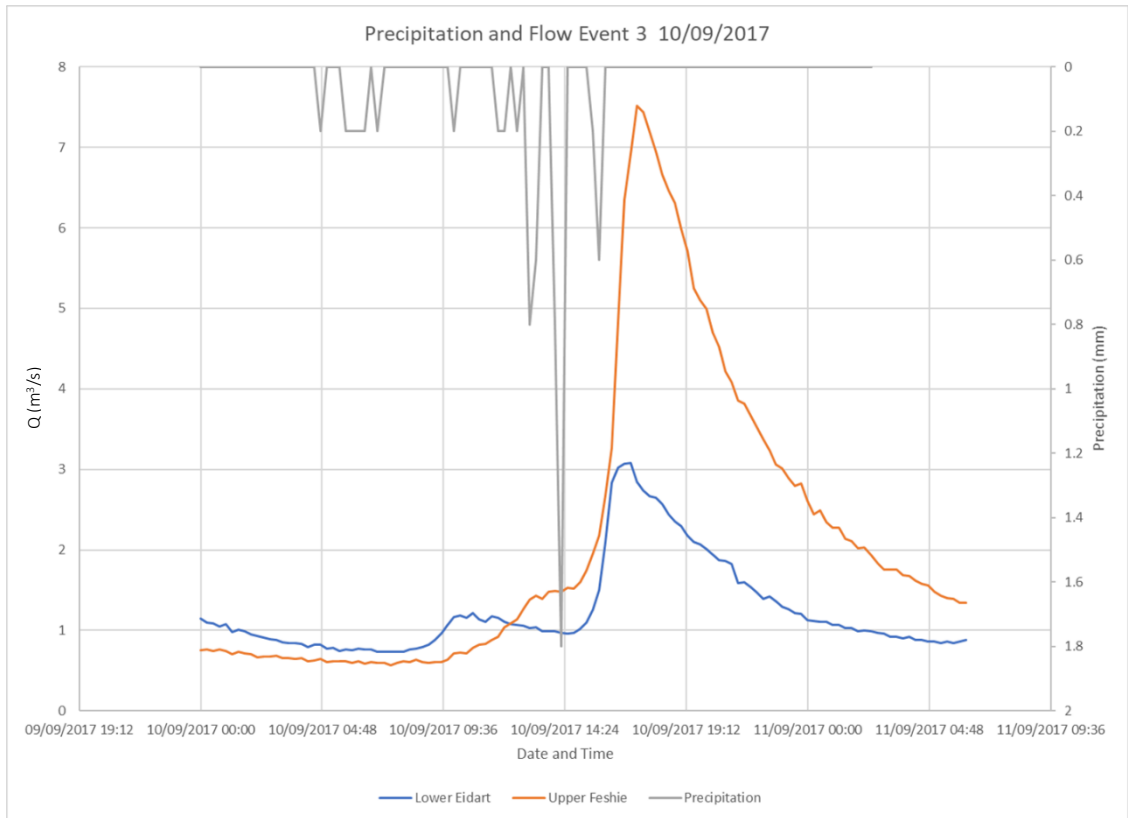


Figure 5.4.1 Cont'd. Comparison Between Upper Feshie and Lower Eidart for 14 Events.

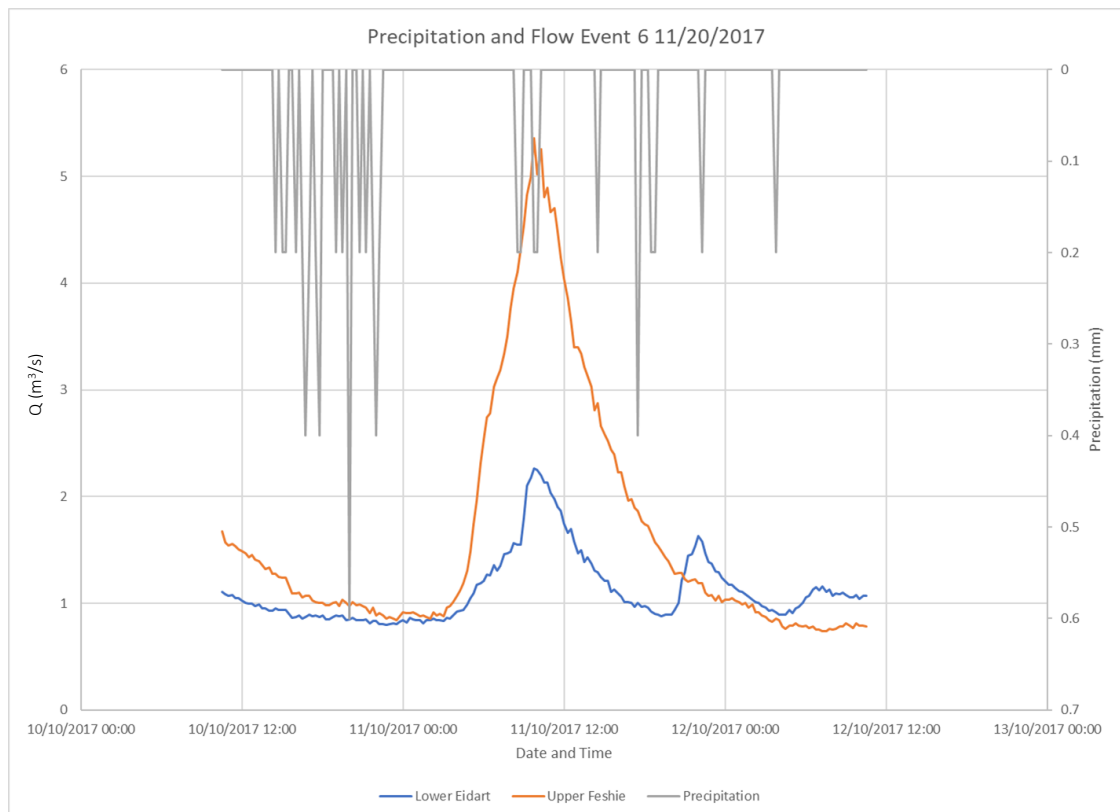
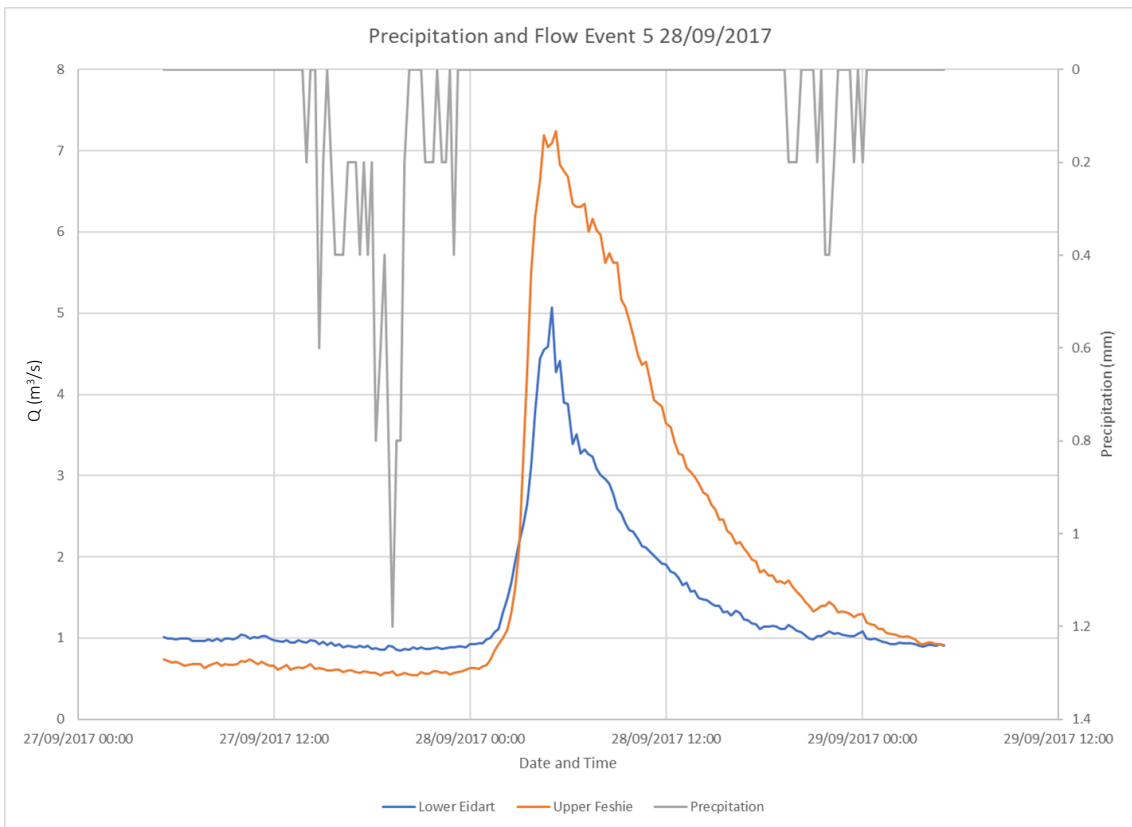


Figure 5.4.1 Cont'd. Comparison Between Upper Feshie and Lower Eidart for 14 Events.

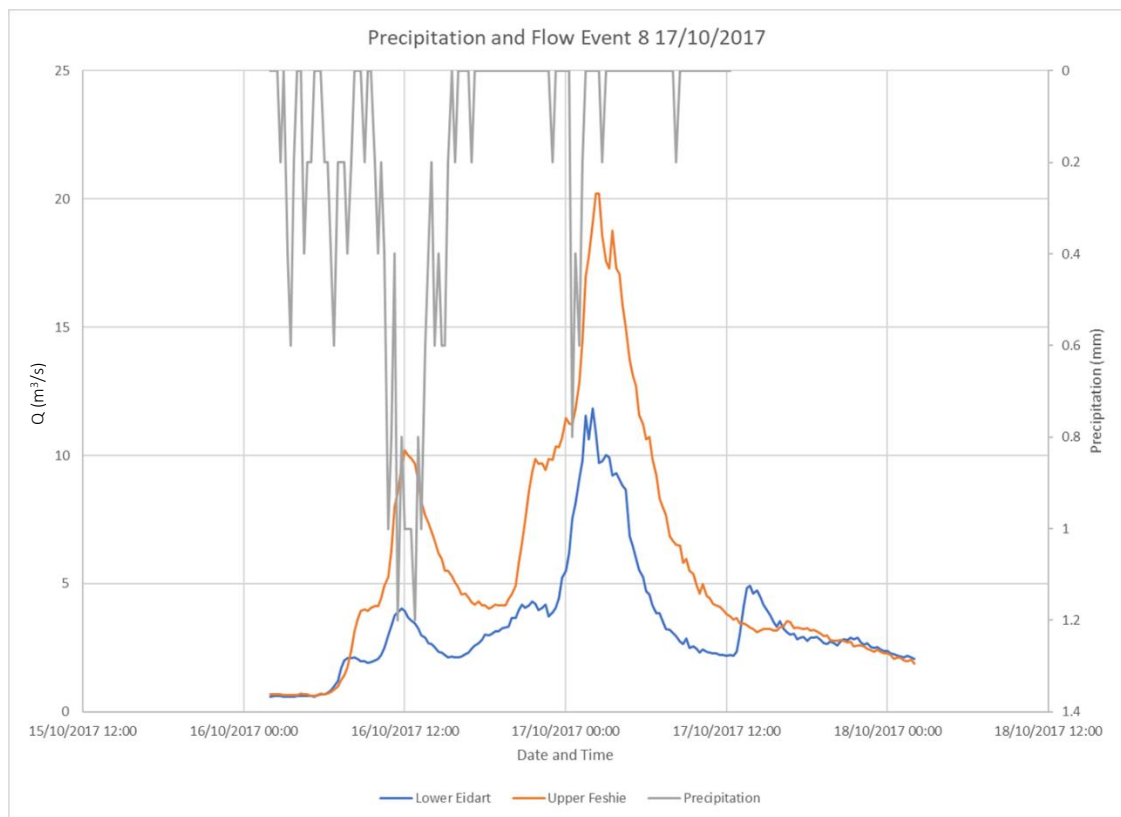
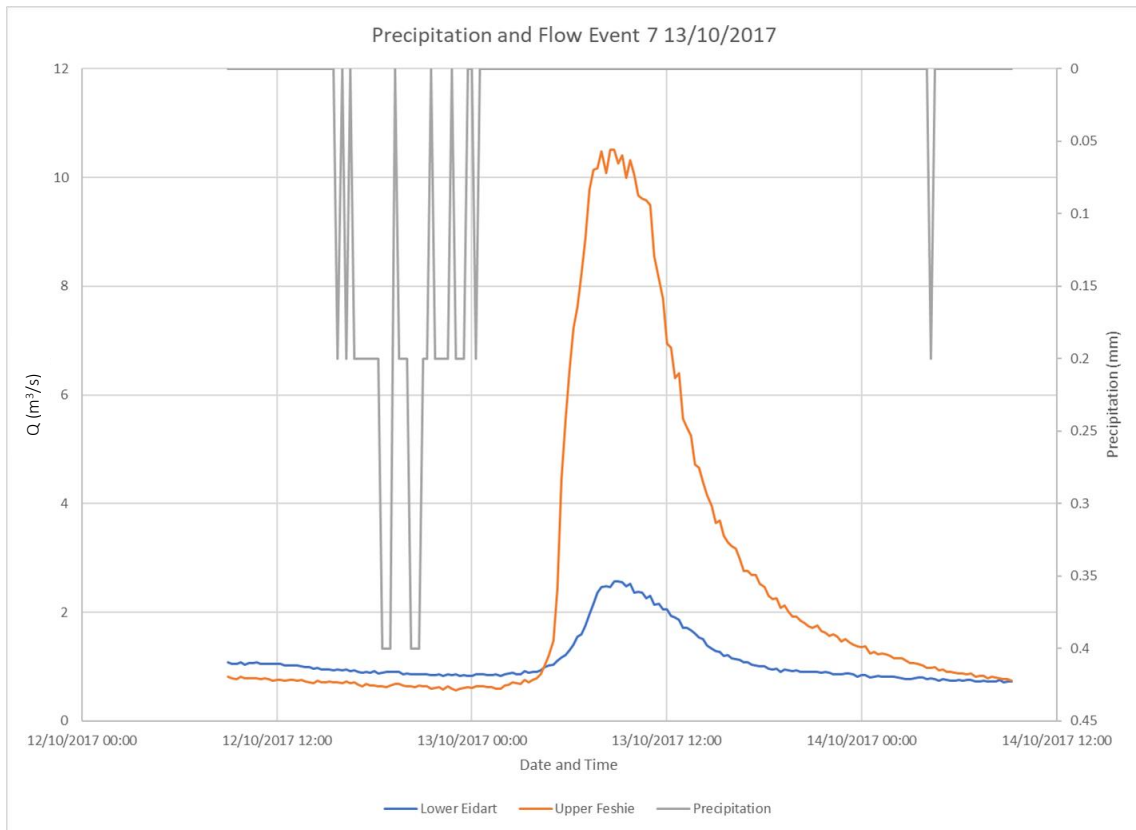


Figure 5.4.1 Cont'd. Comparison Between Upper Feshie and Lower Eidart for 14 Events.

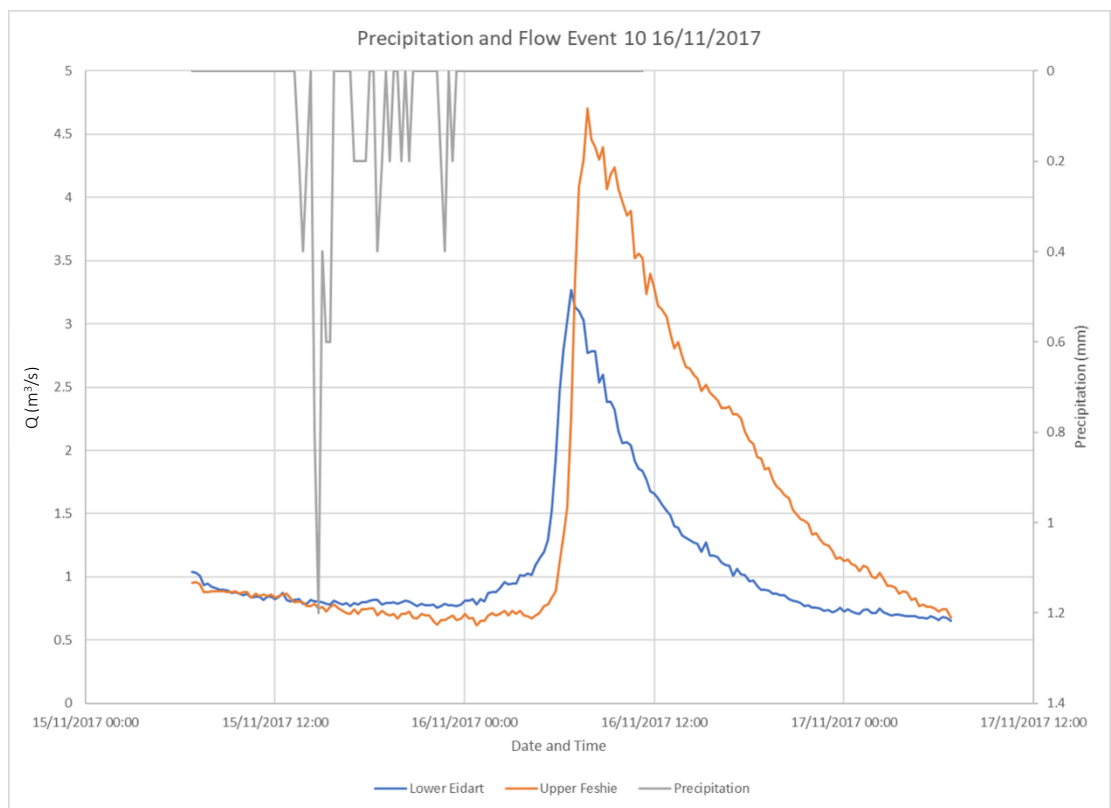
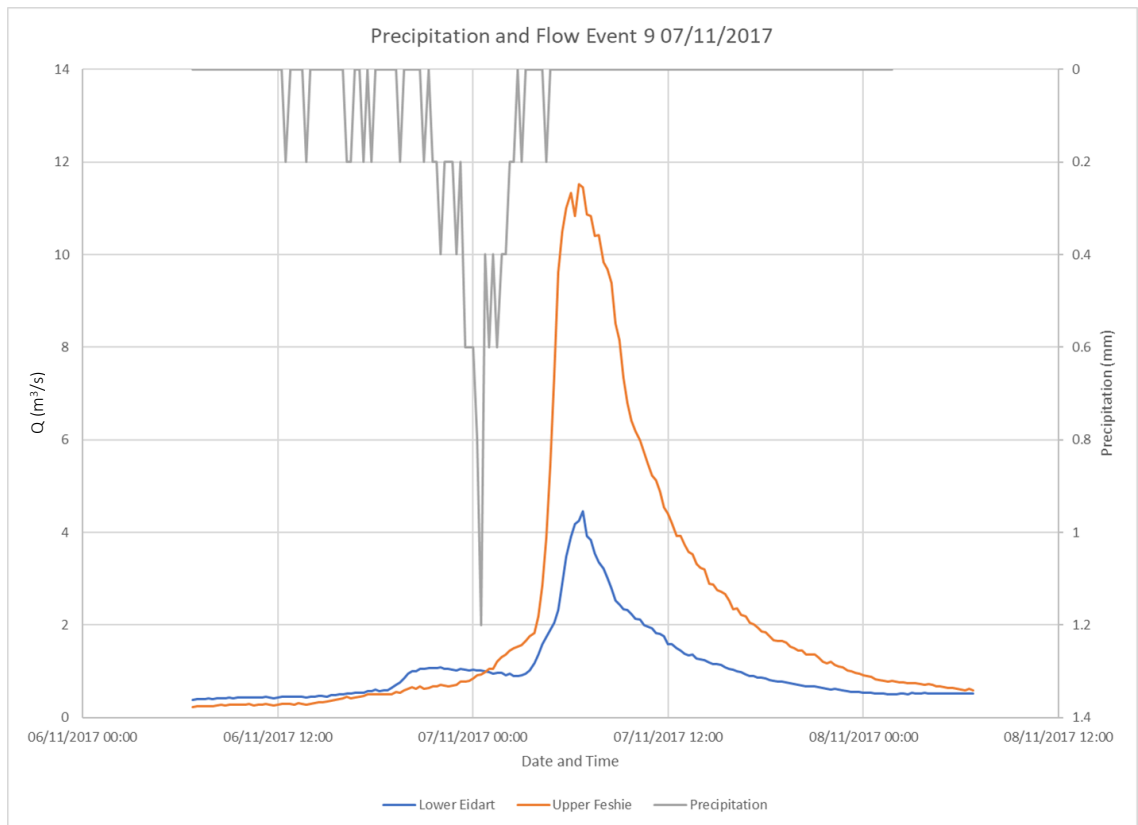


Figure 5.4.1 Cont'd. Comparison Between Upper Feshie and Lower Eidart for 14 Events.

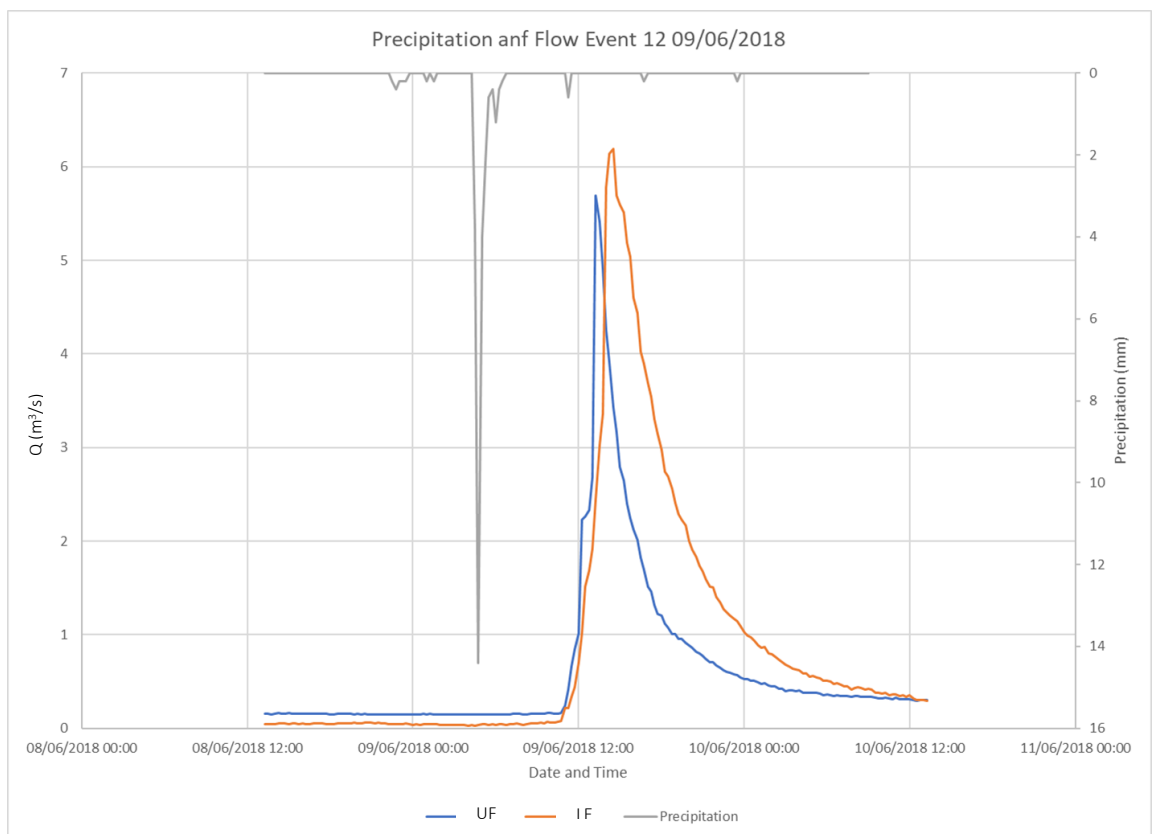
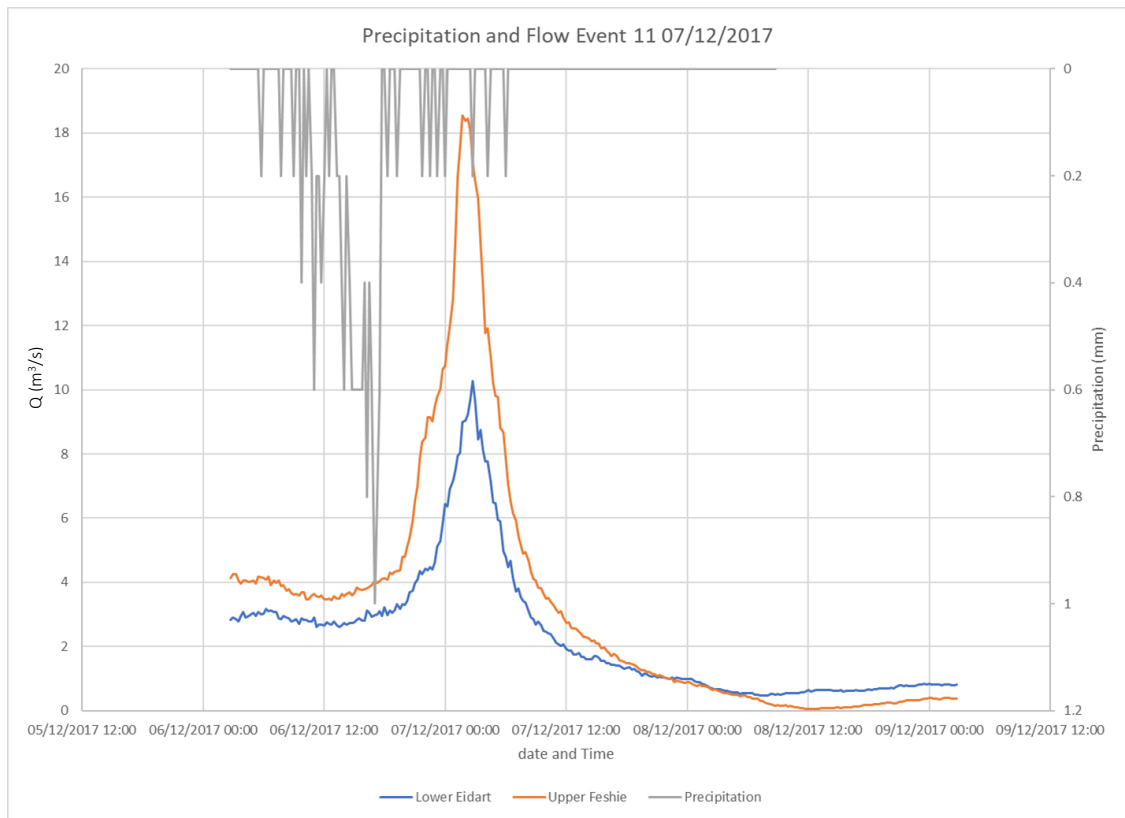


Figure 5.4.1 Cont'd. Comparison Between Upper Feshie and Lower Eidart for 14 Events.

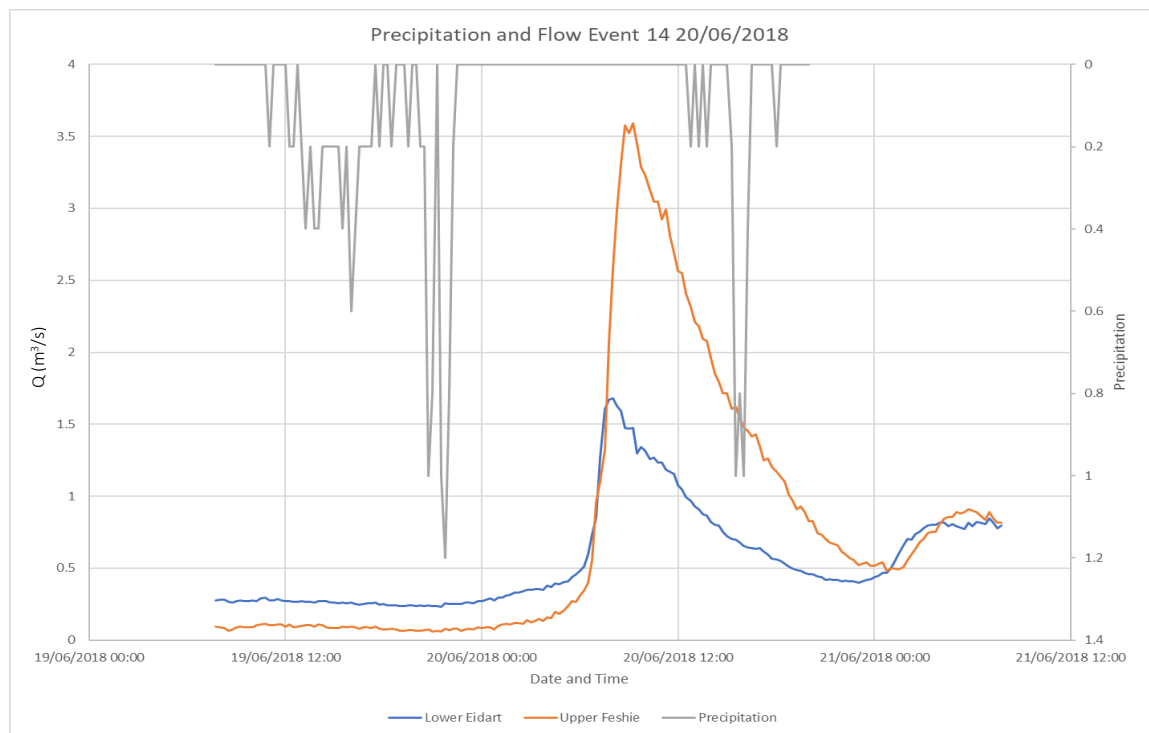
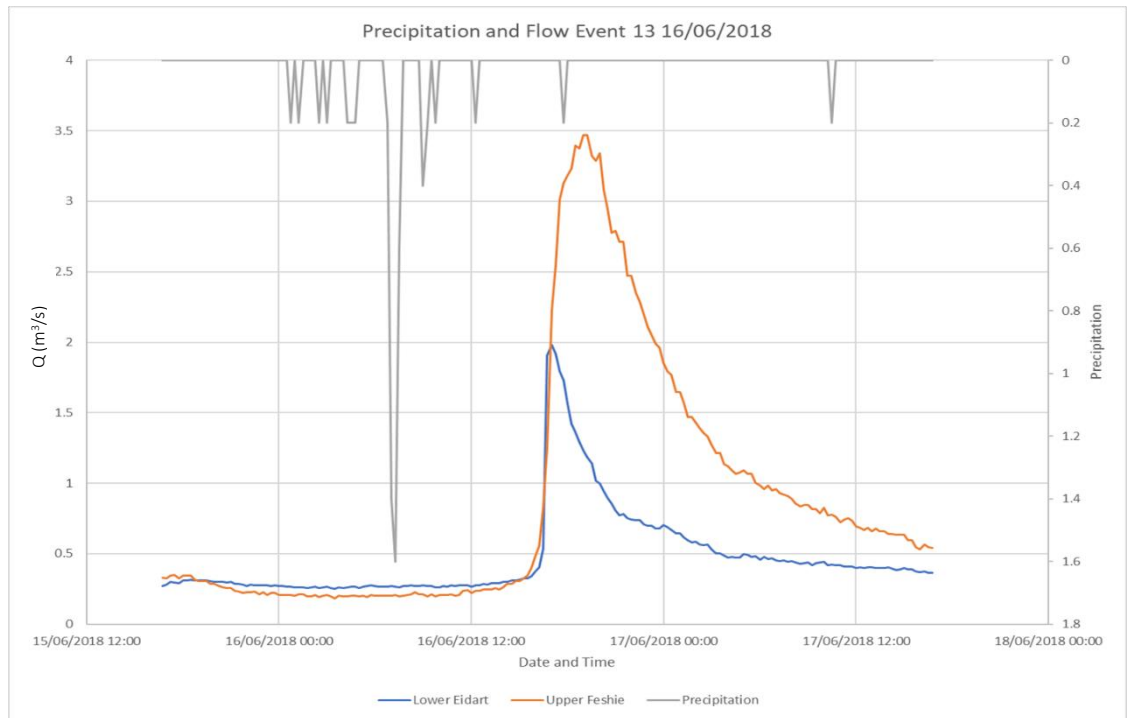


Figure 5.4.1 Cont'd. Comparison Between Upper Feshie and Lower Eidart for 14 Events.

Initially, there is variability in peak discharge and peak discharge timing between the catchments. The greatest peak discharge can be observed in Event 9 from Upper Feshie. The greatest difference in peak is 1.5 hours in Event 4, followed closely by 1.25 hours in Event 1 and Event 14. The smallest difference in timing was 0.25 hours, which was the most common result in Events 2, 3, 5, 6, 7, 8, and 9. Event 13 shows a 0.5-hour difference between the catchments and finally Events 10 and 12 have a difference in timing at peak discharge of 1 hour.

Table 5.4.1 Summary Table of all 14 Analysed Events.

Event ID	Lower Eidart			Upper Feshie			Δ Timing (hours)	Δ Peak (m3/s)
	Date and Time	Peak Stage (m)	Peak Discharge (m3/s)	Date and Time	Peak Stage (m)	Peak Discharge (m3/s)		
1	23/08/2017 09:45	1.43	5.42	23/08/2017 11:00	1.50	10.40	1.25	15.82
2	25/08/2017 19:00	1.36	4.50	25/08/2017 19:15	1.29	5.27	0.25	9.77
3	10/09/2017 17:00	0.84	3.49	10/09/2017 17:15	0.90	7.51	0.25	11.01
4	11/09/2017 11:30	0.84	10.81	11/09/2017 13:00	0.91	5.49	1.50	16.30
5	28/09/2017 05:00	0.88	5.07	28/09/2017 05:15	0.94	7.24	0.25	12.31
6	11/10/2017 10:30	1.09	2.13	11/10/2017 10:15	1.29	5.25	0.25	7.38
7	13/10/2017 09:00	1.15	2.58	13/10/2017 08:45	1.50	10.51	0.25	13.09
8	17/10/2017 02:00	1.82	11.84	17/10/2017 02:15	1.79	10.20	0.25	22.03
9	07/11/2017 06:45	1.33	4.46	07/11/2017 06:30	1.51	11.52	0.25	15.98
10	16/11/2017 06:45	1.21	3.27	16/11/2017 07:45	1.25	4.70	1.00	7.97
11	07/12/2017 02:45	1.74	7.82	07/12/2017 01:15	1.75	15.88	0.50	23.69
12	09/06/2018 13:15	1.39	5.69	09/06/2018 14:15	1.30	6.19	1.00	0.49
13	16/06/2018 17:00	1.07	1.98	16/06/2018 17:30	1.18	3.01	0.50	4.99
14	20/06/2018 08:00	1.03	1.68	20/06/2018 09:15	1.21	3.59	1.25	5.27
Mean		1.23	5.05		1.31	7.63		
		Mean Δ Stage (m)	Mean Δ Peak Discharge (m3/s)					
		0.08	2.57					

5.5 Results of Lag Time Analysis

Using the time difference between the peak of the precipitation event and the corresponding peak discharge in each catchment, a lag time could be assigned to each catchment for each event. The results of deriving lag time per event for each catchment can be seen in Table 5.5.1. These results were used as the data for a Mann-Whitney Wilcoxon (MWW) test. The Mann-Whitney test is used to compare the difference of the average of the two lag time datasets which are not normally distributed. These results can be seen in Table 5.5.2.

Table 5.5.1 Summary Table of Lag Times in Each Catchment.

Event ID	Precipitation Peak Date and Time	LE Peak Discharge Date and Time	UF Peak Discharge Date and Time	Δ Timing LE (hours)	Δ Timing UF (hours)
1	23/08/2017 07:30	23/08/2017 09:45	23/08/2017 11:00	2.2	3.50
2	25/08/2017 17:00	25/08/2017 19:00	25/08/2017 19:15	2.0	2.25
3	10/09/2017 15:15	10/09/2017 17:00	10/09/2017 17:15	1.8	2.00
4	11/09/2017 10:30	11/09/2017 11:30	11/09/2017 13:00	1.0	2.50
5	28/09/2017 03:00	28/09/2017 05:00	28/09/2017 05:15	2.0	2.25
6	11/10/2017 05:45	11/10/2017 10:30	11/10/2017 10:15	4.8	4.50
7	13/10/2017 06:00	13/10/2017 09:00	13/10/2017 08:45	3.0	2.75
8	17/10/2017 01:15	17/10/2017 02:00	17/10/2017 02:15	0.7	1.00
9	07/11/2017 04:00	07/11/2017 06:45	07/11/2017 06:30	2.8	2.50
10	16/11/2017 04:30	16/11/2017 06:45	16/11/2017 07:45	2.3	3.25
11	07/12/2017 00:30	07/12/2017 02:45	07/12/2017 01:15	2.2	0.75
12	09/06/2018 11:15	09/06/2018 13:15	09/06/2018 14:15	2.0	3.00
13	16/06/2018 14:45	16/06/2018 17:00	16/06/2018 17:30	2.2	2.75
14	20/06/2018 05:30	20/06/2018 08:00	20/06/2018 09:15	2.5	3.75

In addition to the results present in Table 5.5.2, the characteristics of the lag time in the catchments can be visualised in Figure 5.5.1 with comparative box and whisker plots. Figure 5.5.2 shows that Lower Eidart has a shorter median lag time (2.2 hours) with a smaller interquartile range ($Q_{25} = 2.0$, $Q_{75} = 2.4$ hours). In addition to Upper Feshie having the longer median lag time (2.4 hours) and greater interquartile range ($Q_{25} = 2.3$, $Q_{75} = 3.4$ hours), there is also a greater range of observed lag times within the tested sample (the 14 events). However, there are outliers in Lower Eidart which match the overall range in Upper Feshie, although these were omitted as outliers by the R-Studio software. Table 5.5.2 shows that Lower Eidart was not normally distributed with $P=0.04353$ whereas Upper Feshie was with a Shapiro-Wilk result of $P=0.8846$. Additionally, the result of the MMW test was $P= 0.1171$, showing that there is a statistically insignificant difference between the average lag time of Lower Eidart and Upper Feshie.

Table 5.5.2 Results of the Mann-Whitney Wilcoxon Test.

Results of the Mann-Whitney Wilcoxon Test	
Shapiro-Wilk Normality Test	
W- Value	P- Value
0.9706	0.04253 (LE) 0.8846 (UF)
Mann-Whitney Wilcoxon Test	
W- Value	P- Value
132.5	0.1171

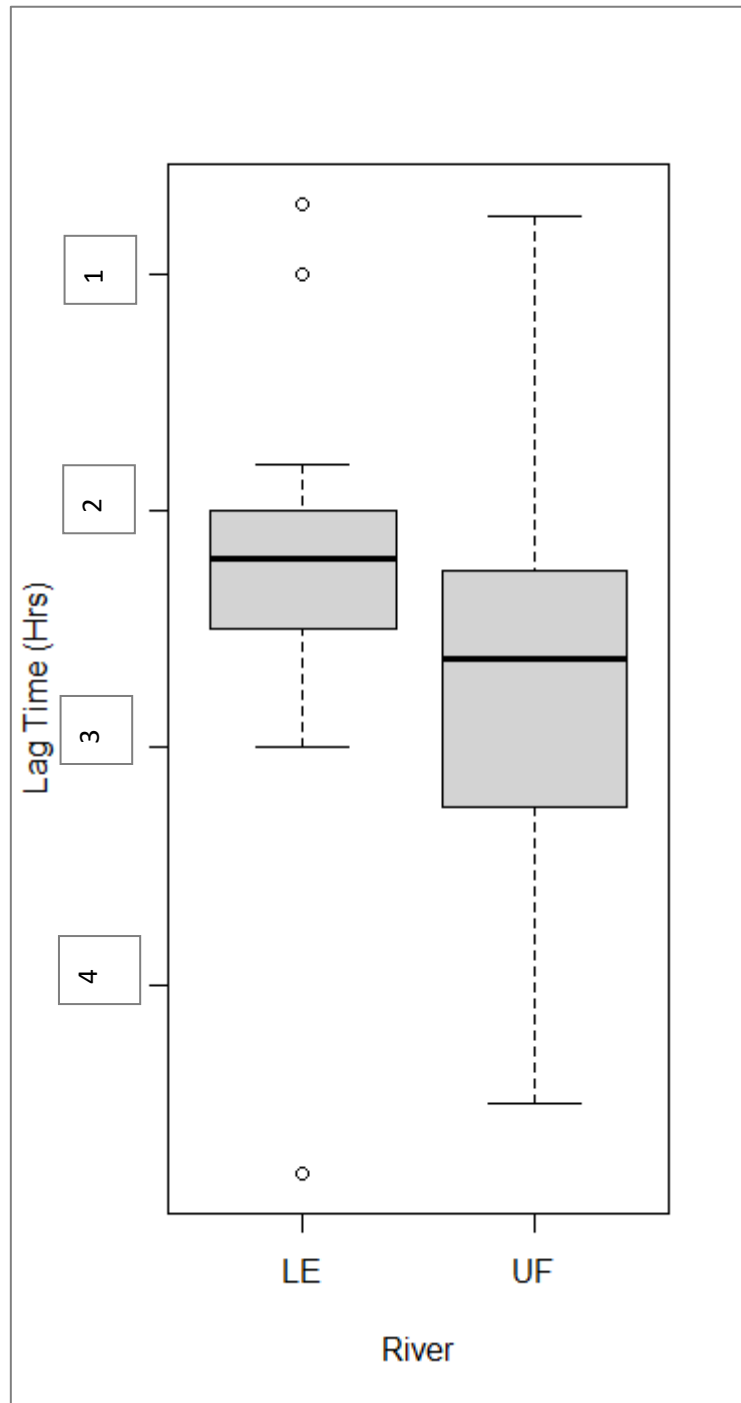


Figure 5.5.1 Visualisation of the Catchment Lag Times.

5.6 Results of Hydrograph Form Analysis

The results of the created median hydrographs can be observed within this section. Figure 5.6.1 displays the median hydrograph for each catchment derived from all 14 flood events.

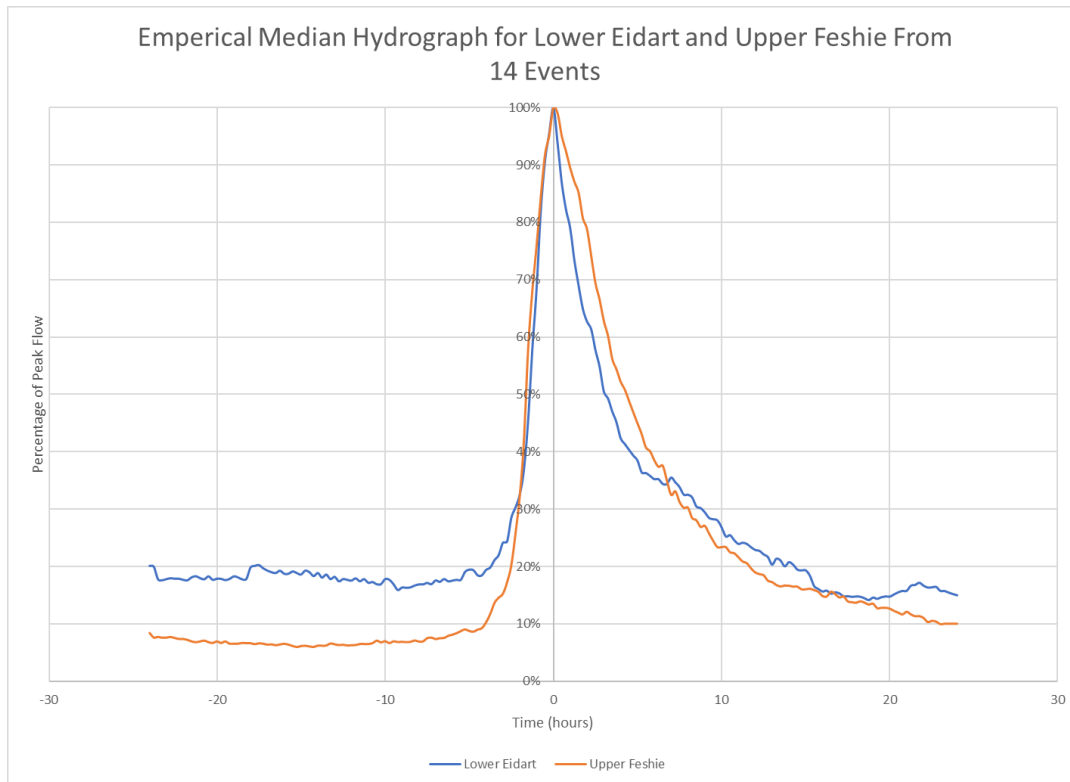


Figure 5.6.1 Median Hydrograph for Lower Eidart and Upper Feshie.

Generally, the two hydrographs have a similar overall form with comparing Upper Feshie and Lower Eidart. For example, Upper Feshie displays a slightly wider profile than Lower Eidart. The rising limb of each hydrograph is extremely similar in gradient and shape and the falling limb of the Lower Eidart is steeper initially than the Upper Feshie due to well-draining subalpine soil and levels out more quickly due to peat-runoff contributions. A greater baseflow is observed in Lower Eidart than in Upper Feshie prior to the characteristic event portrayed which is contrary to the FEH (2022) catchment descriptors. In addition to these characteristic hydrographs, several subsets based on peak flow magnitude and precipitation input were derived and can be seen in Figures 5.6.2, 5.6.3, 5.6.4, 5.6.5, and 5.6.6.

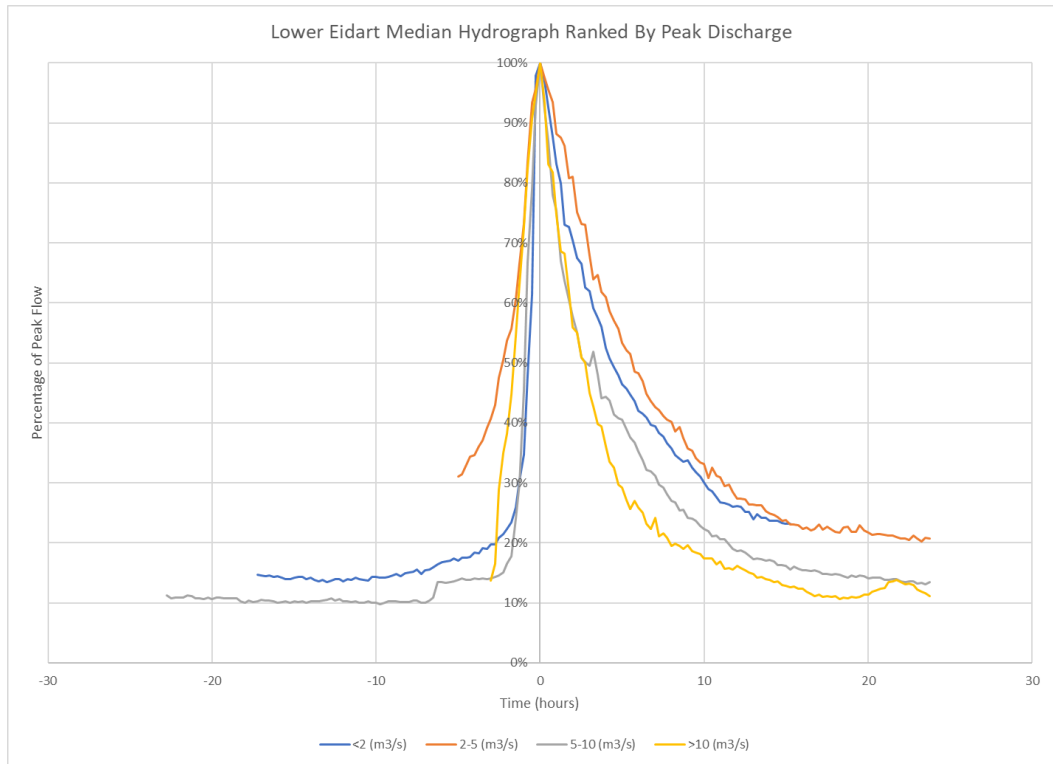


Figure 5.6.2 Median Hydrograph for Lower Eidart Ranked By Peak Discharge

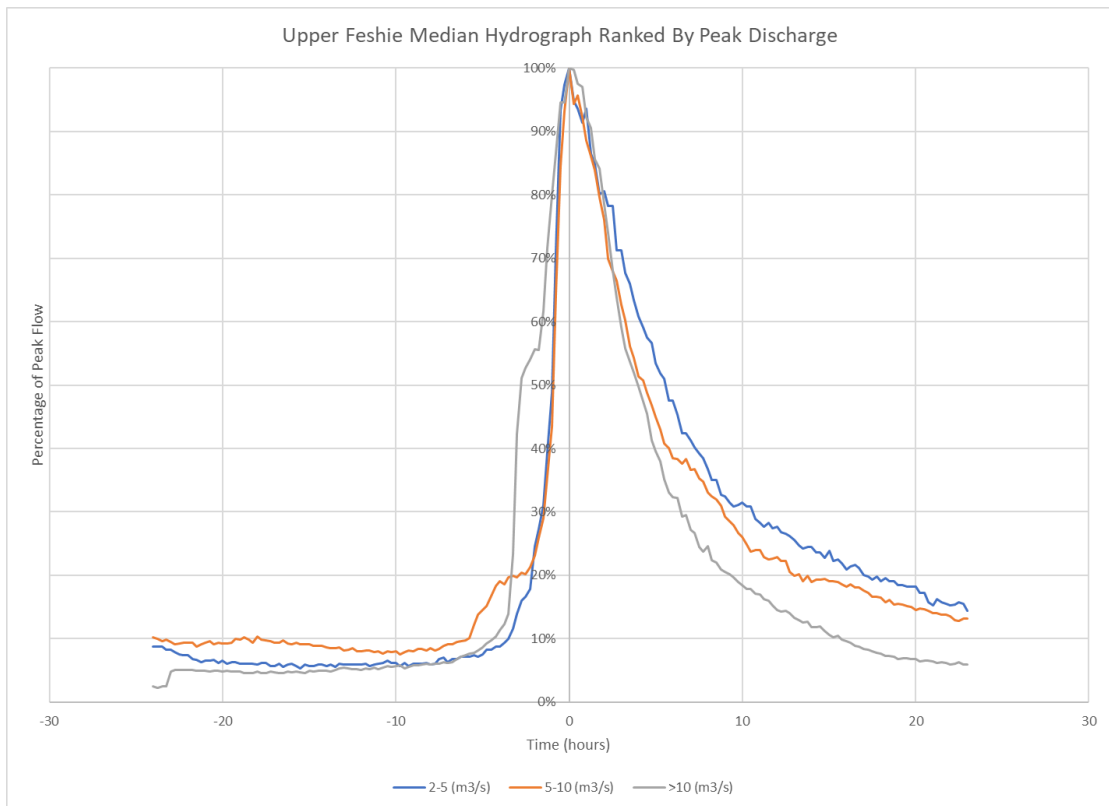


Figure 5.6.3 Median Hydrograph for Upper Feshie Ranked By Peak Discharge

Figures 5.6.2 and 5.6.3 are ranked by the peak magnitude of the events to see how the events may differ in form as the magnitude of the flood event increases. Generally, the mid-range observed floods in Upper Feshie 2-10 m³/s share a similar rising limb shape and the falling limb clearly relates to the size of the event, as expected, as the greater flood events return baseflow more quickly than smaller ones, with a clear order being observed of largest, mid-range, and smallest floods returning to base flow in that respective order. The same trend for the return to baseflow can be observed in Lower Eidart, yet there appears to be some variability in the rising limb, with an absence of adequate data for some of the categories. The ranks of < 2, 5-10 and >10 m³/s share a similar rising limb gradient and form, yet 2-5 m³/s seems to have a less steep rising limb.

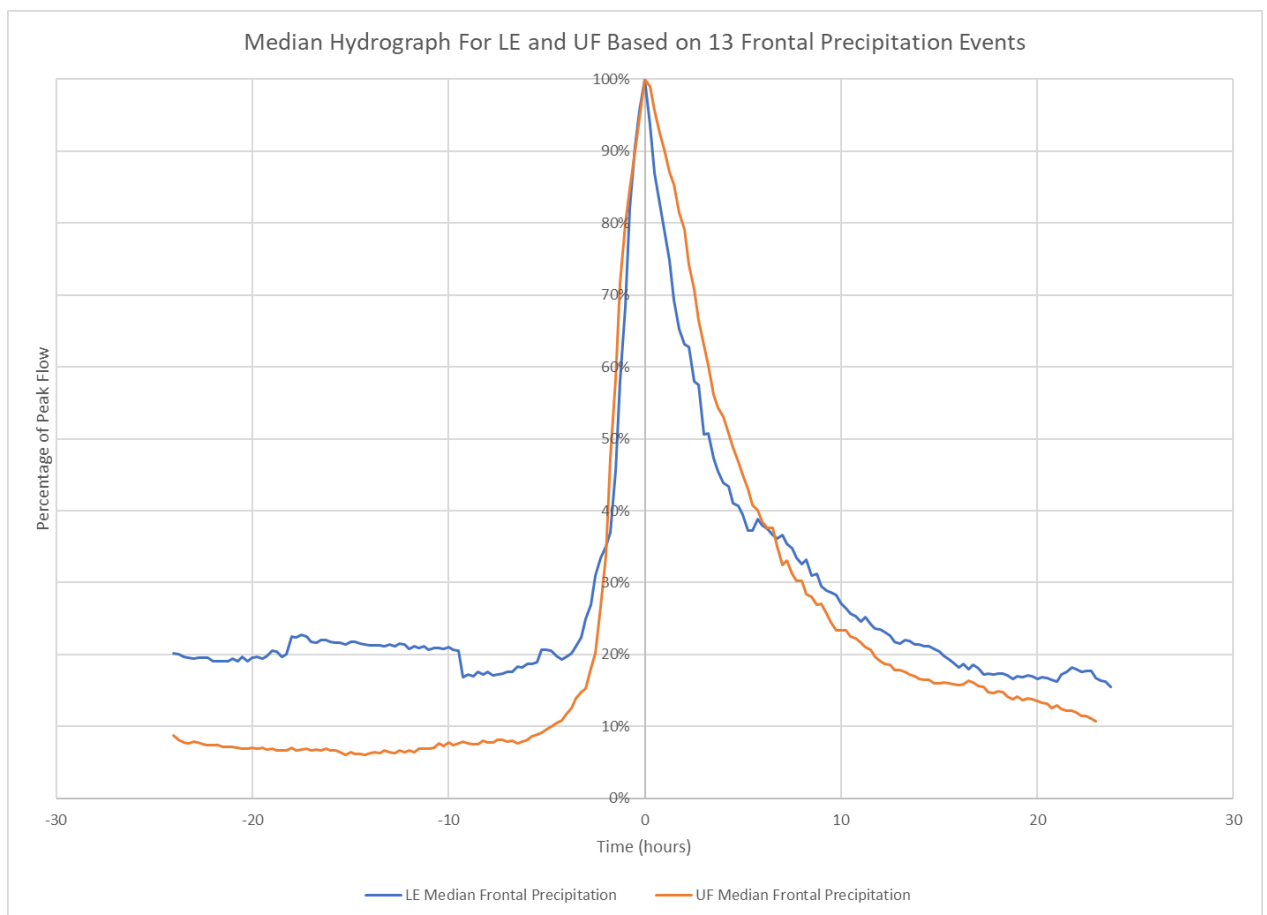


Figure 5.6.4 Median Hydrograph for Lower Eidart and Upper Feshie for Frontal Rainfall Response

Figure 5.6.4 represents a characteristic catchment response of Lower Eidart and Upper Feshie to 13 frontal rainfall events. In addition to Figure 5.6.4, Figures 5.6.5 and 5.6.6 show a comparison between the 13 frontal rainfall events and a single convective rainfall event.

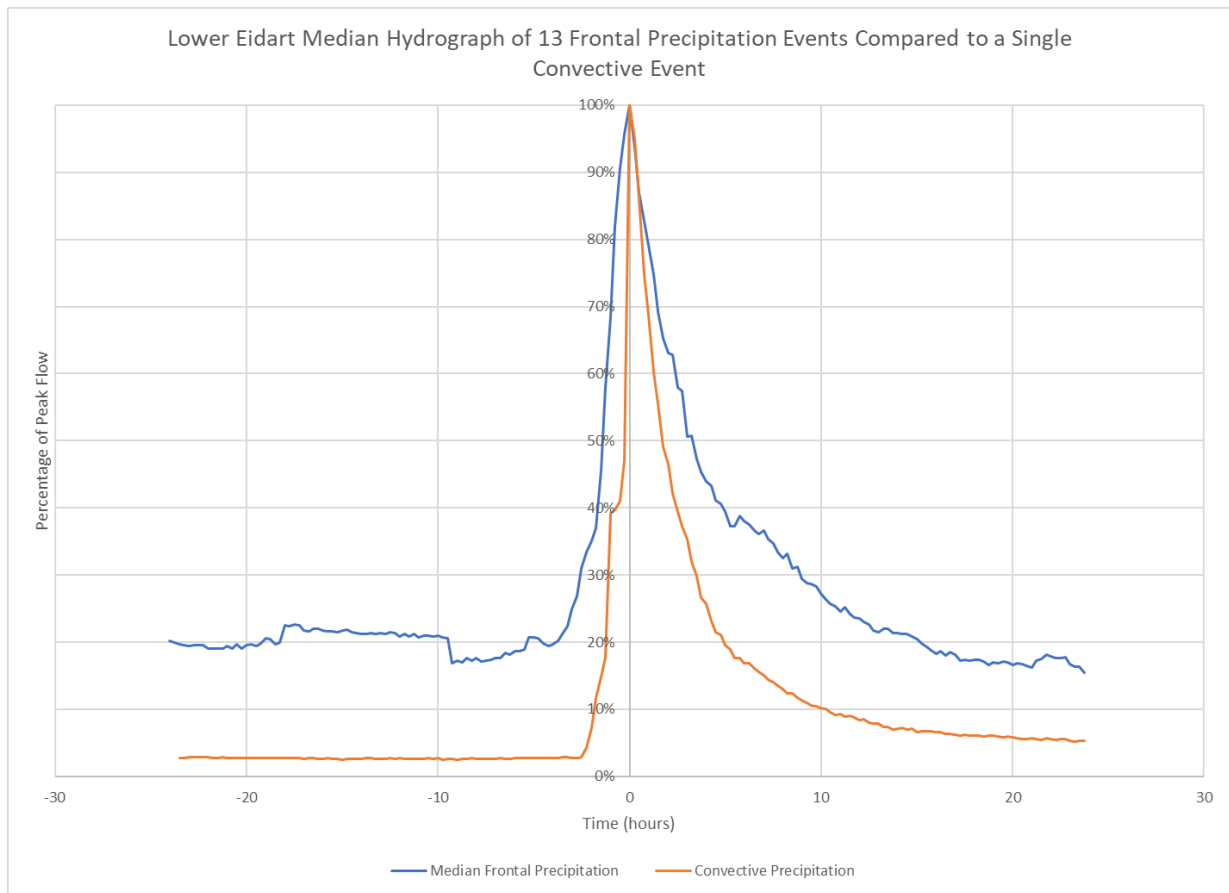


Figure 5.6.5 Lower Eidart Frontal Rainfall Response Compared to Convective Rainfall

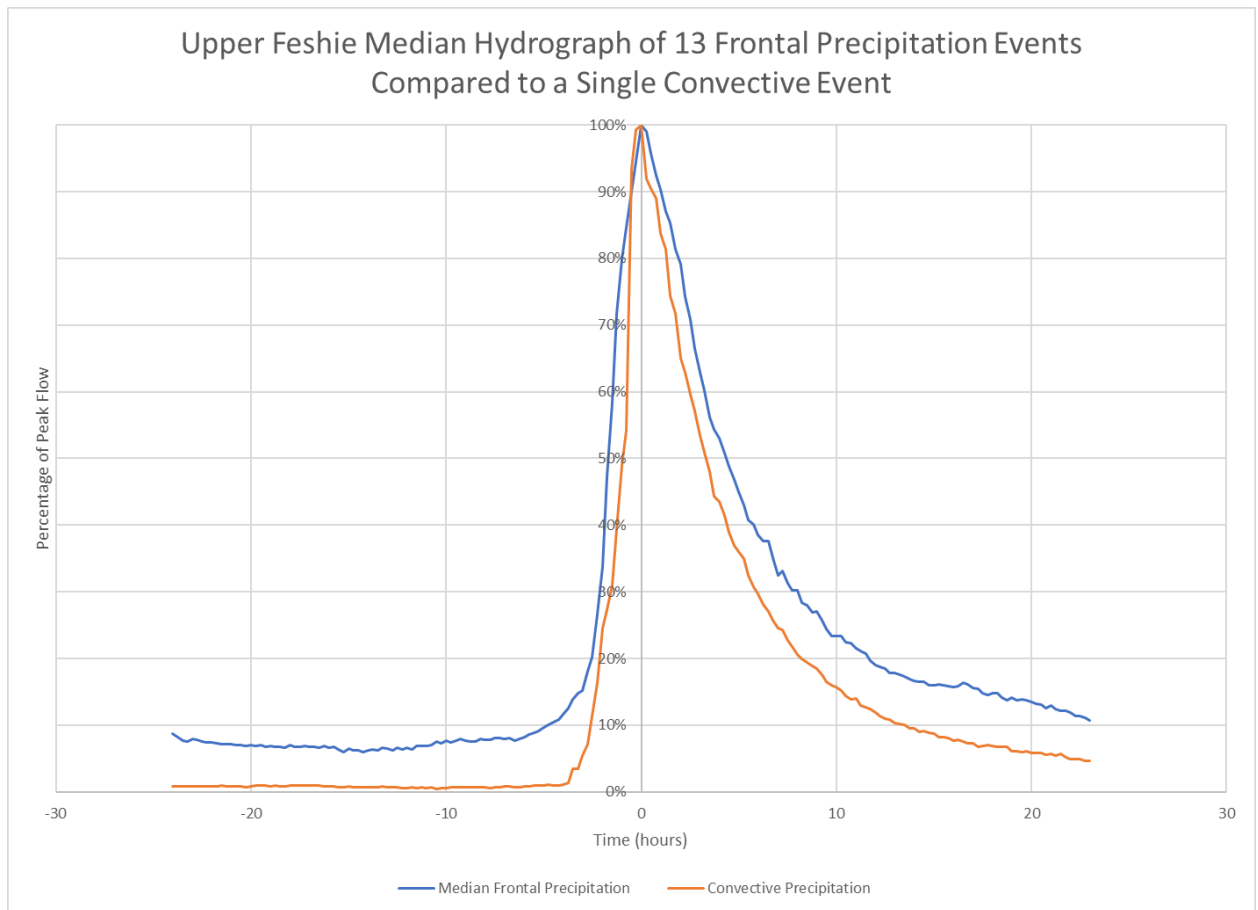


Figure 5.6.6 *Upper Feshie Frontal Rainfall Response Compared to Convective Rainfall*

Figures 5.6.5 and 5.6.6 follow a similar trend whereby the convective rainfall event has a narrower hydrograph shape with a steeper angle at the base of the rising limb when compared to frontal rainfall. The falling limb of the convective events also return the hydrograph to baseflow faster than frontal events. The trend of Lower Eidart, with its greater antecedent flow, having a narrow hydrograph profile remains true throughout all the median hydrographs above.

Finally, the combined flows from each catchment for the 14 events used in this study has led to the creation of a median hydrograph for Upper Feshie Confluence, which can be observed in Figure 6.2.1. The use of combined flows rather than continuous time series is due to lack of availability of time series data due to instrumentation failure. Figure 6.2.1 shows that the antecedent flow between Upper Feshie and Lower Eidart, evening out the increased input baseflow from Lower Eidart is evened out with Upper Feshie, in line with expectations. The combined hydrograph is slightly wider as it has the combined flow, however the rising limb is almost identical to the Lower Eidart and Upper Feshie. There is no dual peak observed in the median hydrograph for the Upper Feshie Confluence. In addition to the median hydrograph for Upper Feshie Confluence, the combined flow for all 14 events were plotted in Figure 6.3.1. Multiple peaks can be observed for each event.

Chapter 6: Discussion

This research set out to meet the three objectives introduced in Chapter 1. The aim which to generate knowledge of the hydrological response of two neighbouring catchments with differing physical characteristics in the Upper Feshie system. The aims and objectives will be addressed, and the findings will be discussed in the following chapter.

6.1 *Choice of Methods*

The production of reliable rating curves which justifiably extend the current ratings that are based on flow gaugings, was the first objective of this research. The initial methodology included the synthesis of a 1D HEC-RAS simulation based on channel geometry and simulated flows to achieve a stage-discharge dataset to calibrate the rating extension. To do this, a high-resolution topographic survey was required as no adequate data of this kind exists in the study areas followed by fitting of the model results before validation in objective 2.

The results of the topographic survey can be observed in Figures 5.1.0-5.1.9 which are derived Digital Terrain Models constructed from the survey. These results were successful in their intended purpose of providing the gradient for the HEC-RAS hydraulic model as gradient is the key downstream boundary condition in steady flow analysis. Visual analysis through contour display in Figures 5.1.4-5.1.6 was efficient for ensuring that the model input topography was representative of the reaches, increasing the confidence in the input parameter of topography.

The results in Figures 5.1.0-5.1.3 are the colour banded results of the topographic survey; they provide general insights into the basal geometry of the channel, for example highlighting the location of the thalweg and changes in gradient due to control features. Figures 5.1.1 and Figures 5.1.3 show channel geometry with control features clearly, Figure 5.1.2 however, shows a deep Thalweg feature with no breaks or changes in colour banding. The implications of this result are that the hydraulic controls were not represented in the DTM, meaning that there will be a low degree of confidence in the input topography which went into the model for Lower Eidart, which Figure 5.1.2 corresponds to. It is believed that this may have adversely affected the HEC-RAS modelling for Lower Eidart.

Figures 5.1.7-5.1.9 are representations of the cross-sectional geometry at each of the three gauges and are the most important result from the topographic survey. The cross section at the gauge was surveyed as a failsafe protocol as this cross section can be used to estimate flow through the $Q = VA$ method. These results have primarily assisted with objective one for their use in the extension of the rating for Lower Eidart, which will be discussed in more detail later in this chapter.

Extension of the rating equation to increase confidence in the stage-discharge relationship at each gauge at higher flows was deemed to require a HEC-RAS 1D model as this seemed to be the optimal approach as it is described in Ramsbottom and Whitlow (2003) to be an approach with a long history of success and the software is freely available. The results of the hydraulic modelling can be observed in Figures 5.2.1-5.2.4 and Table 5.2.1.

The second objective of this research was to validate the rating equations created by the 1D HEC-RAS model independently. The validation process took place in 3 stages, visual analysis, level data application and finally by using the $Q = VA$ method to compare the results. Table 5.3.1 presents a comparison between the HEC-RAS results after the refinement process and those of an integrated approach between the HEC-RAS results and the $Q = VA$ results. Table 5.3.1 shows that upon application to the time series data, the peak discharge for Lower Eidart was $715 \text{ m}^3/\text{s}$ with a mean annual runoff of 1600 mm per year in a period of time series which experienced approximately 1400 mm of rainfall. These results are not acceptable especially when they are compared to Upper Feshie which is a bigger river, showing a peak discharge of $20.2 \text{ m}^3/\text{s}$ and a mean annual runoff of 1268 in the same period. The results for Upper Feshie are permissible which represented success of the results from the Upper Feshie HEC-RAS model. However, the results for Lower Eidart generated from HEC-RAS were evaluated to be unacceptable based on water balance. The Lower Eidart results are not acceptable as Lower Eidart is claimed to receive 1654 mm of runoff depth per year along with 1423 mm for Upper Feshie as presented in existing literature by Soulsby, *et al.*, (2006).

The $Q = VA$ method was required to develop a rating equation for Lower Eidart considering the unsatisfactory results of the HEC-RAS model. The $Q = VA$ method to extend the rating equation at Lower Eidart is an empirical method based on a three-step process, outlined in Figures 5.3.1, 5.3.2 and 5.3.3. The first step includes using the average velocity of observed empirical gaugings which there is confidence in. Once the relationship between stage and velocity has been established then the use of the

relationship between wetted area and stage can inform the formula of $Q = VA$. There is confidence in the surveyed topography of the reach for the cross-sectional area and there is confidence in the empirical gaugings, meaning that this method has a reliable starting point whereas the HEC-RAS modelling is based on the reliability of input parameters which is believed to be the cause of the poor results for Lower Eidart because the complexity of the reach was not fully represented in the input topography.

The results of the $Q = VA$ method to develop the Lower Eidart rating can be observed in Figure 5.3.3 which is a rating curve made up of two parts. The parameters for this equation are in Table 5.3.2 and is joined by the HEC-RAS rating parameters for Upper Feshie in Table 5.3.3. Table 5.3.1 described the peak discharge for the $Q = VA$ method to be $11.8 \text{ m}^3/\text{s}$ and a mean annual runoff of 1183 mm which is considerably more realistic given the environment and time series being used which received 1400 mm of precipitation. The HEC-RAS 1D model is considered to have been partially successful with proper topographic input occurring at Upper Feshie, but not Lower Eidart and the three-stage quality review process has been useful in highlighting the error in the Lower Eidart rating which directly corresponds to objective two in terms of the validation of the results. Additionally, objective one has been met by the $Q = VA$ component of the quality review process, and partially by the HEC-RAS modelling.

Overall, two satisfactory rating equations have been generated though the combination of the HEC-RAS 1D modelling and the $Q = VA$ method for rating extrapolation. The HEC-RAS was used successfully for the site Upper Feshie and was checked against the $Q=VA$ method. The HEC-RAS model for the Lower Eidart was unsatisfactory and so the $Q=VA$ method was used solely for this rating. The combination of visual analysis, application of these to the time series data and in the cross validation between HEC-RAS and $Q = VA$ has successfully facilitated the extension of the current ratings at the gauges for Lower Eidart and Upper Feshie.

6.2 Hydrological Analysis

The third objective was to carry out hydrological analysis using the newly derived and verified rating equations. In this research, 14 events were selected for lag time analysis, which was carried out in conjunction with the creation of a median hydrograph, as a means of filling the knowledge gap in the hydrological response of blanket peat headwater catchments such as Upper Feshie and especially in bare peat and mineral catchments such as the Lower Eidart.

The results of the 14 events can be seen in Table 5.4.1 and show that from the time series used, Lower Eidart has smaller peak discharges compared to Upper Feshie with a maximum and average peak discharge of 11.8 m³/s and 5.1 m³/s being observed, respectively. The maximum and average peak discharge for Upper Feshie was 20.2 m³/s and 7.63 m³/s, respectively. The difference in the average and peak discharge was 8.4 m³/s and 2.57 m³/s respectively. The maximum stage observed for Lower Eidart was 1.82 m and the average stage was 1.23 m. The Upper Feshie catchment showed a maximum stage of 1.79 m and an average stage of 1.31 m. There is a difference in the maximum and average stage of 0.03 m and 0.8 m respectively between the catchments. The average stage of Upper Feshie was higher than Lower Eidart potentially due to the cumulative effect of having a wider hydrograph profile (Figure 5.6.1) but in terms of the peak stage, there is little difference. Both Lower Eidart and Upper Feshie have a catchment size of approximately 30 km² and are in close spatial proximity, difference in these metrics is likely due to physical catchment descriptors, especially soil. There is a dual peak in the median hydrograph displayed in the discharge ranked median hydrograph of the Upper Feshie catchment (Figure 5.6.3) and may be a result of tributary timing. Dual peak hydrographs are often attributed to a rapid overland response and a slower subsurface response (Martinez-Carreras, *et al.*, 2001), however given the low storage characteristics of these catchments described in Chapter 2, this seems less significant than the timing of two large catchment tributaries. There is a small lochan on the tributary named Caochan Dubh (Figure 4.1.3) which may act as a reservoir, attenuating some runoff which could contribute to the second peak of the hydrograph. However, the FARL (reservoir) catchment descriptor from FEH (2022) is 0.977 indicating an insignificant reservoir impact in the Upper Feshie catchment.

The methodology used in this research, of estimating the lag time to peak discharge from subtracting the peak of the hyetograph from the peak of the hydrograph is consistently cited in further literature, such as Snyder (1938), Maidment (1993) and Grantano (2012) as well as Lambord and Hotschlag (2018). Due to this, the methodology used to estimate lag time has ensured a high degree of confidence in the lag time estimates which have been observed in this research (Table 5.5.1) and used as the sample for the statistical analysis of lag time. A total of 14 flood events were selected for analysis through the process described in section Chapter 4, section 4.5.2.

Table 5.5.1 describes the results of the lag time analysis which is graphically presented in Figure 5.5.1 as a box and whisker plot. Figure 5.5.1 highlights that the Lower

Eidart has a median lag time of 2.2 hours and Upper Feshie has a lag time of 2.6 hours. The shorter lag time in the Lower Eidart is attributed to the soil characteristics of the catchment as more than 59% of the catchment is rapidly draining mineral soil with 27% blanket peat observed to be in a low friction, eroding state. Lower Eidart can be compared to Upper Feshie which is more than 65% blanket peat with a further 10% peaty podzol (Soulsby, *et al.*, 2006). This shows that three quarters of the Upper Feshie catchment has more slowly draining soils than Lower Eidart, facilitating some reasoning for Lower Eidart reaching peak discharge first. Additionally, a greater incidence of blanket peat leads to a greater storage potential than mineral soil and a considerably greater surface friction (Shuttleworth, *et al.*, 2019).

Table 5.5.2 shows that the population of lag time values for Lower Eidart was not normally distributed upon use of a Shapiro-Wilk normality test ($P=0.04253$) whereas Upper Feshie was ($P=0.8846$). Therefore, the non-parametric (MWW) test of difference was deemed to be the required test for the lag time analysis. The result of the lag time analysis was $P=0.1171$ which means that the difference of the average lag time in each catchment was not significantly different.

The difference in lag time between the catchments is 0.4 hours, or 23 minutes. Synchrony of tributary timing is accepted to be a key parameter in hydrograph convolution (Pattison, *et al.*, 2014) in addition to catchment descriptors and event precipitation structure. Upper Feshie peaks 23 minutes after the Lower Eidart, which is downstream of the gauge on Upper Feshie so an assumption can be reasonably made that increased synergy between the 2 catchments could lead to an increased flood wave at the confluence if the ongoing regeneration of the Lower Eidart catchment (noted in Chapter 1) leads to an attenuation of surface runoff. This may lead to an increase in the the lag time in the Lower Eidart, bringing the time of peak discharge of the catchments closer together. Natural Flood Management strategies have been shown to slow the flow (Black, *et al.*, 2022), however an increase in overall peak discharge may not occur as the outcome of increased catchment synergy is difficult to predict (Pattison, *et al.*, 2014). However, changes to the hydrograph profile at the confluence (Figure 6.2.1) is expected.

The median hydrograph for Upper Feshie Confluence (Figure 6.2.1) was created by combining the flows from Lower Eidart and Upper Feshie.

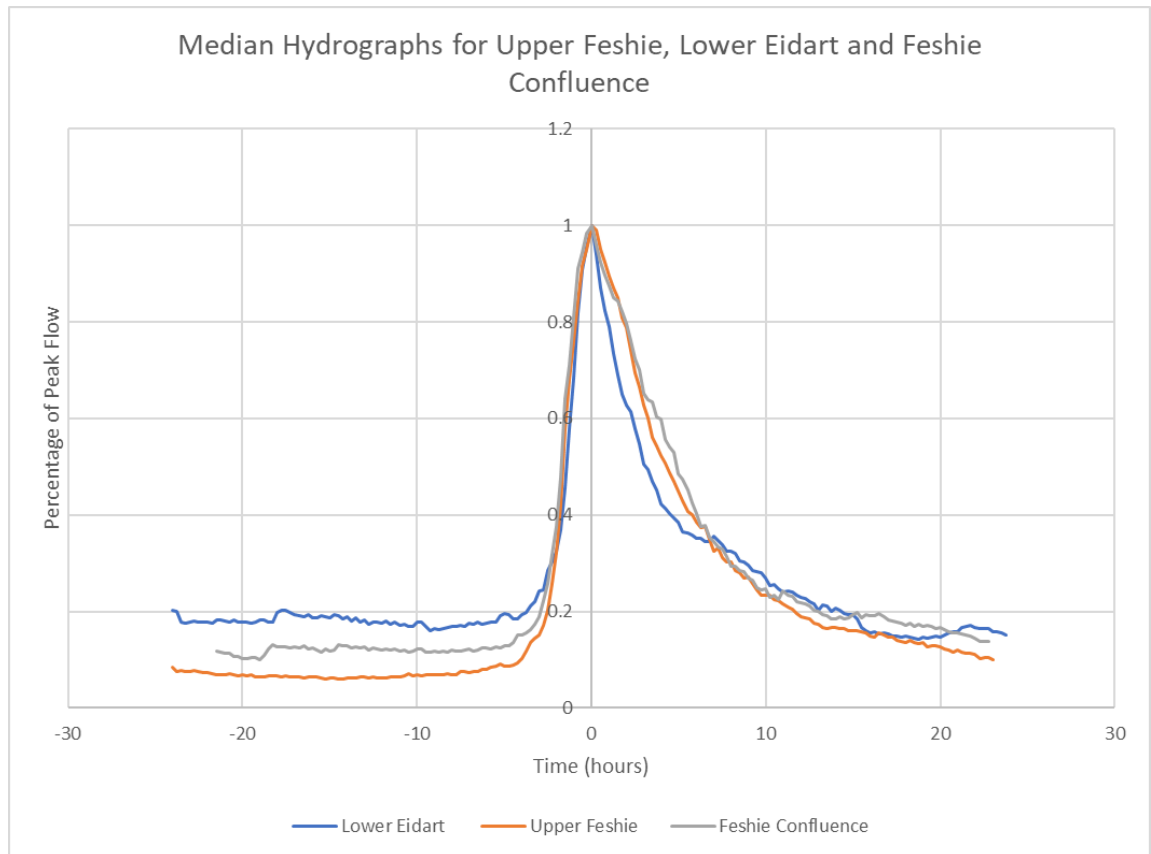


Figure 6.2.1 *The Median Hydrographs for the Study Catchments and Their Confluence*

In addition to lag time analysis, part of the third objective of this research was to create a series of characteristic hydrographs which could be used to compare the catchment response of Lower Eidart and Upper Feshie. The objective has been met with the creation of Figures 5.6.1-5.6.6. The hydrological response of these catchments can be compared in their current state; however, it is also now possible to compare the runoff response of each catchment temporally as regeneration matures.

Again, 14 events were selected to omit snow and snow melt events, as outlined in Chapter 4 so that only floods from uniform rainfall were included. Following the methods of Archer, *et al.*, (2000) a median empirical hydrograph was obtained for each catchment, allowing a comparison on shape to be made. The results of the creation of a median hydrograph for Lower Eidart and Upper Feshie can be observed in Figure 5.6.1 which shows an extremely similar hydrograph shape between the catchments with a nearly identical rising limb and a slightly wider shape for upper Feshie which is attributed to the dominant soil characteristics of the catchment (>65% blanket peat). Lower Eidart has a greater incidence of rapidly draining thin mineral soil (>59% along with >27% peat in an

eroded state) which is thought to be why Lower Eidart displays a narrower hydrograph profile across all flows and in response to both frontal and convective rainfall (Figures 5.6.5 and 5.6.6). The narrow shape of the hydrograph in the Lower Eidart is representative of a quick-flow response of blanket peat environments (Holden and Burt, 2002). Runoff contributions from saturation excess runoff are facilitated by the hydrophobic bare-peat surfaces in the Lower Eidart. Bare peat and peat hags have severely limited infiltration and storage potential so the steep-rise, flashy hydrographs which return to baseflow rapidly are likely due to this.

Figure 5.6.1 also shows that Lower Eidart shows roughly 10% greater baseflow prior to the rising limb than Upper Feshie. The greater baseflow in Lower Eidart may also be a contributing factor to the lower peak discharge in Lower Eidart, because if there is a greater proportion of runoff leaving as baseflow there is less to augment flood peaks. There is a disagreement in the FEH (2022) catchment descriptors and existing literature (Soulsby, *et al.*, 2006) in terms of base flow. FEH (2022) state that Lower Eidart has a lower baseflow than Upper Feshie. The time series used in this study is consistent with Soulsby, *et al.*, (2006), showing greater baseflow contributions from Lower Eidart than Upper Feshie.

To test the sensitivity of the hydrograph shape, a series of subsets were created and can be observed in Figures 5.6.2, 5.6.3, 5.6.4, 5.6.5, and 5.6.6. The Upper Feshie hydrographs show a consistent stepped peak across the range of flows, potentially due to tributary timing higher up the Upper Feshie system which Lower Eidart does not. These peak flow hydrographs do not exhibit a high degree of sensitivity across the range of flows whereby all the subset hydrographs are similar in shape and duration, supporting confidence in the main set observed in Figure 5.6.1.

A subset of these hydrographs was created based on precipitation input. 14 flood events were ranked as frontal or convective based on precipitation intensity. Convective rainfall has a higher intensity with greater rain drop diameter than frontal rainfall (Thurai, *et al.*, 2016) leading to a greater runoff depth over a short period of time. Figures 5.6.5 and 5.6.6 demonstrate that convective rainfall leads to an almost vertical rise in flows and a very steep rising limb whereas frontal rainfall leads to a more subdued catchment response and wider hydrograph profile in both catchments. Frontal rainfall, however, brings persistent long-duration rainfall events (Met Office, 2022) which may be recognisable in Figures 5.6.5 and 5.6.6 due to the flows generated by frontal rain taking longer to return to baseflow. Overall, the catchment response to both types of rainfall is

similar in both catchments, continuing the trend of Lower Eidart having a narrower profile.

6.3 Study Limitations

A potential limitation of this study is limited availability of time series data. However, the year of record provided for this study has presented 14 flood events with corresponding precipitation data which was adequate for generating a comparison of hydrological response between the study catchments. The mountainous environment of the Upper Feshie system makes access for instrument checking, maintenance and calibration flow gauging very difficult especially over the winter months. Consequently, gauging stations can be left unattended for long periods of time in sub-zero conditions so either the instrumentation may freeze, or the data logger may reach capacity and stop logging. An increase in the temporal extent of the continuous time series would be useful in further comparisons of these catchments.

A limitation in this research is the accuracy of the hydraulic modelling. Hydraulic modelling is an extremely versatile tool in civil engineering, flood risk assessment and habitat restoration (Jowett and Duncan, 2011) with a diverse range of literature supporting its use, for example in Kean and Smith; (2005), Lang, *et al.*, (2010), and Muste and Lee (2013). However, the unsatisfactory result of the 1D model in this research led to an output for Lower Eidart which was not usable. Simply put, the channel morphology of the modelled reach of the Lower Eidart is too complex for fully 1D modelling with many step-pool formations which act as stage independent and importantly, stage dependent controls. The reduced confidence in the input topography of the Lower Eidart is due to difficulty in accurately representing the 'weir' style controls at the head of each step-pool. Connection to a 2D domain and a more accurate 'weir' representation as an input inline structure would have increased confidence in the topography and yielded better results.

A final limitation is the omission of the third reach, Upper Feshie Confluence, from the hydrological analysis due to lack of adequate time series. The continuous time series data for Upper Feshie Confluence did not overlap the study period for Upper Feshie and Lower Eidart, which prevented significant hydrological analysis in Upper Feshie Confluence.

Additionally, application of a rating to the time series at Upper Feshie Confluence may also have presented insights into the accuracy of the rating extension for Lower Eidart and Upper Feshie through sense checking the peak flows throughout the 14 flood

events used in this research. A recommendation based on this research would be the extension of the rating equation at Upper Feshie Confluence so that this research may be built upon and consolidated in its aim of attaining knowledge of the runoff regime of these upland blanket peat and mineral catchments. Figure 6.3.1 has been generated by the combination of flows from Lower Eidart and Upper Feshie and shows a series of peaks for most flood events in this study. Hydrological analysis of Upper Feshie Confluence following the methods used in this study may verify the results of the lag time analysis presented in Chapter 5.

6.4 General Implications

This research has increased knowledge of upland hydrological response across spatial and temporal scales. Shuttleworth, *et al.*, (2019) presents catchment scale results for assessing the impact of surface runoff in peatland catchment hydrological response. This study may augment the work of Shuttleworth, *et al.*, (2019) due to the extension of the ratings so that they may be applied to Lower Eidart and Upper Feshie as they naturally regenerate, facilitating a way of recording changes to hydrological response at catchment scale. The extension of these ratings for gauging stations carefully placed in areas of bedrock control will be applicable to data captured over a greater temporal period as flows are projected to increase by up to 40% by 2100 (Arnell, *et al.*, 2021).

Blanket peat environments are efficient carbon sinks (NatureScot 2020) and therefore it is important that knowledge of these environments is attained and validated as peat restoration is of paramount conservation importance at a national scale. Therefore, quantifying changes in catchment response as the blanket peat is restored may be used as a means of quantifying the effect of the restoration. The baseline difference in lag time between the two catchments has been identified as 23 minutes, with the potential for sub-catchment synergy to increase the flood wave from the Upper Feshie if the difference of lag time is reduced by restoration, which signals successful regeneration but may increase flood risk downstream.

Surface runoff attenuation through peat bog restoration is by proxy, a soft flood management measure (Carrick, *et al.*, 2018) as it is categorised as flood attenuation measure which is associated with surface cover change. Black, *et al.*, (2021) presents evidence of catchment scale success in the application of flood risk management through hydrological analysis including lag time to peak discharge. This research may have implications for augmenting knowledge of the effectiveness of soft Natural Flood

Management measures as the overall Feshie catchment is currently being naturally regenerated as mentioned in Chapter 1. Therefore, the analysis of lag time to peak discharge and the creation of a characteristic median hydrograph will stand as a baseline for a temporal comparison of the current hydrological response of Lower Eidart and Upper Feshie and how these catchments may react after a sustained period of regeneration.

Overall, this research serves to bridge the gaps in current knowledge of the hydrological response of upland bare peat and mineral catchments at catchment scale. Additionally, this research may augment the work of Black, *et al.*, (2021) and Shuttleworth, *et al.*, (2019) by presenting a baseline for insights into the spatial and temporal impacts of peatland restoration on flood events and risk in the Scottish Highlands.

Chapter 7: Conclusion

The aim of this study was to compare the hydrological response of two neighbouring blanket peat and bare peat/ mineral sub catchments of the Feshie catchment, Scottish Highlands. For the estimation of flows for the installed river gauging stations, HEC-RAS 1D modelling was found to be successful for Upper Feshie however not Lower Eidart due to the complexity of the reach. The $Q = VA$ method replaced the 1D modelling in the extension of the rating equation for Lower Eidart and yielded more realistic results.

The results of the $Q = VA$ method presented a peak discharge of $11.8 \text{ m}^3/\text{s}$ and a mean annual runoff of 1183 for Lower Eidart which received 1400 mm of rainfall in the study year through the creation of a two-part rating equation. The Upper Feshie results included $20.2 \text{ m}^3/\text{s}$ and 1268 mm for Lower Eidart which received 1400 mm of rainfall in the study year through a three-part equation generated in HEC-RAS.

It is recommended that empirical analyses are used in the place of hydraulic modelling for complex upland catchments as hydraulic modelling is based on assumptions and input parameters, whereas empirical means such as the Vbar method begin from observational data with high confidence.

Analysis of lag time to peak discharge across 14 events showed that Lower Eidart, which predominantly has bare peat (>27%) and exposed mineral soil (>59%) for surface coverage, peaked 23 minutes faster than Upper Feshie. The statistical test found this 23 minute to be statistically insignificant with $P = 0.1171$. In addition to this lag time

analysis, creation of a median hydrograph for both catchments allowed ease of comparison between these catchments in terms of their hydrological response. It was found that both catchments have a very similar hydrological response (Figure 5.6.1) where the gradient of the rising limb of both catchments is remarkably similar. However, Lower Eidart is consistently narrower in profile than Upper Feshie across all synthesised hydrographs which is attributed to the physical soil characteristics of the catchment leading to reduced surface friction, lower storage and more rapid runoff conveyance than Upper Feshie.

Lower Eidart has a higher antecedent flow prior to the simulated hydrograph, potentially explaining why Lower Eidart exhibits much lower peak discharge for two catchments that are both approximately 30 km², however this baseflow observation is inconsistent with prior expectations from literature (Chapter 2, section 2.2) and the FEH (2022) catchment descriptors (Table 3.3.1).

A sensitivity analysis of this hydrograph in terms of the creation of a median hydrograph subset based on flood magnitude (Figures 5.6.2 and 5.6.3) validated the median hydrograph in Figure 5.6.1 because there was little variability in the shape of the hydrographs across the range of flows. A hydrograph subset based on precipitation type were divided into frontal and convective to see how these catchments react to different precipitation input (Figures 5.6.4, 5.6.5 and 5.6.6). The results showed that both catchments respond to convective precipitation more quickly and return to baseflow more quickly than with frontal events. Because all but one of the events were of frontal origin, the general comparison between hydrograph shapes for all events applied equally for the frontal events.

Validation of this research through extension of the rating equation at Upper Feshie Confluence may verify the analyses in this study, which is of national conservation importance as this study may present insights into the effects of natural regeneration on hydrological response of upland catchments.

This research may set the baseline for temporal analysis of changes in the hydrological response of Lower Eidart as the regeneration matures. These temporal comparisons may augment the work of Black, *et al.*, (2021) and Shuttleworth, *et al.*, (2019) as it may help quantify the effectiveness of catchment scale regeneration on surface runoff attenuation as surface runoff is the primary means of runoff conveyance in Lower Eidart and Upper Feshie.

Understandings of catchment scale regeneration is of national importance as peatland restoration is of paramount conservation importance globally, especially in an uncertain time of changing climate. Lower Eidart peaks 23 minutes before the Upper Feshie and if this difference in lag time is reduced by increased surface roughness through natural regeneration, it may lead to enhanced sub catchment synergy which may increase the flood wave at the confluence countering NFM efforts.

Overall, this research presents novel findings of the hydrological response of two neighbouring bare peat and mineral catchments in the Feshie catchment where the Lower Eidart peaks 23 minutes faster than the Lower Eidart and has a consistently narrower hydrograph profile. These results are attributed to the contrasting physical characteristics of these catchments as Lower Eidart has reduced storage capacity and enhanced surface runoff through a great incidence of well-draining mineral soils (>59%) and poor condition peat (>27%) leading to more efficient runoff conveyance when compared to Upper Feshie. Upper Feshie is predominantly peat (>65%) and peaty soil (>10%) which has a greater ability to attenuate runoff through friction and slightly enhanced storage, leading to a wider hydrograph profile and longer lag time. Therefore, the contrasting physical descriptors of the catchments are consistent with the hydrological differences observed, and consistent with the results published by Soulsby., *et al* (2006), while being at odds with the BFI values obtained from the FEH Web Service which indicate a stronger baseflow contribution from the Upper Feshie.

Further research should aid the continuity of these hydrological analyses by validating this study with Upper Feshie Confluence, and by generating interest to continue the research and consolidate the availability of time series meteorological and flow data from these upland catchments. This line of study has a unique and important opportunity to unlock the hydrology of Scottish headwater catchments in broader peat environments and allow for monitoring of hydrological response spatially and temporally in an unprecedented time of climate concerns and conservation drive.

References

- Acrement, G., and Schneider, V. (1989) *Guide for Selecting Manning's Roughness Coefficients for Natural Channels and Flood Plains*. Available: <https://pubs.usgs.gov/wsp/2339/report.pdf>. Accessed: 09/04/2021. USGS.
- Acreman, M. (1989) Extreme Historical UK Floods and Maximum Flood Estimation. *Water and Environment Journal*. Vol 3(4): pp. 404-412. Wiley Online Library.
- Al-Meida, G., and Rodriguez, J. (2011) *Understanding Pool-Riffle Dynamics Through Continuous Morphological Simulations*. *Water Resource Research*. Vol 47(1). AGU.
- Arctic Atlas (2002) *Racomitrium lanuginosum*. Available: https://www.arcticatlas.org/photos/pltspecies/spp_details.php?queryID=rala70. Accessed: 29/09/2022.
- Arnell, N., Kay, A., Freeman, A., Rudd, A., and Lowe, J. (2021) Changing Climate Risk in the UK: A Multi-Sectoral Analysis Using Policy Relevant Indicators. *Climate Risk Management*. Vol 31. Elsevier Online Library.
- Averis, A., and others (names unavailable). (2004) *Illustrated Guide to British Upland Vegetation*. *Joint Nature Conservation Committee*.
- Baldassarre, G., Castellarin, A., and Brath A. (2009) Analysis of the Effects of Levee Heightening on Flood Propagation. *Hydrological Sciences Journal*. Vol 51: pp. 1007-1017. Taylor and Francis
- Baldassarre, G., and Claps, P. (2011) A Hydraulic Study on Applicability of Flood Rating Curves. *Hydrology Research*. Vol 42(1). IWA Publishing.
- Beston, R., and Marius, J. (1969) Source Areas of Storm Runoff. *Water Resource Research*. Vol 5(3): pp. 574-582. Wiley Online Library.
- Bettess, F. (1992) *Surveying for Archaeologists*. University of Durham Department of Archaeology.
- Becker, A. (2005) Runoff Processes in Mountain Headwater Catchments: Recent Understanding and Research Challenges. *Global Change and Mountain Regions*. Vol 23: pp. 283-295. Springer.

- Beniston, M. (2012) Focus Article. Is Snow in the Alps Receding or Disappearing? *WIREs Climate Change*. Vol 3: pp. 349-385.
- Betsholtz, A., and Nordlof, B. (2017) Potentials and Limitations of 1D, 2D and Coupled 1D-2D Flood Modelling in HEC-RAS. *Masters Thesis*. Water Resource Engineering, Lund University.
- Bessar, M., Matte, P., and Anctil, F. (2020) Uncertainty Analysis of a 1D Hydraulic Model with Adaptive Calibration. *Water*. Vol 12: pp. 561. MDPI.
- Biodiversity Ireland (2022) *Nardus Stricta Heath*. Available: <https://biodiversityireland.ie/ivc-classification-explorer/he4/he4b/>. Accessed: 29/09/2022.
- Black, A., and Burns, C. (2002) Re-Assessing Flood Risk in Scotland. *Science of the Total Environment*. Vol 294(1): pp. 169-184. Elsevier Online.
- Black, A., Peskett, L., MacDonald, A., Young, A., Spay, C., Ball, T., Thomas, H., and Werrity, A. (2021) Natural Flood Management, Lag Time and Catchment Scale: Results from an Empirical Nested Catchment Study. *Journal of Flood Risk Management*. Vol 14(3):e12717. Wiley Online Library
- Boorman, D., Hollis, J., and Lilly, A. (1995) Report No. 126. Hydrology of Soil Types: A Hydrologically- Based Classification of the Soils of the United Kingdom. *NERC*.
- Bonnell, M. (1998) Selected Challenges in Runoff Generation Research in Forests from the Hillslope to Headwater Drainage Basin Scale. *Journal of American Water Resource Association*. Vol 34: pp. 765-785. Wiley Online Library.
- Bragg, O. (2002) Hydrology of Peat-Forming Wetlands in Scotland. *Science of the Total Environment*. Vol 294(1-3): pp. 111-129. Elsevier Online.
- Brunner, G. (2001) HEC-RAS River Analysis System Users' Manual, US Army Corps of Engineers. Hydraulic Engineering Centre, Davis (2001).
- Buttle, J. (1998) Fundamentals of Watershed Hydrology. *Isotope Tracers in Catchment Hydrology*. pp. 1-50. Elsevier.
- Bullard, J., McTanish, G., and Martin, P. (2007) Establishing Stage-Discharge Relationship in Multiple-Channelled Ephemeral Rivers: A case Study of

- Diamantina River, Australia. *Geophysical Research*. Vol 45(3): pp. 233-245. Wiley Online Library.
- Burt, T., and Holden, J. (2022) Changing British Temperature and Rainfall Gradients in the British Uplands. *Climate Research*. Vol 43(3). Research Gate.
- Casas, A., Benito, G., Thorndycraft, V., and Rico, M. (2006) The Topographic Data Source of Digital Terrain Models as a Key Element in the Accuracy of Hydraulic Flood Modelling. *earth Surface Processes and Landforms*. Vol 31(4): pp. 444-456. Wiley Online Library.
- Caviedes-Voullieme, d., Morales-Hernandez, M., Lopez-Marijuan, I., and Garcia-Navarro, P. (2014) Reconstruction of 2D Riverbeds by Appropriate Interpolation of 1D Cross-Sectional Information for Flood Simulation. *Environmental Modelling & Software*. Vol 61: pp. 206-228. Elsevier Online.
- Carrick, J., Rahim, M., Adjei, C., Kalee, H., Banks, S., Bolam, F., Luna, I., Clark, B., Cowton, J., Domingos, I., Golicha, D., Gupta, G., Grainger, M., Hasanaliyeva, G., Hodgson, D., Capel, E., Magistrali, A., Merrell, I., Oikeh, I., Othman, M., Mudiyansele, R., Samuel, C., Sufar, E., Watson, P., Zakira, N., and Stewart, G. (2018) Is Planting Trees the Solution to Reducing Flood Risks? *Journal of Flood Risk Management*. Vol 12(2). Wiley Online Library.
- Ceola, S., Montanari, A., Krueger, T., Dyer, F., Kreibich, H., Westerberg, I., *et al.*, (2016) Adaption of Water resource Systems to Changing Society. *Hydrological Sciences Journal*. Vol 61(16): pp. 2803- 2817. Taylor and Francis.
- Charman, D. (2009) in *Encyclopaedia of Inland Waters*. Elsevier Publications.
- Chow, V. (1959) *Open Channel Hydraulics*. McGraw-Hill, New York.
- Clifford, N. (1993) Differential Bed Sedimentology and the Maintenance of Riffle-Pool Sequences. *CATENA*. Vol 20(5): pp. 447-468. Elsevier Online.
- Clayton, J., and Kean, J. (2010) establishing Multi-Scale Stream Gauging Network in the Whitewater Basin, Kansas, USA. *Water Resources Management*. Vol 61(16): pp. 2803-2817. Springer.
- Conway, V., and Millar, A. (1960) The Hydrology of Some Small Peat Covered Catchments in the Northern Pennines. *Journal of the Institute of Water Engineers*. Vol 14: pp. 415- 425. Institute of Water.

- Coxon, G., Freer, J., Westerberg, I., Wagener, T., Woods, R., and Smith, J., P. (2015) A Novel Framework for Discharge Uncertainty Quantification Applied to 500 UK Gauging Stations. *Water Resource Research*. Vol Vol 51: pp. 5531-5546. Wiley Online Library.
- Crawford, G. (1991) Estimation of Suspended-Sediment Rating Curves and Mean Suspended Sediment Loads. *Journal of Hydrology*. Vol 129: pp. 331-348. Elsevier Online.
- Cris, R., Buckmaster, S., Bain, C., and Reed, M. (eds) (2014) Global Peatland Restoration Demonstrating Success. Edinburgh: ICUN UK National Committee Peatland Programme.
- Craft, C. (2016) in *Creating and Restoring Wetlands*. Elsevier Publications.
- Damman, A. (1986) Hydrology, Development, and Biogeochemistry of Ombrogenous Peat Bogs with Special Reference to Nutrient Relocation in a Western Newfoundland Bog. *Journal of Botany*. Vol 64(2): pp. 156. Canadian Science Publishing.
- Deasy, C., Titman, A., and Quinton, J. (2014) Measurement of Flood Peak Effects as a Result of Soil and Land Management. *Journal of Environmental Management*. Vol 132: pp. 304-314. Springer.
- De Jong, C. (2015) Challenges for Mountain Hydrology in the Third Millennium. *Frontiers in Environmental Science*. Available: <https://www.frontiersin.org/articles/10.3389/fenvs.2015.00038/full>. Accessed: 02/05/2021.
- Degetto, M., Gregoretti, C., and Bernard, M. (2015) Comparative Analysis of the Differences Between Using LiDAR Contour Based DEMs for Hydrological Modelling of Runoff Generating Debris Flows in the Dolomites. *Frontiers in Earth Science*. Vol 3(21). Frontiers Media.
- Dingman, S. (1981) Elevation: a Major Influence on the Hydrology of New Hampshire and Vermont, USA. *Hydrological Sciences Journal*. Vol 26(4): pp. 399-413. Taylor and Francis Online.
- Dimitriadis, P., Tegos, A., Oikonomou, A., Pagana, V., Koukouvinos, A., Mamassis, N., Koutsoyiannis, D., and Efstratiadis, A. (2016) Comparative Evaluation of 1D and

- Quasi-2D Hydraulic Models Based on Benchmark and Real-World Applications for Uncertainty Assessment in Flood Mapping. *Journal of Hydrology*. Vol 534: pp. 478-492. Elsevier Online.
- Dottori F., Martina, M., and Todoni, E. (2009) A Dynamic Rating Curve Approach to Indirect Discharge Measurement. *Hydrology and Earth System Sciences*. Vol 13: pp. 847- 836. Copernicus Publications.
- Dunne, T. (1978) Field Studies of Hillslope Flow Processes. *Hillslope Hydrology*. Wiley.
- Dunne, T., and Dietrich, W., E. (1990) Experimental Investigation of Horton Overland Flow on Tropical Hillslopes. *Z. Geomorphology. N.F* Vol 35: pp. 40-59. Berlin Stuttgart.
- Ebert, K. (2009) Terminology of Long-Term Geomorphology: A Scandinavian Perspective. *Progress in Physical Geography*. Vol 33: pp. 163-182. Sage Publications.
- Eggesman, R., Haithwaite, A., Gross-Brauckmann, G., Kuster, E., Naucke, W., Scich, M., and Schweikle, V. (1993) Physical Processes and Properties of Mires. *Mires, Processes, Exploration and Conservation*. 1993: pp. 172-262. Wiley Online Library.
- Evans, M., Burt, T., and Warburton, J. (1999) Runoff Generation and Water Table Fluctuations in Blanket Peat; Evidence from UK Data Spanning the Dry Summer of 1995. *Journal of Hydrology*. Vol 221(3): pp. 141-160. Elsevier Online.
- Evans, M., Allot, T., Holden, J., Flitcroft, C., and Bon, A (2005) Understanding Gully Blocking in Deep Peat. *Moors for the Future Report*. Number 4. Available: <http://citeseerx.ist.psu.edu/viewdoc/download?doi=10.1.1.117.2678&rep=rep1&type=pdf>. Accessed: 15/03/21.
- Fang, X., Cleveland, T., Garcia, C., Thompson, D., and Malla, R. (2005) *Literature Review on Timing Parameters*. No. 0-4696-1; p. 82. Lamar University.
- Flores, R. (2014) in *Coal and Coalbed Gas*. Elsevier Publications.
- Gao, J., Holden, J., and Kirkby, M. (2016) The Impact of Land Cover Change on Flood Peaks in Peatland Basins. *Journal of Hydrology*. Vol 389(3): pp. 336-343. Elsevier Online.

- Greicke, O., and Smithers, J. (2014) Review of Methods Used to Estimate Catchment Response Time for Purpose of Peak Discharge Estimation. *Hydrological Sciences Journal*. Vol 59(11): pp. 1935-1971.
- Gregoretto, C., Degetto, M., Bernard, M., Crucil, G., Pimazzoni, A., De Vido, G., Berti, M., Simoni, A., and Lanzoni, S. (2016) Runoff of Small Rocky Catchments: Field Observations and Hydrological Modelling. *Water Resources Research*. Vol 52(10): pp. 8138-8158. Wiley Online Library.
- Gilman, K. (1994) *Hydrology and Wetland Conservation*. pp. 101. John Wiley and Sons.
- Gilvear, D., and Watson, A. (1995) The Use of Remotely Sensed Imagery for Mapping Wetland Water Table Depths: Insh Marshes, Scotland. *Hydrology and Hydrochemistry of British Wetlands*. (1995): pp. 419-430. Wiley Online Library.
- Gleason, C. (2015) Hydraulic Geometry of Natural Rivers: A review and Future Directions. *Processes in Physical Geography*. Vol 39(3): pp. 337-360. SAGE Journals.
- Global Biodiversity Information Facility (2022) *Sphagnum Fuscum* Available: <https://www.gbif.org/species/2669215> Accessed: 29/09/2022.
- Gorham, E., and Rochefort, L. (2003) Peatland Restorations: A Brief Assessment with Special Reference to Spagnum Bogs. *Wetlands Ecology and Management*. Vol 11: pp. 109-119. Springer.
- Goodfellow, B., Skelton, A., Martel, S., Stroeven, A., Jansson, K., and Hattestrand, C. (2014) Controls of Tor Formation, Cairngorm Mountains, Scotland. *JGR Earth Surface*. Vol 119(2): pp. 225- 246. Wiley Online Library.
- Gosling, R. (2014) Assessing the Impact of Projected Climate Change On Drought Vulnerability in Scotland. *Hydrology Research*. Vol 45(6): pp. 906-816. IWA Publishing.
- Grayson, R., Holden, J., and Rose, R. (2010) Long-Term Change in Storm Hydrographs in Response to Peatland Vegetation Change. *Journal of Hydrology*. Vol 389: pp. 336-343. Elsevier.

- Grantano, G. (2012) Estimating Basin Lagtime and Hydrograph Timing Indexes Used to Characterise Stormflows for Runoff Quality Analysis. *US Geophysical Survey Scientific Investigation Science Report*. United States Geophysical Survey.
- Hankin, B., and Beven, K. (1998) Modelling Dispersion in Complex Open Channel Flows: Equifinality of Model Structure. *Stochastic Hydrology and Hydraulics*. Vol 12(6): pp. 377. Springer
- Hardy, R., Bates, P., and Anderson, M. (1999) The Importance of Spatial Resolution in Hydraulic Models for Flood Plain Environments. *Journal of Hydrology*. Vol 216(1): pp. 124-136. Elsevier Online.
- Harmal, R., King, K., Haggard, B., Wren, D., and Sheridan, J. (2006) Practical Guidance for Discharge and Water Quality Data Collection on Small Watersheds. *Transactions of the ASABE*. Vol 49(4): pp. 397-948. E-Library ASABE.
- Hawkins, R., Ward, J., Woodward, D., and Mullem, A. (2009) Curve Number Hydrology: State of Practice. *American Society of Civil Engineers*.
- Hagemann, H., Hagemann, S., and Rockel, B. (2015) On the Role of Soil Moisture in the Generation of Heavy Rainfall During the Oder Flood Event in July 1997. *Tellus A: Dynamic Meteorology and Oceanography*. Vol 61(1). Taylor and Francais Online.
- Hale, V., and McDonnell, J. (2016) Effect of Bedrock Permeability on Stream Baseflow mean Transit Time Scaling Relations: 1 A Multiscale Catchment Comparison. *Water Resources Research*. Vol 52: pp. 1358-1374. AGU.
- Hewlett, J., and Hibbert, A. (1967) Factor Affecting the Response of Small Watersheds to Precipitation in Humid Areas. *Forest hydrology*. New York: Pergamon.
- Herschy, R. (1993) The Velocity- Area Method. *Flow Measurement and Instrumentation*. Vol 4(1): pp. 7-10. Elsevier Online.
- Herschy, R. (1999) *Hydrometry- Principles and Practices*. John Wiley and Sons, Chichester: pp. 376.
- Hirabayashi, Y., Mahendran, R., Koirala, S., and others. (2013) Global Flood Risk Under Climate Change. *Nature Climate Change*. Vol 3: pp. 816-821. Nature.
- Hirsch, R., and Archfield, S. (2015) Flood Trends: Not Higher but More Often. *Nature Climate Change*. Vol 5: pp 189-199. Nature Publishing.

- Horton, R. (1937) Hydrolic Interrelations of Water and Soils. *Soil Science Society of America*. Vol 1.
- Holden, J., and Burt, T. (2003a) Runoff Production in Blanket Peat. *Water Resources Research*. Vol 39(7): pp. 1191. AGU.
- Holden, J., and Burt, T. (2003b) Hydrological Studies on Blanket Peat: The Significance of the Acrotelm- Catotelm Model. *Journal of Ecology*. Vol 91: pp. 86-102. Wiley Online Library.
- Holden, J. (2006) Peatland Hydrology. *Peatlands: Evolution Records of Environmental and Climatic Change*. Elsevier Online.
- Holden, J., Chapman, M., Evans, G., Hubacek, K., Kay, P., and Warburton, J. (2007) Vulnerability of Organic Soils in England and Wales. *Special Report to DEFRA*.
- Holden, J., Kirby, M., Lane, S., Milledge, D., Brookes, C., Holden, V., and McDonald, A. (2008) Overland Flow Velocities and Roughness Properties in Peatlands. *Water Resources Research*. Vol 44(6). AGU.
- ICUN (2014) *ICUN UK Committee Peatland Programme Briefing Note No.7*.
- Kean, J., and Smith, J. (2005) Generation and Verification of Theoretical Rating Curves in the Whitewater Basin, Kansas. *Journal of Geophysical Research*. Vol 110. Wiley Online Library.
- Kiang, J., Gazorian, C., McMillan, H., Coxon, G., Le Coz, J., Westerberg, I. *et al.*, (2018) A Comparison of Methods for Streamflow Uncertainty.
- Ingram, H., A., P. (1978) Soil Layers in Mires: Function and Terminology. *Journal of Ecology*. Vol 55(3): pp. 711-724. JSTOR.
- Ingram, H., A., P. (1983) Hydrology. Mires, Swamp, Bog, Fen and Moor. *Ecosystems of the World*. Vol 4(A): pp 76-158. Elsevier Online.
- Ingram, H., A., P., and Bragg, O. (1984) The Diplomatic Mire: Some Hydrological Consequences. *Proceedings of the 7th International Peat Congress*. Vol 1: pp. 220-234. AGRIS.
- Ingram, H, A, P. (1989) Mires as Cultural Landscapes. *Conserving Peatlands, CAB International*. pp. 159-161. Wallingford.

- ICUN (2020) *Position Statement: Peatlands and Trees*. Available: <https://www.iucn-uk-peatlandprogramme.org/sites/default/files/header-images/Resources/IUCN%20UK%20PP%20Peatlands%20and%20trees%20position%20statement%202020.pdf>. Accessed: 09/03/2021.
- Jarvie, H., Neal, C., Smart, R., Owen, R., Fraser, D., Forbes, I., and Wade, A. (2001) Use of Continuous Water Quality Records for Hydrograph Separation and to Assess Short Term Variability and Extremes in Acidity and Dissolved Carbon Dioxide for the River Dee, Scotland. *Science of the Total Environment*. Vol 265: pp. 85-98. Elsevier Online.
- James, A., and Roulet, N. (2009) Antecedent Moisture Conditions and Catchment Morphology as Controls on Spatial Patterns of Runoff Generation in Small Forest Catchments. *Journal of Hydrology*. Vol 377(3): pp. 351-366. Elsevier Online.
- Jigsaw Cambridge (2021) Step-By-Step Guide to Dumpy Level Survey. Available: [step by step guide to dumpy level survey.pdf \(jigsawcambs.org\)](http://www.jigsawcambs.org/step-by-step-guide-to-dumpy-level-survey.pdf). Accessed: 15/05/2021.
- Keleman, J., C., and Ingram, H., A., P. (1999) The Use of Large Bottomless Lysimeters in the Determination of Water Balances for a Raised Mire. *Hydrological Processes*. Vol 13: pp. 101- 111. Wiley Online Library.
- Kiczko, A., and Miro-Swiatek, D. (2018) Impact of Uncertainty of Flood Plain Digital Terrain Model on 1D Hydrodynamic Flow Calibration. *Water*. Vol 10: pp. 1308. MDPI.
- Kjeldson, T., and Jones, D. (2010) Predicting the Index Flood in Ungauged UK Catchments: On the Link Between Data-Transfer and Spatial Error Modelling. *University of Bath*.
- Kjeldson, T., Jones, D., and Morris, D. (2014) Using Multiple Donor Sites for Advanced Flood Estimation in Ungauged Catchments. *Water Resource Research*. Vol 50(8): pp. 6636-6657. AGU.
- Lange, J., Greenbaum, N., Husary, S., Ghanem, M., Leibundgut, C., and Schick, A. (2003) Runoff Generation from Successive Simulated Rainfalls on a Rocky Semi-Arid Mediterranean Hillslope. *Hydrological Processes*. Vol 17: pp. 279-296. Wiley Online Library.

- Lane, S., Morris, J., O'Connell, P., and Quinn, P. (2007) *Managing the Rural Landscape. Future, Flooding and Coastal Erosion Risks*. pp. 297-319. Thomas Telford, London.
- Lang, M., Pobanz, K., Renard, B., RenoUpper Feshie, E., and Saquet, E. (2010) Extrapolation of Rating Curves by Hydraulic Modelling, With Application to Flood Frequency Analysis. *Hydrological Sciences Journal*. Vol 55(6): pp. 883-989. Wiley Online Library.
- Lam, N., Nathanson, M., Lundgren, N, Rehnstorm, R., and Lyon, S. (2015) A Cost-Effective Laser Scanning Method for Mapping Stream Channel Geometry and Roughness. *Journal of the American Water Resources Association*. Vol 51(5): pp. 1211-1220. Wiley Online Library.
- Lambord, P., and Holtschlag, D. (2018) Estimating Lag to Peak Between Rainfall and Peak Streamflow with A Mixed-Effect Model. *Journal of American Water Resources Association*. Vol 54(4): pp. 949-961. Wiley Online Library.
- Leopold, L., and Maddock, T. (1953) *The Hydraulic Geometry of Stream Channels and Some Physiographic Implications*. *Geological Survey Professional Paper 252*. United States Government Printing Office.
- Le Coz, J., Renard, B., Bonnfait, L., Branger, F., and Le Boursicaud, R. (2014) Combining Hydraulic Knowledge and Uncertain Gaugings in the Estimation of Hydrometric Rating Curves: A Bayesian Approach. *Journal of Hydrology*. Vol 509: pp. 573- 587. Elsevier Online.
- Lee, K., and Muste, M. (2017) Refinement of the Fread Method for Improved Tracking of Stream Discharges During Unsteady Flows. *Journal of Hydraulic Engineering*. Vol 143(6): pp. ASCE Library.
- Ledingham, J., Archer, D., Lewis, E., Fowler, H. and Kilsby, C. (2019) Contrasting Seasonality of Storm Rainfall and Flood Runoff in the UK and Some Implications for Rainfall-Runoff Methods of Flood Estimation. *Hydrology Research*. Vol 50(5): pp. 1309–1323. IWA.
- Lindsay, R., and Immirzi, P. (1996) *An Inventory of Lowland Raised Bogs in Great Britain*. Scottish National Heritage research and Monitoring report no. 78.

- Lindsay, R., Charman, D., J., Everingham, F., O'Rielly, R., M., Palmer, M., A., Rowell, T., A., and Stroud, D., A. (1988) *The Peatlands of Caithness and Sutherland. The Flow Country*. Nature Conservancy Council.
- Lorenz, R., Jaeger, E., and Senevirante, S. (2010) Persistence of Heat Waves and its Link to Soil Moisture Memory. *Geophysical Research Letters*. Vol 37(9). AGU Publications.
- Low, R. (2020) *The Hydrology of Peatlands*. Available: https://www.youtube.com/watch?v=113e-XcP4mg&ab_channel=NPTWildlife. Accessed: 26/01/2021.
- Lukas, S., Merritt, J., and Mitchell, W. (2004) The Quaternary of the Central Grampian Highlands. *Quaternary Research Association*.
- Maidment, D. (1993) *Handbook of Hydrology*. New York: McGraw-Hill.
- Mansell, M. G. (1997) The Effect of Climate Change on Rainfall Trends and Flooding Risk in the West of Scotland. *Hydrology Research*. Vol 28(1): pp. 37-50. IWA Publishing.
- Martinez-Carreras, N., Christophe, H., Laurent, G., Klaus, J., Juilleret, J., Francois, Iffly, J., McDonnell, J., and Laurent, P. (2001). On the Trail of Double Peak Hydrographs. *EGU General Assembly Conference Abstracts*. Harvard
- Marston, R. (2010) Geomorphology and Vegetation on Hillslopes: Interactions, Dependencies, and Feedback Loops. *Geomorphology*. Vol 116(3): pp. 206-217. Elsevier.
- MacDonald, P. (2016) Change in Glen Feshie. Available: <https://www.eca.ed.ac.uk/sites/default/files/PMacdonald-ChangeInGlenFeshie-SNH-Nos-AW2016-PDF.pdf>. Accessed: 11/05/2021. Scottish National Heritage.
- Marston, R., and Marston, B. (2017) Mountain Hydrology. *in International Encyclopaedia of Geography*. pp. 4532-4540. Research Gate.
- Mansanarez, V., Westerberg, I, Lam, N., and Lyon, S. (2019) Rapid Stage-Discharge Rating Curve Assessment Using Hydraulic Modelling in an Uncertainty Framework. *Water Resource Research*. Vol 55(11): pp. 9765-9787. Wiley Online Library.

- McCoy, R. (2005) *Field Methods in Remote Sensing*. The Guilford Press: New York.
- McCuen, R. (2009) Uncertainty Analysis of Watershed Time Parameters. *Journal of Hydraulic Engineering*. Vol 14(5): pp. 490-498. Springer.
- McMillan, H., Krueger, T., and Freer, J. (2012) Benchmarking Observational Uncertainties for Hydrology: Rainfall, River Discharge and Water Quality. *Hydrological Processes*. Vol 26(26): pp. 4078- 4111. Wiley Online Library.
- McMillan, H., Seibert, J., Paterson-Overlier, A., Lang, M., White, P., and Snelder, T. *et al.*, (2017) How Uncertainty Analysis of Streamflow Data Can Reduce Cost and Promote Robust Decisions in Water Management Applications. *Water Resource Research*. Vol 53: pp. 5220-5228. Wiley Online Library.
- McMillan, H., Westerberg, I., and Krueger, T. (2018) Hydrology Data Uncertainty and its Implications. *WIREs Water*: pp. 1319. Wiley Online Library.
- McPherson, B. (2022) *New Climate Predictions Summary for Scotland*. Available: <https://www.historicenvironment.scot/about-us/news/new-climate-projections-summary-for-scotland/#:~:text=Scotland%20will%20experience%20warmer%2C%20wetter,wetter%20and%202.7%20degrees%20warmer>. Accessed: 16/09/2022.
- Metcalf, P., Beven, k., Hankin, B., and Lamb, R. (2018) A New Method, With Application, for the Analysis of the Impacts on Flood Risk of Widely Distributed Enhanced Hillslope Storage. *Hydrology and Earth System Science*. Vol 22(4): pp. 2258-2605. European Geosciences Union.
- Mesa-Mingorance, J., and Ariza-Lopez, F. (2020) Accuracy Assessment of Digital Elevation Models (DEMs): A Critical Review of Practices of the Past Three Decades. *Remote Sensing*. Vol 12(6). MDPI.
- Met Office (2022) *What Are the Different Types of Rain?* Available: <https://www.metoffice.gov.uk/weather/learn-about/weather/types-of-weather/rain/types-of-rain>. Accessed: 04/06/2022.
- Mimikou, M. (1984) Regional Relationships Between Basin Size and Runoff Characteristics. *Hydrological Sciences Journal*. Vol 29(1): pp. 63-73. Taylor and Francis Online.

- Miller, S. (1994) Handbook for Agrohydrology: Chapter 6. 1st edition. *Natural Resources Institute*.
- Milly, P. (1994) Climate, Soil Water Storage, and the Average Annual Water Balance. *Water Resources Research*. Vol 30&7): pp. 2143-2156. Wiley Online Library.
- Milly, P., Dunne, K., and Vecchia, A. (2005) Global Pattern Trends in Streamflow and Water Availability in a Changing Climate. *Nature*. Vol 438: pp. 347-350. Nature Publishing.
- Min, S., Zhang, X., Zwiers, F., and Hegrel, G. (2011) Human Contributions to More-Intense Precipitation Extremes. *Nature*. Vol 470: pp. 378-381. Nature.
- Milledge, D., Odoni, N., Allot, T., Evans, M., Pilkington, M., and Walker, J. (2015) Annex 6 in Flood Risk Modelling in Pilkington, *et al.*, Restoration of Blanket Bogs; Flood Risk Reduction and Other Ecosystem Benefits. Final Report of Making Space for Water Project: Moors and the Future Partnership, Edale.
- Morvan, H., Knight, D., Wright, N., Tang, X., and Crossley, A. (2008) The Concept of Roughness in Fluvial Hydraulics and its Formulation in 1D, 2D and 3D Numerical Simulation Models. *Journal of Hydraulic Research*. Vol 36: pp. 191-208. Taylor and Francis.
- Montanari, A., Young, G., Saveninje, H., Hughes, D., Wagener, T., Ren, L., *et al.*, (2013) ‘Panta-Rhei- Everything Flows’. Change in Hydrology and Society. *Hydrological Sciences Journal*. Vol 58(6): pp. 1256-1275. Taylor and Francis.
- Muste, M., and Lee, K. (2013) Quantification of Hysteric Behaviour in Stream Flow Rating Curves. *Proceedings of the 35th IAHR World Congress, Chengdu, China*. 8-13 September 2013.
- Nagy, L., Grabherr, G., and Thompson, D. (2003) Alpine Biodiversity in Europe. *Ecological Studies*. Vol 167. Springer
- NatureScot (2015) *Scotland’s National Peatland Plan: Working for Our Future*. Available: <https://www.nature.scot/doc/scotlands-national-peatland-plan-working-our-future>. Accessed: 04/06/2022.
- NatureScot (2020) *Peatland Action Study: Whats The Connection Between Peat and Carbon Storage*. Available: <https://www.nature.scot/doc/peatland-action-case-study-whats-connection-between-peat-and-carbon->

[storage#:~:text=As%20peat%20is%20formed%20in,peat%2C%20the%20balanc e%20is%20disturbed](#). Accessed: 04/06/2022.

- NatureScot (2022) *Montane Scrub and Treeline Woodlands*. Available: <https://www.nature.scot/landscapes-and-habitats/habitat-types/woodland-habitats/montane-scrub-and-treeline-woodlands>. Accessed: 29/09/2022.
- Nutt, N., and Perfect, C. (2011) Allen Water Natural Flood Management: Scoping Study. Report by CRESS and Halcrow to the Scottish Environment Protection Agency Stirling. SEPA.
- Pappenberger, F., Beven, K., Horritt, M., and Blazkova, S. (2005) Uncertainty in the Calibration of Effective Roughness Parameters in HEC-RAS Using Inundation and Downstream Level Observations. *Journal of Hydrology*. Vol Vol 302: pp. 46-69. Elsevier Online.
- Pan, C., and Shangguan, Z. (2006) Runoff Hydraulic Characteristics and Sediment-Generation in Sloped Grassplots Under Simulated Rainfall Conditions. *Journal of Hydrology*. Vol 331(1-2): pp. 178-185.
- Pall, P., Aina, T., Stone, D., Stott, P., Nozawa, T., Hilberts, A., Lohmann, D., and Allen, M. (2011) Anthropogenic Greenhouse Gas Contributions to Flood Risk in England and Wales in Autumn 2000. *Nature*. Vol 470: pp. 382-385. Nature.
- Pattison, I., Lane, S., Hardy, R., and Reany, S. (2014) The Role of Tributary Relative Timing and Sequencing in Controlling Large Floods. *Water Resource Research*. Vol 50(7): pp.5444-5458. Wiley Online Library.
- Penna, D., Meerveld, T., Gobbi, A., Borga, A., and Fontana, D. (2011) The Influence of Soil Moisture on Threshold Runoff Generation Processes in an Alpine Headwater Catchment. *Hydrology and Earth System Science*. Vol 15(3): pp. 689-702. European Geosciences Union.
- Pederson, O., Aberle, J., and Ruther, N. (2019) Hydraulic Scale Modelling of the Rating Curve for a Gauging Station with Challenging Geometry. *Hydrology Research*. Vol 50(3): pp. 825- 836. Wiley Online Library.
- Phillips, J., and Tadayon, S. (2006) *Selection of Manning's Roughness Coefficients for Natural and Constructed Vegetated and Non-Vegetated Channels, and Vegetation*

Maintenance Plan Guidelines for Vegetated Channels in Central Arizona. 1st Edition. United States Geological Survey

Phillips, W., Hall, A., Mottram, R., Fifeld, L., and Sugden, D. (2006) Cosmogenic ¹⁰Be and ²⁶Al Exposure Ages of Tors and Erratics, Cairngorm Mountains, Scotland: Timescales for the Development of a Classic Landscape of Selective Linear Glacial Erosion. *Geomorphology*. Vol 73(3): pp. 222-245. Elsevier Online.

Price, J., and Whitehead, G. (2001) Developing Hydraulic Thresholds for Sphagnum Recolonisation on an Abandoned Cutover Bog. *Wetlands*. Vol 21(1): pp. 32-40. Research Gate.

Provenzale, A., and Palazzi, F. (2011) Assessing Climate Change Risks Under Uncertain Conditions. *Engineering Geology for Society and Territory*. Vol 1. Springer.

Pilgrim, D., Cordery, I., and Baron, B. (1982) Effects of Catchment Size on Runoff Relationships. *Journal of Hydrology*. Vol 58(3): pp. 205-221. Elsevier Online Library.

Pitman, A., De Noblet- Ducourde, N., Avila , F., Alexander, L., Boisier J., and others. (2010) Effects of Land Cover Change on Temperature and Rainfall Extremes in Multi Model Ensemble Situations. *Earth System Dynamics*. Vol 3: pp. 213-231. Copernicus Publications.

Price, J., Evans, C., Evans, M., Allott, T., and Shuttleworth, E. (2016) Chapter 5: Peatland Restoration and Hydrology. *Peatland Restoration and Ecosystem Services*. Cambridge University Press.

Quinton, W., and Hayashi, M. (2005) The Flow and Storage of Water in the Wetland-Dominated Central Mackenzie River Basin: Recent Advances and Future Directions. University of Calgary.

Quesada , B., Vautard, R., You, P., Hirschi, M., and Senevirante, S. (2012) Asymmetric European Summer Heat Predictability from Wet and Dry Southern Winters and Springs. *Nature Climate Change*. Vol 2: pp. 736-741. Nature.

Rantz, S. (1982) Measurement and Computation of Streamflow. Vol 2: Computation of Discharge USGS Water Supply Paper: pp. 2175. US Government Printing Office.

RSGS (2014) Rewilding Glenfeshie. *The Geographer*, Winter 2014/15, p21.

- Ringrose, S., and Mignon, P. (1997) Analysis of Digital Elevation Data from the Scottish Highlands and Recognition of Pre-Quaternary Elevated Surfaces. *Paleosurfaces, Recognition, Reconstruction and Paleoenvironmental Interpretation*. The Geological Society, London.
- Riestad, S., Peterson- Overlier, A., and Bogetveit, L. (2007) Setting Up Rating Curves Using Hec-Ras. *Journal of Nordic Water Association*. Vol 3: pp. 30. Springer.
- River Levels UK (2020) Feshie at Feshie Bridge. Available: <https://riverlevels.uk/feshie-feshie-bridge#.X8047Nj7Q2x>. Accessed: 06/12/2020.
- Robertson, R., A., Nicholson, I., A., and Hughes, R. (1968) Runoff Studies in a Peat Catchment. *Proceedings of the Second International Peat Congress*. International Peat Society. pp. 161-166.
- Robinson, M., and Newson, M., D. (1986) Comparison of Forest and Moorland Hydrology in an Upland Area with Peat Soils. *International Peat Journal*. Vol 1: pp. 49-68. Elsevier Online.
- Robinson, S. (2006) Carbon Accumulation in Peatlands, Southwestern Northwest Territories, Canada. *Canadian Journal of Soil Science*. Vol 86(2). Research Gate.
- Rocheftort, L. (2000) Sphagnum- A Keystone Species in Habitat Restoration. *Bryologist*. Vol 103(3): pp. 503-508. JSTOR
- Rogers, P., Soulsby, C., Petry, J., Malcolm, I., Gibbins, C., Dunn, S. (2004) Groundwater Surface Interactions in a Braided River: A tracer Based Assessment. *Hydrological Processes*. Vol 18(7): pp. 1315-1332. Wiley Online Library.
- Royal Society for the Protection of Birds (2021) *Making Space for Natural processes: Forest to Bog Restoration at RSPB Forsinard Flows Reserve*. Available: <https://www.nature.scot/sites/default/files/2017-07/Make%20space%20for%20natural%20processes%20-%20Forsinard%20Flows%20-%20Flows%20final%20web%20draft%203.pdf>. Accessed: 09/03/2021 Scottish National Heritage.
- Roulet, N., Moore, J., Bubier, J., and Lafleur, P. (1992) Northern Fens: Methane Flux and Climatic Change. *Tellus*. Vol 33: pp. 100-105. Taylor and Francis Online.
- Rumsby, B., McVey, R., and Brasington, J. (2001) The Potential for High Resolution Fluvial Archives in Braided Rivers: Quantifying Historic Reach-Scale Channel

and Flood Plain Development in the River Feshie, Scotland. In: Maddy, D., Macklin, G., and Woodward, J. (eds) *River Basin Sediment Systems- Archives of Environmental Change*. Balkema Publishing.

Schmidt, A. (2002) Analysis of Stage-Discharge Relations for Open-Channel Flows and their Associated Uncertainties (Doctoral Dissertation). Retrieved from IDEALS. University of Illinois.

Scott, P., Stone, D., and Allen, M. (2014) Human Contribution to the European Heatwave of 2003. *Nature*. Vol 432: pp. 610-614. Nature.

Schoener, G., and Stone, M. (2019) Impact of Antecedent Soil Moisture on Runoff from a Semiarid Catchment. *Journal of Hydrology*. Vol 569: pp. 627-636. Elsevier Online.

Senevirante, S., koster, R., Guo, Z., Dirmeyer, P., Kowalczyk, E., and others. (2006a) Soil Moisture Memory in AGCM Simulations: Analysis of Global Land-Atmosphere Coupling Experiment (GLACE) data. *Journal of Hydrometeorology*. pp. 1090-1112. American Meteorological Society.

Shuttleworth, E., Evans, M., Pilkington, M., Walker, J., Milliedge, D., and Allott, T. (2019) Restoration of Blanket Peat Moorland Delays Stormflow from Hillslopes and Reduces Peak Discharge (Accepted Manuscript) *Journal of Hydrology*. Durham University.

Smith, R., Bragg, O., M., Jefferies, C., and Ingram, H., A., P. (1995) Use of a Simple Mixing Model for the Separation of Storm Flow in a Peaty Catchment. In Black AR, Johnson RC, editors. Proceedings of the BHS Fifth National Hydrology Symposium. Wallingford: Institute of Hydrology, 1995: 5.1-5.7.

Smith, R., Bragg, O., and Ingram, H., A., P. (1999) Area Separation of Streamflow in an Upland Catchment with Partial Peat Cover. *Journal of Hydrology*. Vol 219: pp. 46-55. Elsevier Online.

Smith, K. (2013) *Environmental Hazards: Assessing Risk and Reducing Disaster*. 6th eds. Taylor and Francais.

Snyder, F. (1938) Synthetic Unit-Graphs. *EoS, Transactions American Geophysical Union*. Vol 19(1): pp. 447-454.

- Soulsby, C., Wade, A., Smart R., and Helliwell, R. (2002) Water Quality in the Uplands: a Hydrological Perspective on Catchment Hydrochemistry. *Science of the Total Environment*. Vol 294(1): pp. 73-94. Elsevier Online.
- Soulsby, C., Tetzlaff, D., Rodgers, P., Dunn, S., and S. Waldron (2006) Runoff processes, Stream Water Residence Times, and Controlling Landscape Characteristics in a Mesoscale Catchment: An Initial Evaluation. *Journal of Hydrology*. Vol 325: pp.197-221. Elsevier Online.
- Stoker, J. (1957) Water Waves. *Interscience*. New York (1957).
- Stewart, A., and Lance, A. (1983) Moor-Drainage: A Review of Impacts of Land Use. *Journal of Environmental Management*. Vol 17. pp. 81-99. Pascal Francis Institute.
- Stransky, D., Bares, V., and Fatka, P. (2007) The Effect of Rainfall Measurement Uncertainties on Rainfall-Runoff Processes Modelling. *Water Sciences and Technology*. Vol 55(4): pp. 103-111. IWA Publishing
- Thomas, D., and Black, R. (1970) Partial Area Contributions to Storm Runoff in a Small New England Watershed. *Water Resource Research*. Vol 6(5): pp. 1296-1311. Wiley Online Library.
- Timbadya, P., Patel, P., and Porey, D. (2011) Calibration of HEC-RAS Model on the Prediction of Flood for Lower Tapi River, India. *Journal of Water Resource and Protection*. Vol 3: pp 805.
- Tomkins, K, (2014) Uncertainty in Streamflow Rating Curves: Methods, Controls and Consequences. *Hydrological Processes*. Vol 28(3): pp. 464-481. Wiley Online Library.
- Trivedi, M., Morecroft, M., Berry, P., and Dawson, T. (2008) Potential Effects of Climate Change on Plant Communities in the Three Montane Nature Reserves in Scotland, UK. *Biological Conservation*. Vol 141(6): pp. 1665-1675. Elsevier Online.
- Trenbeth, K., (2011) Changes in Precipitation with Climate Change. *Climate Research*. Vol 47: pp. 123-138. Climate Services for Sustainable Development.
- Uddin, H. (2020) Dumpy Level Survey for Profile Levelling and Contouring. Available: [Dumpy Level Survey for profile levelling and contouring – QGEO \(theqgeo.com\)](https://www.theqgeo.com). Accessed: 15/05/2021.

- Uhlenbrook, S., and Leibundgut, C. (1997) Runoff Formation During Floods in Different Spatial Scales. *Water and Soil*. Vol 29: pp. 13-22. Springer.
- United Kingdom Centre for Ecology and Hydrology (2022) *Ratings and Datums*. Available: <https://nrfa.ceh.ac.uk/ratings-datums>. Accessed: 08/04/2021.
- United Kingdom Centre for Ecology and Hydrology (2022) *Why Monitor Upland Catchments?* Available: <https://www.ceh.ac.uk/why-monitor-upland-catchments>. Accessed: 05/04/2021.
- United Kingdom Centre for Hydrology and Ecology (2022) FEH Web Service. Available: <https://fehweb.ceh.ac.uk/GB/map>. Accessed: 11/05/2021.
- United States Army Corps of Engineers (2022) HEC-RAS. Available: <https://www.hec.usace.army.mil/software/hec-ras/download.aspx>. Accessed: 27/06/2021.

Appendices

Appendix A: Survey Derivation Report

A derivation report is an account of the corrections applied to topographic observations which are taken relative to no known location. The base station becomes an area of known high accuracy after post processing and these observations are therefore corrected to be in line with OS Datum Newlyn.

10/27/21, 2:01 PM Point Derivations

cbec eco-engineering UK Ltd		Phone: +44 (0) 1463 718831	
Unit 11, Beta Centre		cbecoeng.co.uk	
Stirling University Innovatin Park		info@cbecoeng.co.uk	
Stirling FK9 4NF			
United Kingdom			

Project File Data		Coordinate System	
Name:		Name:	United Kingdom/Ordnance Survey
Size:		Datum:	Ordnance Survey
Modified:	26/10/2021 12:26:52 (UTC:1)	Zone:	OS National Grid (OSTN15)
Time zone:	GMT Standard Time	Geoid:	OSGM15 (United Kingdom)
Reference number:		Vertical datum:	Newlyn
Description:		Calibrated site:	
Comment 1:			
Comment 2:			
Comment 3:			

Additional Coordinate System Details

Local Site Settings			
Project latitude:	?	Ground scale factor:	1
Project longitude:	?	False easting offset:	0.000 m
Project height:	50.000 m	False northing offset:	0.000 m

Point Derivations

Resultant Coordinates for point: Feshie Base							
Easting		Northing		Elevation		Height	
290550.537 m		787559.587 m		593.047 m		646.347 m	
Data	Used to calc.	Status	ΔEast (Metre)	ΔNorth (Metre)	Distance (Horiz) (Metre)	ΔElevation (Metre)	ΔHeight (Metre)
Adjusted (Local)	NEch	Enabled	0.000 m	0.000 m	0.000 m	0.000 m	0.000 m
FAUG → Feshie Base		Enabled	0.003 m	-0.006 m	0.007 m	0.013 m	0.013 m
DUDE → Feshie Base		Enabled	0.010 m	-0.002 m	0.010 m	0.004 m	0.004 m
BRAE → Feshie Base		Enabled	-0.005 m	-0.001 m	0.005 m	-0.008 m	-0.008 m
KILN → Feshie Base		Enabled	0.009 m	-0.001 m	0.009 m	0.020 m	0.020 m

file:///C:/Users/Ashley/AppData/Local/Temp/TBC Temporal/ftbq0y1q_hud/Rpt15774bac.html 1/4

10/27/21, 2:01 PM

Point Derivations

INVR → Feshie Base	Enabled	-0.009 m	0.012 m	0.015 m	-0.013 m	-0.013 m
--------------------	---------	----------	---------	---------	----------	----------

Survey Data used to calculate point: [Feshie Base](#)

Precision Confidence Level: **DRMS**

GNSS vectors

Tolerance of meaned vectors (Metre)
 Max horizontal tolerance of mean: **0.0500**
 Max vertical tolerance of mean: **0.0800**

Source	H. Prec. (Metre)	V. Prec. (Metre)	Length (Metre)	ΔX (Metre)	ΔY (Metre)	ΔZ (Metre)
FAUG → Feshie Base FAUG → Feshie Base (PV5)	0.0062 m	0.0171 m	57031.5573 m	20071.9455 m	52474.6231 m	-9804.5634 m
DUDE → Feshie Base DUDE → Feshie Base (PV20)	0.0082 m	0.0197 m	79587.5063 m	-49656.5175 m	-53809.6445 m	31191.7230 m
BRAE → Feshie Base BRAE → Feshie Base (PV2)	0.0055 m	0.0160 m	25103.3588 m	2356.7701 m	-24890.9399 m	-2250.6376 m
KILN → Feshie Base KILN → Feshie Base (PV14)	0.0135 m	0.0265 m	65212.6025 m	-44999.2759 m	35060.5482 m	31599.1560 m
INVR → Feshie Base INVR → Feshie Base (PV9)	0.0081 m	0.0176 m	63167.7697 m	50651.1518 m	21730.0760 m	-30861.4930 m

Coordinates

Source	Easting (Metre)	Northing (Metre)	Elevation (Metre)	Height (Metre)
Adjusted (Local)	290550.537 m	787559.587 m	593.047 m	646.347 m

Resultant Coordinates for point: [feshie base 2](#)

Easting	Northing	Elevation	Height

file:///C:/Users/Ashley/AppData/Local/Temp/TBCTemporal/tbq0y1q.hud/Rpt15774bac.html

2/4

10/27/21, 2:01 PM Point Derivations

		290419.212 m	788042.689 m	566.790 m	620.084 m		
Data	Used to calc.	Status	Δ East (Metre)	Δ North (Metre)	Distance (Horiz) (Metre)	Δ Elevation (Metre)	Δ Height (Metre)
Adjusted (Local)	NEch	Enabled	0.000 m	0.000 m	0.000 m	0.000 m	0.000 m
FAUG → feshie base 2		Enabled	-0.004 m	-0.008 m	0.009 m	0.012 m	0.012 m
DUDE → feshie base 2		Enabled	-0.001 m	0.011 m	0.011 m	0.006 m	0.006 m
BRAE → feshie base 2		Enabled	0.002 m	-0.003 m	0.003 m	0.005 m	0.005 m
KILN → feshie base 2		Enabled	0.005 m	0.001 m	0.006 m	-0.033 m	-0.033 m
INVR → feshie base 2		Enabled	-0.002 m	0.004 m	0.004 m	-0.003 m	-0.003 m
Survey Data used to calculate point: feshie base 2							
Precision Confidence Level: DRMS							
GNSS vectors							
Tolerance of meaned vectors (Metre)							
Max horizontal tolerance of mean: 0.0500							
Max vertical tolerance of mean: 0.0800							
FAUG → feshie base 2	H. Prec. (Metre)	V. Prec. (Metre)	Length (Metre)	Δ X (Metre)	Δ Y (Metre)	Δ Z (Metre)	
feshie base 2 → FAUG (PV4)	0.0053 m	0.0153 m	56735.3871 m	-19646.8909 m	-52358.4949 m	9565.1366 m	
DUDE → feshie base 2	H. Prec. (Metre)	V. Prec. (Metre)	Length (Metre)	Δ X (Metre)	Δ Y (Metre)	Δ Z (Metre)	
feshie base 2 → DUDE (PV19)	0.0060 m	0.0158 m	80025.4207 m	50081.5619 m	53925.7697 m	-31431.1387 m	
BRAE → feshie base 2	H. Prec. (Metre)	V. Prec. (Metre)	Length (Metre)	Δ X (Metre)	Δ Y (Metre)	Δ Z (Metre)	
feshie base 2 → BRAE (PV1)	0.0048 m	0.0161 m	25162.0878 m	-1931.7069 m	25007.0821 m	2011.2230 m	
KILN → feshie base 2	H. Prec. (Metre)	V. Prec. (Metre)	Length (Metre)	Δ X (Metre)	Δ Y (Metre)	Δ Z (Metre)	
feshie base 2 → KILN (PV13)	0.0095 m	0.0256 m	65560.4829 m	45424.2991 m	-34944.4134 m	-31838.6236 m	
INVR → feshie base 2	H. Prec. (Metre)	V. Prec. (Metre)	Length (Metre)	Δ X (Metre)	Δ Y (Metre)	Δ Z (Metre)	

file:///C:/Users/Ashley/AppData/Local/Temp/TBC Temporal/fg0iy1q_hud/Rpt15774bac.html 3/4

10/27/21, 2:01 PM

Point Derivations

	(Metre)					
feshie base 2 --> INVR (PV8)	0.0073 m	0.0184 m	62670.0331 m	-50226.0849 m	-21613.9339 m	30622.0722 m
Coordinates						
Source	Easting (Metre)	Northing (Metre)	Elevation (Metre)	Height (Metre)		
Adjusted (Local)	290419.212 m	788042.689 m	566.790 m	620.084 m		

Date: 27/10/2021 13:45:50	Project:	Trimble Business Center
---------------------------	----------	-------------------------

Appendix B: *Code Used for R-Studio*

A series of programming code used to undertake a Mann-Whitney Wilcoxon Test.

```
setwd("C:/Users/Downloads")
river1<-read.csv("Lag.csv")
attach(river1)
river2<-as.factor(river)
shapiro.test(count[river2=="LE"])
# data: count[river2 == "LE"]
# W = 0.87041, p-value = 0.04253
shapiro.test(count[river2=="UF"])
# Shapiro-Wilk normality test
# data: count[river2 == "UF"]
# W = 0.9706, p-value = 0.8846
wilcox.test(count~river2)
# data: count by river2
# W = 132.5, p-value = 0.1171
# alternative hypothesis: true location shift is not equal to 0
```